

**INVESTIGATION OF LONG TERM AGEING IN SOLID INSULATING  
MATERIAL BY STUDYING THE EFFECT OF VARIATION OF  
PARAMETERS AND WAVELET TRANSFORM ANALYSIS ON REAL  
TIME DATA ON PARTIAL DISCHARGE**

Thesis Submitted to  
**The Maharaja Sayajirao University of Baroda**

In Partial Fulfillment of the Requirements for  
The Degree of Doctor of Philosophy  
(Electrical Engineering)

By  
Chirag K. Vibhakar

Guided by  
Mrs. S. A. Kanitkar  
(Retd.) Prof. & Head  
Electrical Engineering Department



Faculty of Technology & Engineering  
M. S. University of Baroda  
Vadodara - 390 001  
November 2011

**DEDICATED TO**

*My Parents, wife*

*and*

*My Son*

# DECLARATION

**CHIRAG K. VIBHAKAR** hereby declare that the work reported in this thesis titled **‘INVESTIGATION OF LONG TERM AGEING IN SOLID INSULATING MATERIAL BY STUDYING THE EFFECT OF VARIATION OF PARAMETERS AND WAVELET TRANSFORM ANALYSIS ON REAL TIME DATA ON PARTIAL DISCHARGE’** submitted for the award of degree of

**DOCTOR OF PHILOSOPHY**

**IN**

**ELECTRICAL ENGINEERING**

is original and was done by me in **THE DEPARTMENT OF ELECTRICAL ENGINEERING, FACULTY OF TECHNOLOGY AND ENGINEERING, THE MAHARAJA SAYAJIRAO UNIVERSITY OF BARODA, VADODARA.**

I take privilege in declaring that the work is developed, structured and prepared by me solely. Further, I declare that the work is not part of any declared or published work partly or fully for the award of any degree or academic qualifications of this university or of any other institution of examining body in India and abroad.

Place: Vadodara

**(Chirag K. Vibhakar)**

Date:

# CERTIFICATE

*This is to certify that the thesis entitled 'Investigation of Long Term Ageing in Solid Insulating Material by Studying the Effect of Variation of Parameters and Wavelet Transform Analysis on Real Time Data on Partial Discharge' submitted by Shri Chirag. K. Vibhakar, incorporates the bonafide results of the investigation carried out by him in the department of electrical engineering, under my direct supervision and guidance. This is also to certify that the thesis contains his original contribution and no degree or diploma or distinction has been conferred on him before, either in this or any other university.*

Date:

Place: Vadodara

**Mrs. S. A. KANITKAR**

*Research Guide*

*(Retd.) Prof. & Head*

*Email id : smitakanitkar@yahoo.com*

*Electrical Engineering Department*

*Faculty of technology and Engineering*

*M. S. University of Baroda, Vadodara*

**Prof. S. K. SHAH**

*Head of the Department*

*Electrical Engineering Department*

*Faculty of technology and Engineering*

*M. S. University of Baroda, Vadodara*

**Dean**

*Faculty of technology and Engineering*

*M. S. University of Baroda, Vadodara*

# ACKNOWLEDGEMENTS

First and foremost, special thanks and deepest sense of gratitude to my guide Prof. Mrs. S. A. Kanitkar, (Retired Professor of Electrical Engineering, Faculty of Technology and Engineering, M. S. University Baroda) who gave me the opportunity to research in this area and continuously motivated me from the start to completion stage. The thesis in its present form is the result of her inspiration, enthusiasm and trust instilled in me. I wish to take this opportunity to express my sincere thanks for her encouragement, support and invaluable guidance during entire research span.

I am grateful to Mr. Shailesh Patel (senior testing engineer, PD Test. Unit, ERDA), Mr Amit Patel (CEO, ECS Vadodara), Mr. Ritesh Patel (Testing Engineer, TRIL, Ahmedabad), Mr Mohan (Manager AREVA, Vadodara) and Prof. K. R. Siddhapura (Assistant Professor, HOD of Electrical Engineering Department, D. I. T., Rajkot) for their guidance and help during the various phases of the work.

I am very much thankful to all the faculty members of the Department of Electrical Engineering, Faculty of Technology and Engineering, M. S. University, Baroda, for their continuous inspiration and key suggestions during the various stages of the work presentations.

I am also very much thankful to Dr. A. R. Chudasama (Department of Electrical Engineering, Faculty of Technology and Engineering, M. S. University, Baroda) and Dr. V. J. Pandiya (Asst. Prof., Department of electrical engineering, PDPU, Gandhinagar) for their key suggestions during the various stages of work.

I would like to express my sincere thanks and deep sense of gratitude to Hon. Pravinbhai Maniar (Chairmen of V.V.P. Engg. College,Rajkot) who has taught a lot through his silent ethical way of working, Dr. S. P. Parikh (Principal of V.V.P Engg. College, Rajkot) for his continuously mentoring and valuable discussions, all my colleagues of V.V.P. engineering college and unmentioned names for providing their direct or indirect help.

I would like to thank Almighty for not letting me down at the time of crisis and showing me silver lining in the dark clouds.

I am deeply indebted to my parents, wife, son, and friends for their encouragement and support throughout the study.

**Chirag. K. Vibhakar**

# ABSTRACT

Solid dielectric materials are used in all kinds of electrical circuits and devices to insulate different voltage potentials. Insulating materials are used extensively in Electrical High Voltage (HV) systems. Following observations are noticed during the insulation operation:

- Severe cracks formation
- Sudden breakdown of insulation without any abnormal indication
- Above observations noticed under normal operating conditions and/or after long duration

Such behavior has been attributed to the long duration breakdown by internal discharges. This electrical discharge is referred to as Partial discharge (PD).

Insulator (dielectric) testing plays important role in HV system. The conventional test (i.e. power frequency and impulse) consists of applying a specific voltage for a short duration to check failure occurrence. The failure tests evaluate performance of the equipments. Such-tests enable detection of grossly defective insulation, but they don't give any assurance against gradual deterioration and eventual failure in service by thermal or electro chemical deterioration. The integrity and quality of insulation is checked by various tests like power frequency voltage withstand test, loss angle measurement, insulation resistance measurement, impulse voltage withstand test etc. But, with above measurements, the minor insulation flaws and inefficient processing of insulation cannot be identified. In many cases, insulator fails due to high insulation resistance and short operation time. Many experiments were carried out to understand the phenomena and progressive deterioration of the insulation. It was found that such failures are only due to phenomenon named PD.

PD is a localized electrical discharge in any insulator. The air gap or void in the solid insulation material creates localized electrical discharge. This discharge is restricted to a small part of the dielectric which partially bridges the insulation between the conductors.

The significance of PD Measurement is to detect insulating material life, which is under construction or in service/use. PD measurement provides a sensitive and non destructive method of insulation system evaluation and of incipient defects detection. Partial Discharge (PD) is an

important tool for improving the reliability of HV insulating system. It is very sensitive and non destructive method for insulation ageing evaluation of any HV equipment. Although having small magnitude, PD deteriorates progressively and makes equipment/insulation failure.

Thus, the main purpose of present interest in PD characteristics tests has following prominent views:

1. The internal discharges characteristics and its amount can be determined and this knowledge can be utilized to control the quality of insulation during different process in manufacturing because it discharge is directly related to the amount of gas or moisture presence in the insulation, the impregnation process and the casting process.
2. The PD detection can be used for finished insulation products like bushings, capacitors, cables, insulators, machine winding insulators etc. as non destructive test.
3. During PD measurement there is noticeable contribution of noise. So, effective noise elimination technique helps in better estimation on PD.

Partial Discharge are related with various aspects such as temperature, pressure etc. A critical study of the existing literature reveals that the existing models relating electrical stress, ageing effect and life of insulation material are purely empirical. Thus, there is a need for PD analysis for insulating material by varying direct affecting parameters like temperature. Short term ageing tests on insulating material are not reached at the standardization stage. There is limited information availability of PD data for both normal and/or adverse conditions. PD measurement technique and exact analysis is obtained under standard condition. PD varies if some of the parameter changes, which affect the dielectric strength of solid insulating material.

During the first attempt, investigations are performed on epoxy insulators by applying HV ageing tests under different voltage and temperature conditions. Also, the effect of temperature is monitored for PD as part of investigation. Experiments are carried out on widely employed simple epoxy resin based high-voltage insulation electrode systems, having a pin hole (cavity). Before placing epoxy insulator at high voltage assembly, it is passed from X-ray unit to check the size of pin hole. Each insulator temperature is regulated from  $-5^{\circ}\text{C}$  to  $150^{\circ}\text{C}$  inside thermal chamber during the experiment. Performed ageing mechanism analysis, simple phenomenological ageing and life effects are proposed. It gives a new approach and tool for the

problem of future applications on electrical components. The investigation and modeling of ageing test focused on temperature and wasted energy in the epoxy during ageing. During this attempt, it is found that the signal (having PD) contains significant amount of noise. So, it is necessary to remove the noise from original signal.

During the second attempt, noise removal from original signal is carried out as a prime task. There are some methods available to remove noise namely, statistical analysis, Wavelet Transform (WT) analysis etc. WT is capable to operate in real time and hence it is appropriate choice for PD extraction. Also, hardware implementation and realization is also possible for the same. WT is an extension of Short-Time Fourier Transform (STFT) which allows variable-sized window and produces a time-scale view of the signal (instead of time-frequency). In essence, the technique decomposes a signal into time shifted and scaled versions of an original (or mother) wavelet. It is capable of providing the time and frequency information simultaneously. WT constitutes combinations of high pass and low pass filters, which filters out either high frequency or low frequency components from the signal. There are many such filter stages. The WT has the procedure where the time domain signal passes through various filters. This procedure is repeated every time for some portion of the signal corresponding to some frequencies which are being removed from the signal. Also, WT has one more characteristic of shifting and scaling. Shifting and scaling of a wavelet means delaying or hastening its beginning and stretching or compressing the original wavelet respectively. There is a correspondence between scaling and frequency. This process removes noise from acquired signal. This is called signal de-noising. Signal de-noising has two important WT parameters, WT Threshold value determination and WT function selection.

**Following work is carried out during WT analysis:**

1. Real time data acquisition for HV transformers
2. WT method is carried out on simulated signal and acquired signal.
3. A new method is envisaged for optimum WT threshold function selection, based on acquired signal analysis on time domain.

In first exercise, a program is developed which can extract PD pulses from data. This program is linked to simulated signal and real time acquired signal. The simulated signal is generated using

modeling of PD signals and noise whereas real time data is acquired from Transformers at Transformers and Rectifiers India Ltd. (TRIL located near Bavala, Gujarat, India and Areva T&E located at Vadodara, Gujarat, India). From various set of signals, PD data is acquired; analyzed and satisfactory results are derived.

In the second exercise, signal de-noising for PD detection is emphasized by WT Threshold function selection. The threshold function selection helps to remove/retain signal during analysis. It is important when the acquired signal has more noise contribution than original PD signal. Here, signal (having PD pulses and noise) analysis is focused on different threshold function selections. The analyses are carried out in two phases; (1) analysis on acquired signals and (2) WT analysis for different threshold functions. Finally, it compares both the results and suggests which WT threshold function will give fruitful results based on original signal determination.

***Flow of Report:***

The thesis progressively discusses the approach employed in order to achieve the above objectives as follows:

Chapter-1 Discuss the importance of solid insulating material in practice, ageing and breakdown of solid insulating material, significance of PD measurement, recognition of PD, definition of PD and the same in solid insulating material.

Chapter-2 Discuss the Fundamental of PD and measurement methods like basic PD equivalent circuit, Various PD quintiles, PD measuring system within the PD test circuit, calibration of PD detectors in a complete test circuit, source and reduction of disturbances, Origin and recognition of discharge.

Chapter-3 Discuss the Measurement and analysis of solid insulating material ageing test under the effect of temperature on partial discharges.

Chapter-4 Discuss the fundamentals of Fourier transforms, its variants (DFT, FFT) and cover in depth view of Wavelet Transform including its application to PD analysis.

Chapter-5 Discuss the Wavelet Transform application for PD detection and analysis with data acquisition, WT suitability check for PD Measurement, method for estimating WT threshold function, results and conclusion on WT analysis.

Chapter-6 Discuss the conclusions from suggested techniques and related simulation results presented in the thesis. Possible steps for future developments and research in this area is also briefly suggested.

In summary, this thesis focuses on the problems encountered by the conventional PD measurement during testing of solid insulating material and specifically focused on temperature and noise contribution. The main goal is to describe the life of epoxy resin systems subjected to PD activity under thermal stress conditions (which are higher and lower than the ambient temperature as well as above the glass transition temperature ( $T_g$ )). During second phase, WT is applied for checking simulated data and real time data. It is derived that, WT can extract the PD signals effectively by simulating PD and noise. Subsequently, WT is further considered for different threshold function and threshold value selection. Finally, a conclusion is derived to optimum threshold function selection based on the acquired signal.

# Table of Contents

<b>Dedication</b>	<b>i</b>
<b>Declaration</b>	<b>ii</b>
<b>Certificate</b>	<b>iii</b>
<b>Acknowledgement</b>	<b>iv</b>
<b>Abstract</b>	<b>vi</b>
<b>Table of Contents</b>	<b>xi</b>
<b>List of Figures</b>	<b>xiv</b>
<b>List of Tables</b>	<b>xvii</b>
<b>List of Symbols</b>	<b>xviii</b>
<b>List of Abbreviations</b>	<b>xxi</b>
<b>List of Chemical Composition</b>	<b>xxii</b>
<b>Chapter-1 Introduction</b>	<b>1</b>
1.1 General	2
1.2 Significance of Partial Discharge (PD) Measurement	5
1.3 Recognition of Partial Discharge	7
1.4 Definition of Partial Discharge	8
1.5 Characteristics of Partial Discharge	10
1.6 Causes of PD in Solid Insulating Material	11
1.7 Various Parameters Affecting PD	13
1.8 PD Behavior Under Different Voltage Condition	16
1.9 Work Objectives	18
<b>Chapter-2 Fundamentals of Partial Discharges &amp; Their Measuring Methods</b>	<b>19</b>
2.1 Basic PD Equivalent Circuit	20
2.2 The Recurrence of Discharge	25
2.3 PD Currents	28
2.4 Various PD Quantities	31

2.5	Various PD Measurement Methods	34
2.6	PD Measuring System Within the PD Test Circuit	36
2.7	Calibration of PD Detectors in a Complete Test Circuit	60
2.8	Digital Instruments for PD Measurement	62
2.9	Source of Interference and Reduction of Disturbances	66
2.10	Origin and Recognition of Discharge	71
<b>Chapter-3</b>	<b>Measurement and Analysis of Solid Insulating Material Ageing Test Under the Effect of Temperature on Partial Discharges</b>	<b>76</b>
3.1	Introduction	77
3.2	PD Measurement for Solid Insulating Material at different Temperatures	79
3.3	PD Modeling	81
3.4	Results and Analysis	83
3.5	Conclusions	88
<b>Chapter-4</b>	<b>Wavelet Transform (WT)</b>	<b>89</b>
4.1	Introduction	90
4.2	Discrete Fourier Transform (DFT) and Fast Fourier Transform (FFT)	93
4.3	Introduction to Wavelet Transforms	96
4.4	Wavelet and Multi-Resolution Analysis Mathematical Representation	101
4.5	Wavelet Transform and Multilevel Representation	105
4.6	Review of Wavelet Applications in Power Systems	115
4.7	Wavelet Transform as Applied to PD Analysis	118
<b>Chapter-5</b>	<b>Practical Application of WT for PD Detection and Analysis</b>	<b>122</b>
5.1	Introduction	123
5.2	Data Acquisition at Laboratory	124
5.3	WT Suitability Check for PD Measurement	128
5.4	Method for Estimating WT Threshold Function	129
5.5	Results	138

5.6	Conclusion on WT Analysis	159
<b>Chapter-6</b>	<b>Conclusion and Future Scope</b>	<b>160</b>
	<b>Publications</b>	<b>163</b>
	<b>References</b>	<b>166</b>
	<b>Appendix</b>	<b>174</b>

## List of Figures

Figure No.	Figure Title	Page No.
1.1	Solid insulation with gas filled void	9
2.1	Simulation of a PD test objects	20
2.2	The PD test object $C_t$ within a PD test circuit	22
2.3	Sequence of cavity breakdown under alternating voltages	26
2.4	Measurement of PD current $i(t)$ – low sensitivity circuit	28
2.5	Measurement of PD current – high sensitivity circuit	29
2.6	Basic Partial Discharge Detection Test Circuit – Straight Detection	37
2.7	Correct Relationship Between Amplitude and Frequency to Minimize Integration Errors for a Wide-band System	39
2.8	Principle of ‘Wide-band’ PD Measuring System	42
2.9	Elliptical Display	46
2.10	Output Voltage Signals $U_{out}$ of a Wide-band PD Detector with $\Delta f = 45$ to 440 kHz for Two Different Input Pulses	47
2.11	Narrow-band Amplifier Responses	51
2.12	Response of a Simple Narrow-band Circuit with $\Delta f = 10$ kHz; $f_m = 75$ kHz	55
2.13	Block Diagram of a Quasi-peak RIV Meter Including Weighting Circuit Compared with PD Narrow-band PD Detector	56
2.14	Variation of CISPR Radio Interference Meter Reading with Repetition Frequency $N$ , for Constant Input Pulses	58
2.15	The Usual Circuit for the Calibration of a PD Measuring Instrument MI within the Complete Test Circuit.	61
2.16	The Pattern of a Phase-resolved PD Measurement for a Moving Metal Particle within a GIS.	65
2.17	An Example of a $\phi - q - n$ Diagram	66
2.18	Differential PD bridge (Balanced Circuit)	70

<b>Figure No.</b>	<b>Figure Title</b>	<b>Page No.</b>
2.19	Polarity Discrimination Circuit	71
2.20	Origin and Recognition of Discharges	72
3.1	Electrical Set-up for PD Measurement	80
3.2	PD Vs. Applied Voltage (kV) at Different Temperatures.	85
3.3	Stress Vs life at -5° C Temperature	86
3.4	Stress Vs life at 30° C Temperature	86
3.5	Stress Vs life at 60° C Temperature	86
3.6	Stress Vs life at 100° C Temperature	87
3.7	Stress Vs life at 120° C Temperature	87
3.8	Stress Vs life at 150° C Temperature	87
4.1	A Simple Sinusoidal Function	91
4.2	Time – Frequency Representation of a Sinusoidal Function	92
4.3	Examples of Different Wavelet Functions	98
4.4	Approximation of (a) the Input Signal and (b) Approximation of the Input Signal using Haar Scaling Function	107
4.5	Multilevel representation of an input signal using the Haar scaling function	109
4.6	Moving to a Finer Space using the Wavelet, $\Psi_{j,k}(t)$ and Scaling Function, $\Phi_{j,k}(t)$	111
4.7	Multilevel Representation of an Input Signal using Wavelet Function	113
4.8	One Stage MRA and Wavelet Filters	114
4.9	Five Level Multi-Resolution Signal Decomposition	115
4.10	Evolution of Wavelet Publication in Power System	116
4.11	Percentage Usage of Wavelet publications in different power system areas	117
4.12	The Hard and Soft Threshold Function	122

<b>Figure No.</b>	<b>Figure Title</b>	<b>Page No.</b>
5.1	Block Diagram of PD Measurement Setup	125
5.2	Data Acquisition Setup for PD Measurement	126
5.3	Power Transformer Setup as a Test Object	126
5.4	Measurement Record Diagram	127
5.5	Block Diagram for PD Simulated Data	129
5.6	Flow of the Analysis	130
5.7	Block Diagram for acquired signal analysis	131
5.8	Analysis on Data Set-1 ( $R_{pos}$ and $R_{neg}$ are High)	133
5.9	Analysis on Data Set-13 ( $R_{pos}$ and $R_{neg}$ are Low)	133
5.10	Block Diagram for WT analysis	134
5.11	Flowchart of Signal Analyses	135
5.12	Simulated PD pulses, noise and pulled out PD Pulses	140
5.13	Recorded waveform using Mtronics software	142
5.14	Effect of hard and soft threshold selection on data set-1 to 13	144
5.15	Comparison of Hard threshold Gain with Actual Signal (for $p=2$ ) Available from X' mer-1	158
5.16	Comparison of Hard threshold Gain with Actual Signal (for $p=2$ ) Available from X' mer-2	159

## List of Tables

<b>Table No.</b>	<b>Table Title</b>	<b>Page No.</b>
2.1	Different Sources of Disturbances and their remedy for suppression	68
2.2	Interpreting the origin of discharge	74
3.1	Applied Voltage and Partial Discharge Measurements	85
3.2	Stress and Life at different temperatures	88
5.1	Simulated pulse Characteristics	128
5.2	Measured PD at different conditions as per standard	139
5.3	Data analysis on various acquired data sets	143

## List of Symbols

$\epsilon_r$	Relative permittivity of the solid dielectric
d	Thickness of dielectric
t	Thickness of cavity
$C_c$	Capacitance of cavity
$C_b$	Capacitance of dielectric in series with cavity
$C_a$	Capacitance of rest of the dielectric
$V_c$	Voltage across cavity
E	Over-voltage Stress
$E_c$	Electric Field strength across cavity
i (t)	Discharge current
$\delta_{qc}$	Lost charge from $C_c$
$V_e$	PD extinction voltage
$V_i$	PD inception voltage
$i_t$	Displacement current through $C_t$
I	The average discharge current
D	The quadratic rate
P	The discharge power
Z	Impedance
$C_k$	Coupling capacitor
$C_t$	Test object capacitance
Q	Apparent charge
$q_m$	Measured charge
$i_t(t)$	Displacement current

$i_k$	Displacement current through $C_k$
$Z_{mi}$	Input impedance of measuring system
$C_a$	Test object capacitance
$f_m$	Mid-band frequency
$Z(f)$	Transfer impedance
$\Delta_f$	Frequency bandwidth
$T_r$	Pulse resolution time
$\alpha$	Damping angle
$L$	Inductance
$f_0$	Resonance frequency
$T_r$	Resolution time
$G(j\omega)$	Transfer function
$\omega_m$	Mid-band angular frequency
$\Delta\omega$	Angular bandwidth
$G_0$	Scale factor
$F(\omega)$	Phase shift
$\tau$	Full length of the response
$Q$	Quality factors
$T$	Electrical discharging time constant
$k_i$	The scale factor for the instrument
$f(N)$	The non-linear function of $N$
$\tan \delta_K$	Dissipation factor
$T_g$	Material glass transition temperature
$\Phi_k(t)$	A set of vectors
$L$	Hilbert space

$\Psi_{a,b}$	Wavelet function
$\delta_\lambda^H$	Hard threshold function
$\delta_\lambda^S$	Soft threshold function

## List of Abbreviations

PD	Partial Discharge
HV	High Voltage
IEC	International Electro Technical Commission
A.C.	Alternating Current
D.C.	Direct Current
CD	Coupling Device
CC	Connecting Cable
OL	Optical Link
MI	Measuring Instrument
CRO	Cathode Ray Oscilloscope
CISPR	International Special Committee on Radio Interference
RDV	Radio Disturbance Voltage
RIV meter	Radio Interference Voltage meter
GIS	Gas-Insulated Substations
VHF	Very High Frequency
UHF	Ultra High Frequency
DSPs	Digital Signal Processors
FFT	Fast Fourier Transform
DFT	Discrete Fourier Transform
IFT	Inverse-Fourier-Transforming
CWT	Continuous Wavelet Transform
WT	Wavelet Transform
WS	Wavelet Series
DWT	Discrete Wavelet Transform
MRA	Multi-Resolution Analysis

## List of chemical compositions

O <sub>3</sub>	Ozone
NO <sub>2</sub>	Nitrogen Dioxide
CY 225, Hy 925	A Feeder Silica Flore C Epoxy Resin

# **Chapter-1**

## **Introduction**

## 1.1 GENERAL <sup>[1-3]</sup>

Power is the basic need for the economic development of any country. Availability of electricity has been the most powerful vehicle for fuelling economic development and social change throughout the world. Government across the globe has given utmost priority to projects related to generation, transmission and distribution of electrical energy economically and efficiently.

Engineers design the transmission network for efficient energy transfer with consideration of economic factors, network safety and redundancy. These networks deploy components such as power lines, cables, circuit breakers, switches, insulators and transformers etc.

Bulk Transmission of power over long distances on high voltages transmission lines is indispensable. High voltage apparatus requires careful design of its insulation and the electrostatic field profiles for diverse conditions. The principle media of insulation are gases, vacuum, solid, and liquid, or a combination of these.

Solid dielectric materials are used in all kinds of electrical circuits and devices to insulate different voltage levels. A good insulator should be of low dielectric loss, having high mechanical strength, free from gaseous inclusions and moisture, and should also be resistant to thermal and chemical deterioration. Solid dielectrics vary widely in their origin and properties. They may be natural organic substances, such as paper, cloth, rubber, etc. or inorganic materials, such as mica, glass and ceramics or synthetic materials like epoxy resin, plastics etc. All organic materials (produced from vegetable or animal matter) have similar characteristics. They are good insulators and can be easily adopted for practical applications. However, their mechanical and electrical properties always deteriorate rapidly when the temperature exceeds 100 °C. Therefore, they are generally used after treating with a varnish or impregnation with oil. Examples are paper and press board used in cables, capacitors and transformers.

Inorganic materials, unlike the organic materials, important inorganic materials use glasses and ceramics. They are widely used for the manufacture of insulators, bushings etc., because of their resistance to atmospheric pollutants and their excellent performance under varying conditions of temperature and pressure. Synthetic polymers are the polymeric materials, which possess excellent insulating properties and can be easily fabricated and applied to the apparatus. These are generally divided into two groups, the thermoplastic and the thermosetting plastic types. They have characteristics like low melting temperatures in the range 100-120 °C, flexible, mold ability and extrude at temperatures below their melting points. They are widely used in bushings, insulators etc. Their electrical use depends on their ability to prevent the absorption of moisture.

Study of the ageing and breakdown of solid dielectrics have extreme importance in insulation. Below are described characteristics of each insulating materials in case of applying electric field:

- After breakdown solid insulators get permanently damaged
- Gaseous insulators fully recover their dielectric strength after the applied electric field removed and
- Liquid insulators partly recover their dielectric strength after the applied electric field removed

If the solid insulating material is truly homogeneous and free from imperfections, its breakdown stress will be as high as 10 MV/cm. This is the 'intrinsic breakdown strength', and can be obtained under carefully controlled laboratory conditions. However, in practice, the breakdown fields are very much lower than this value. The breakdown occurs due to many mechanisms. Generally, the surface breakdown occurs rapidly than in the solid itself, which is more frequent cause of trouble in practice. The breakdown of insulation can occur due to mechanical failures, which are caused by the mechanical stresses produced by the electrical fields. This is called "electromechanical" breakdown. Also, the breakdown occurs due to chemical

degradation caused by the heat generated (due to dielectric losses) in the insulating material. This process is cumulative and more severe in the presence of air and moisture. When breakdown occurs on the surface of an insulator, it can be a simple flashover or formation of a conducting path on the surface. When the conducting path is formed, it is called "tracking", and results in the degradation of the material. Surface flashover normally occurs when the solid insulator is immersed in a liquid dielectric. Surface flashover is the most frequent cause of trouble in practice. Porcelain insulators for use in transmission lines must therefore be designed to have a long path over the surface. In porcelain high voltage insulators of the suspension type, the length of the path over the surface will be 20 to 30 times greater than solid. Even though, the surface breakdown is the most common form of failure. The failure of solid insulation by discharge, which occurs in the internal voids and cavities of the dielectric, called partial discharges. It is receiving much attention in present research, which determines relation between the ageing or life and stress characteristics of the material. The energy dissipated in the partial discharges causes' further deterioration of the cavity walls, which raise further evolution of gas. This is a cumulative process eventually leading to breakdown. In practice, it is not possible to eliminate partial discharges, but it can be estimated under specified operating conditions. Also, the design engineer should attempt to raise the discharge inception level by carefully choosing electric field distributions and eliminating voids. This requires a very high quality control during manufacturing and assembly. In some applications, the effect of the partial discharges can be minimized by vacuum impregnation of the insulation. For high voltage applications, cast epoxy resin used as extensively, but great care should be exercised during casting.

High voltage switchgear, bushings, cables, and transformers are typical devices for which partial discharge effects should be considered in design.

## 1.2 SIGNIFICANCE OF PARTIAL DISCHARGE MEASUREMENT<sup>[2,3]</sup>

The significance of partial discharges on life of insulation has long been recognized and is extremely important means to detect the life of insulating materials, which are under construction, already existing or are in service. Measurement of partial discharges provides a sensitivity method of evaluating the performance of an insulation system and of detecting incipient defects.

Insulating materials under normal operating conditions after a long period of satisfactory service, have been found to develop cracks and sudden breakdown without abnormal indications. Such behavior has been attributed to long duration breakdown by internal discharge and surface track formation. Track formation of conductive paths has been found internally to precede the breakdown and partial discharge inside the insulating material play an important part in creation of such paths.

Even the equipments over potential test may still have a dangerously high level of partial discharges under service condition, which could lead its deterioration, and premature failure. The conventional over potential tests (i.e. power frequency and impulse) consist merely of applying more than three times the working voltage for short duration and if there is no failure the equipment is considered to be satisfactory. Such tests enable detection of grossly defective insulation but they give no assurance against gradual deterioration and eventual failure in service by thermal or electro chemical deterioration or erosion or chemical degradation by partial discharge.

There is further a danger that electrical discharges may cause deterioration during the a.c. over voltage test itself which may go unnoticed and it is possible for failure to occur on the reapplication of the high voltage, Where as it may not have occurred in service. Greater emphasis, therefore has to be placed on the measurement

of discharge at normal potential instead of the over potential test and on no destruction and diagnostic testing of electrical apparatus in service.

Partial Discharge (PD) is an important tool for improving the reliability of HV insulating system. It is a method for insulation ageing evaluation of any HV equipment. Although having small magnitude, PD deteriorates progressively and makes equipment insulation failure.

Significance of partial discharge can be explained with following important points:

- The significance of partial discharge is to detect the life of insulating materials, which are under construction, already existing or in service.
- It is an important tool to detect air gaps/voids in solid insulation. Gas bubbles in liquid/composite insulation. So it warns the user at the initial stage of the corrosion in insulations so that severe damage to the electrical instruments can be averted.
- Presence of unwanted/foreign particles (like metallic or magnetic materials), loose connection on the high or low voltage terminals, sharp points in the H.V equipments insulation are the common factors for frequently rise in PD. So, PD is the prime most important test, which shows the deficiencies effectively.
- Sometimes, manufacturing units are unable to maintain required standard of perfection in insulating media. Improper processing or drying of insulation is the major challenges at the industrial level. These parameters can be easily detected by the Partial Discharge methodology.

### **1.3 RECOGNITION OF INTERNAL DISCHARGE <sup>[3]</sup>**

Partial discharges have been known for many years as a cause of deterioration in insulants. However, the subject did not receive much attention in the past as the insulants were worked at comparatively low electrical stress and the shape and design of equipments were such risk of failure from such discharge was low. With the advent of new type of insulants, the economic necessity of working at higher stresses and need for better control of tests, the study of partial discharges assumed considerable importance in electrical apparatus and insulation systems. Thus main purpose of prevent interest in discharge characteristics rests on two prominent view.

- (1) The internal discharge characteristics and its amount can be determined and this knowledge can be utilized to control the quality of insulation at different process in its manufacturing. As the discharge directly relate to the amount of gas or moisture present in the insulation, the impregnation process and the casting process can definitely be improved.
- (2) Another interest lies in the suggestion that the discharge detection can be introduced for testing of finished insulating products like bushing cable, current transformer, line insulators and machine winding insulation etc. as non destructive test.

## 1.4 DEFINITION OF PARTIAL DISCHARGE <sup>[2,3]</sup>

Partial Discharge (PD) is a “localized electrical discharge in any insulator”. The air gap or void in the solid insulation material creates localized electrical discharge. This discharge is restricted to a small part of the dielectric which partially bridges the insulation between the conductors and which may or may not occur adjacent of the conductor.

Partial discharge is in general a consequence of local electrical stress concentrations in the insulation or on the surface of the insulation. Generally such discharges appear as pulses of duration of much less than 1  $\mu$ s.

PDs are thus localized electrical discharges within any insulation system as applied in electrical apparatus, components or systems. PD is restricted to a part of the dielectric materials, which is partial bridging between the electrodes (where the voltage is applied). The insulation may consist of solid, liquid, gaseous or any combination of these materials. The term ‘partial discharge’ includes a wide group of discharge phenomena:

- (i) Internal discharges occurs in voids or cavities within solid/liquid dielectrics
- (ii) Surface discharges on the boundary of different insulation materials
- (iii) Corona discharges occurs in gaseous dielectrics in the presence of inhomogeneous fields
- (iv) Continuous impact of discharge in solid dielectric forming discharge channels (treeing).

Although the magnitude of such discharge is usually small they can cause progressive deterioration and ultimate failure, so that it is essential to detect their presence as non destructive control test.

Some dielectric such as most of gases and some fluids can withstand partial discharge for a very long time while solid insulating materials deteriorate under condition of partial discharge until sooner or later breakdown occurs.

In solid dielectrics discharges happen only in case of strong inhomogeneity, either in the material or in the electric field (sharp electrodes). Partial discharge is not located in highly stressed gas region. Anyhow, such a gas region is produced by discharge itself. The gas region can be transitory as in fluids or permanent as in solids. Figure-1.1 shows schematically three examples of such cavities in solids, each of them representing a case with typical behavior. Figure-1.1(a) indicates a void, fully surrounded by the insulating material. Figure-1.1(b) shows void adjacent to one of the electrodes and figure-1.1(c) shows a pre-breakdown channel which has grown from a highly stressed part of the dielectric at the electrode, although being very narrow and highly insulating, such a channel should also be understood as a gas filled void.

Nowadays, composite insulating materials (consisting of solid-solid, solid-liquid, or liquid-liquid gas insulants) are operated at very high stresses. Also, gaseous pockets and material insulation are introduced in system due to manufacturing difficulties and special limitation. The presence of PD in insulation systems is becoming inevitable and their study has assumed great importance. The various causes of internal discharge are discussed in the succeeding section.

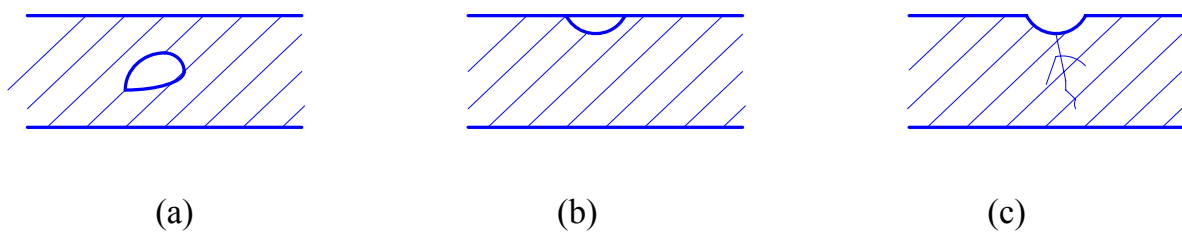


Figure-1.1 Solid insulation with gas filled void (a) void apart from electrodes, (b) void adjacent to electrode, (c) void as pre-breakdown channel (Tree)

## 1.5 CHARACTERISTICS OF PARTIAL DISCHARGE <sup>[3]</sup>

Partial discharge measurement methods have some desirable characteristics, which governs the entire test systems and its equivalent parameters. Some of them are:

- In solid dielectrics; partial discharge occurs only in the case of strong inhomogeneity in either the material (gaseous void, surface contact to gas or fluid) or in the electric field (sharp electrode). The voltage applied across the gaseous cavity, the stress in the gaseous insulation is ' $\epsilon$ ' times the stress applied voltage (where  $\epsilon$  is the relative permittivity of the solid dielectric).
- If the voltage across the gaseous insulation attains its breakdown level, it gives rise to a discharge. This discharge inception voltage depends upon the nature and geometry of cavity, the inherent nature of the solid dielectric and the nature of the voltage applied.
- If discharge persists for longer time, then the insulating materials weaken day by day.

## **1.6 CAUSES OF PARTIAL DISCHARGE IN SOLID INSULATING MATERIALS <sup>[3]</sup>**

A common cause for internal discharges is the inclusion of gas filled cavities in the solid insulation during manufacturing process. Air included in the cavity forms a low permittivity region surrounded by high permittivity region of solid insulation. When the insulation is under electrical stress, concentration of stress takes place in the region of low permittivity. If the stress in cavity increases beyond the breakdown stress of the gas it breaks down and the cavity discharges.

Discharges occur in the regions of high stresses due to intense local fields, which exceed the breakdown strength. The continued exposure of the insulation to these partial discharges can lead to progressive deterioration followed by complete electrical breakdown. Often partial discharges in voids are followed by surface discharge along interlayer spaces to perpendicular to the main field, particularly in cables and transformers leading to tracking in the insulation system. Sometimes the discharges strike the insulation at a point away from the electrode and after progressing along the surface penetrate into the insulation leading to a growth of tree like channels. Often in most cases of breakdown either by treeing or by tracking partial discharges form an integral part of the breakdown mechanism.

Besides the insulation of air filled cavities inside the insulation, there are other low permittivity areas present in the insulation medium. Imperfect impregnation would leave bubbles in the layers or defective adhesion to metal parts would have trapped air, which under breaks down.

The moisture content of oil filled insulation is also important because under stress; the heat produced may vapourise the moisture forming the air filled voids. Another common cause of discharge is the delamination of the bushing layers at edges. If the bonding is not perfect, a foil may come off lamination and provides a low permittivity region to air trap.

All these causes have been investigated for their interest in manufacturing industries and they forward different discharge behaviors, which can be observed with suitable detection circuit. Their study and observation can be used to control the different stages in process of manufacturing for optimum economy and quality.

## 1.7 VARIOUS PARAMETERS AFFECTING PD <sup>[3]</sup>

Various parameters affecting PD occurrences are described below:

### (a) Internal Discharges:

There are many variables affecting the rate of deterioration in dielectric. The deterioration increases with the number of discharges and is consequently proportional to the frequency of applied voltage and is dependent on the amplitude of this voltage. It also depends on the intensity of the discharge and the nature of the dielectric.

### (b) Frequency:

The number of discharge increases proportionally with frequency. The life of dielectric under voltage is consequently inversely proportional to frequency, unless the frequency is so high that thermal breakdown is initiated and voltage life is shorter than expected. If DC voltage is applied, the number of discharges is small; consequently the voltage life at DC voltage is many times that at AC voltage.

### (c) Stress:

The number of discharge increases with increasing stress in the dielectric. Moreover the mechanism of deterioration is affected by stress, e.g. the formation of pits the condition for the propagation of channels are reached sooner at a higher stress. Consequently, the Effect of stress upon voltage life is very large, the voltage life decreases as the 7<sup>th</sup> to 9<sup>th</sup> power of stress.

### (d) Discharge Magnitude:

The discharge magnitude increases with the depth of the cavity and its area. The voltage life is not affected by the surface of the cavity but it is affected by its

depth. Consequently the Correlation between discharge and discharge magnitude and voltage life is uncertain. Only with very large discharges the voltage life is definitely short. In that case the large discharge magnitude is certainly indicating a large cavity depth. Moreover, thermal efforts may co-operate.

(e) Cavity Depth:

Voltage life is shorter if the cavity is deeper.

(f) Thickness of Dielectric:

It is possible that the effect of insulator thickness is of minor importance. The time until treeing sets in is the same for all insulator thickness if stresses are identical. The penetration of tress leads to breakdown in a few voltage cycles and has in this way little effect on the total to breakdown.

(g) Type of Insulator:

Different types of insulator have different resistance to charges. Mica and glass are known to have good resistance to discharges. Polythene, PVC and polystyrene are less resistant, whereas rubber and tetrafluoroethylene is easily attacked by discharge.

(h) Self Extinction of Discharges:

A complication for study of voltage life is the fact that discharges in cavities and surface sometime extinguish because of semi-conducting layers formed by discharge themselves. Rogers investigated these phenomena in cavities in polythene, PVC and rubber. In nearly all cavities embedded in a dielectric, discharge are extinguished or become intermittent. If the ratio diameter to cavity depth is small the extinction tends to be more complete.

(i) Temperature:-

It is well known from various studies in the past that temperature has profound influence on partial discharges in the insulating materials. Increase in temperature results in to considerable increases in amount of partial discharges there by reducing the life of high voltage equipments. Any manufactured insulation is expected to have a life of the order of 25 to 40 years. Discharge tests for such a long period are, obviously, impossible. It is then necessary to reduce the testing time by increasing process of ageing of insulation, bearing all the whole that ageing process is an equivalent as due to discharge. One of the important accelerated life tests on the insulating material is thermal accelerated test by ageing the insulation at higher temperature than the working one.

Cavities adjacent to a conductor show pattern of behavior, which also depends upon cavity diameter. During periods of rest the original conditions are regained, after four days resting the inception voltage recovers almost to the original value. The self extinction of discharge is temporary and repeatable effect. At higher frequency (e.g. 1000 c/s) the discharges are not extinguished.

## 1.8 PD BEHAVIOR UNDER DIFFERENT VOLTAGE CONDITIONS <sup>[3]</sup>

Partial Discharge depends upon magnitude of applied voltage and its wave shape, the basic nature of the insulation, geometry of insulation etc. Thus, the mechanism of re-establishing the electric field in the cavity will be greatly influenced by the type of voltage applied. In the case of direct voltages, the potential distribution is controlled by conducting currents only, therefore a very small repetitions rate  $n$  compared to tests with alternating voltages has to be expected. In contrast to the repetitions rate, the discharge itself and therefore PD quantity related to single pulse should not be very much different between AC and DC.

Superposition of harmonics on AC voltage increases the discharge recurrence frequency in proportional to increased peak voltage. Also, when the harmonic amplitude voltage value increases beyond the inception value, the discharge may occur at all harmonic maxima and minima. In addition, the number of discharges and damage are greatly increased.

Discharge damage due to impulse voltage condition offers a simulation more correct to field condition existing. Insulation in its service time is not expected to bear a long period of over voltage but it may experience number of impulse as produced by switching surge and lightning. Naturally it seems more important that discharge be studied in detail under impulse voltage conditions. Unfortunately such a study has been limited partly due to inadequacy of problem of detection of such impulse discharge. The difficulty with impulse detection is that of the rejection of the residual test voltage from the signal due to discharges in the frequency range of 100 Mc/s.

It is likely that impulse breakdown process in slide breakdown is initiated gaseous cavities. Investigations have proved that the inception voltage for an impulse stress is much greater than that during AC 50 c/s tests. The critical field gradient, i.e. inception stress is function of electrode shape, applied voltage and any space charge present in the field. During the short time application of an impulse, space charge cannot form as readily as for 50 c/s application. It should be expected that space

charge would be more effective in the 50 c/s case and discharge inception stress is lower. Inception voltage under impulse stress differs as to whether impulse is positive or negative.

## **1.9 WORK OBJECTIVES**

The main objectives of the intended study in this are:

1. To study and investigate the long-term ageing in solid insulating material by effect of variation of parameters on Partial discharge.
2. To recognize and understand the problem areas associated with partial discharge measurement of solid insulating material.
3. To work upon, develop and present some techniques using signal processing analytical tools like Wavelet Transform, to de-noising the partial discharge signal.
4. To test the robustness of suggested techniques by extensive simulation studies.

## **Chapter-2**

# **Fundamental of Partial Discharge & Measuring Methods**

## 2.1 BASIC PD EQUIVALENT CIRCUIT <sup>[2]</sup>

For the evaluation of the fundamental quantities related to a PD pulse, simulation of the test object is carried out by the simple capacitor arrangement. Figure-2.1(a) shows solid or fluid dielectric materials between the two electrodes or terminals A and B, and a gas-filled cavity.

The electric field distribution within this test object is simulated by partial capacitance, which is possible as long as no space charges disturb this distribution. Electric field lines within the cavity are represented by  $C_c$  and those starting or ending at the cavity walls form the two capacitances  $C_b'$  and  $C_b''$  within the solid or fluid dielectric. All field lines outside the cavity are represented by  $C_a = C_a' + C_a''$ . Due to realistic geometric dimensions involved, and as  $C_b = \frac{C_b' C_b''}{(C_b' + C_b'')}$  the magnitude of the capacitances will then be controlled by the inequality

$$C_a \gg C_c \gg C_b \quad \dots (2.1)$$

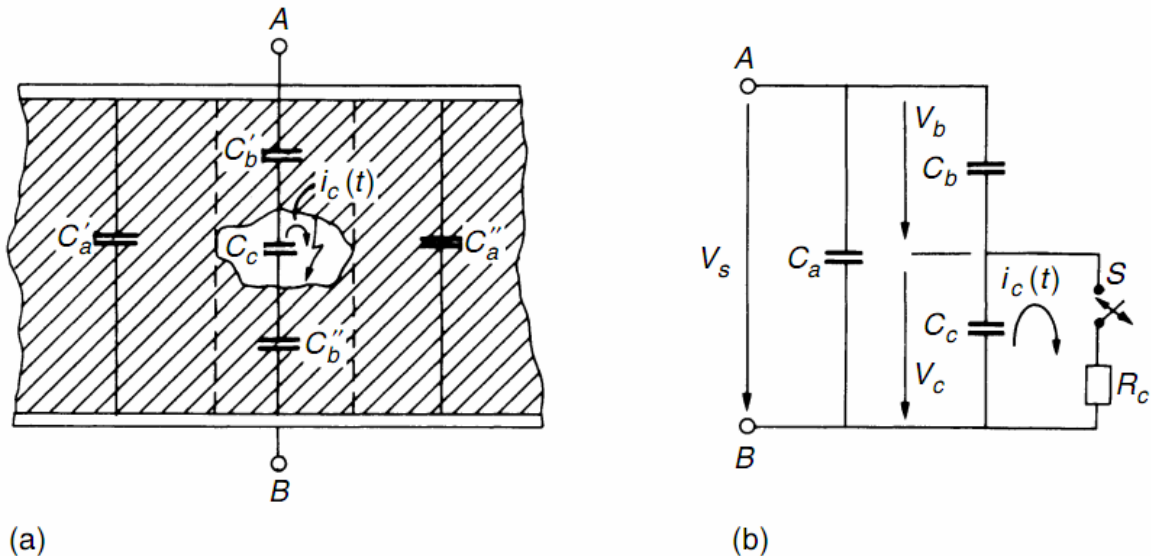


Figure-2.1 Simulation of a PD test objects (a) Scheme of an insulation system comprising a cavity. (b) Equivalent circuit

This void will become the origin of a PD if the applied voltage is increased and the field gradients in the void are strongly enhanced by the difference in permittivity as well as by the shape of the cavity. For an increased value of an A.C. voltage, the discharge will appear first at the crest or rising part of a half-cycle. This gas discharge creates electrons as well as negative and positive ions, which are driven to the surfaces of the void. It forms dipoles or additional polarization of the test object. This physical effect reduces the voltage across the void significantly. Within the model these effect causes the cavity capacitance  $C_c$  to discharge largely. If the voltage still increase or decrease by the negative slope of an A.C. voltage, new field lines are built up and hence the discharge phenomena is repeated during each cycle. If increased D.C. voltages are applied then one or only a few partial discharges will occur during the rising part of the voltage. In case of constant voltage, the discharges will stop as long as the surface charges deposited on the walls of the void do not recombine or diffuse into the surrounding dielectric.

This phenomenon is simulated by the equivalent circuit that is shown in Figure-2.1(b). Here, the switch  $S$  is controlled by the voltage  $V_c$  across the void capacitance  $C_c$ , and  $S$  is closed only for a short time, during which the flow of a current  $i_c(t)$  takes place. The discharge current  $i_c(t)$ , which cannot be measured, would have a shape as governed by the gas discharge process and would in general be similar to a Dirac function, i.e. this discharge current is generally of a very short pulse in the nanosecond range.

It is assumed that the sample was charged to the voltage  $V_a$  but the terminals A and B are no longer connected to a voltage source. If the switch  $S$  is closed and  $C_c$  becomes completely discharged then the current  $i_c(t)$  releases a charge  $\delta_{qc} = C_c \delta V_c$  from  $C_c$ , a charge which is lost in the whole system, assumed for simulation. By comparing the charges within the system pre and post discharge, it is derived that the voltage drop across the terminal is

$$\delta V_a = \{C_b / (C_a + C_b)\} \times \delta V_c \quad \dots(2.2)$$

This voltage drop contains no information about the charge  $\delta q_c$ , but it is proportional to  $C_b \delta V_c$ , a magnitude related to this charge, where  $C_b$  increases with the geometric dimensions of the cavity.

$\delta V_a$  is clearly a quantity that could be measured. It is a negative voltage step with a rise time depending upon the duration of  $i_c(t)$ . The magnitude of the voltage step is quite small and although  $\delta V_c$  is in a range of  $10^2$  to  $10^3$  V; but the ratio  $C_b/C_a$  will always be very small according to Eq.2.1. Thus, a direct detection of this voltage by the measurement input voltage would be a tedious task. The detection circuits are based upon another quantity, which can immediately be derived from a nearly complete circuit shown in Figure-2.2.

The test object (Figure-2.1.a) is now connected to an A.C. voltage source  $V$ . An impedance  $Z$ , either comprises only the natural impedance of the lead between voltage source and the parallel arrangement of  $C_k$  and  $C_t$  or enlarged by a PD-free inductance or filter. It may disconnect the ‘coupling capacitor’  $C_k$  and the test specimen  $C_t$  from the voltage source during the short duration PD phenomena and  $C_k$  is a storage capacitor or quite a stable voltage source during the short period of the partial discharge.

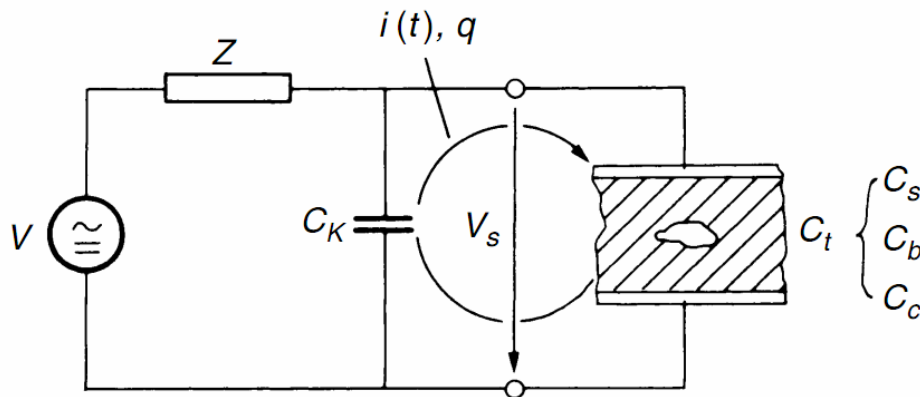


Figure-2.2 The PD test object  $C_t$  within a PD test circuit

It releases a charging current or the actual 'PD current pulse',  $i(t)$  between  $C_k$  and  $C_t$  and tries to cancel the voltage drop  $\delta V_a$  across  $C_t \approx (C_a + C_b)$ . If  $C_k \gg C_t$ , then  $\delta V_a$  is completely compensated and the charge transfer provided by the current pulse  $i(t)$  is given by

$$q = \int i(t) = (C_a + C_b) \delta V_a \quad \dots(2.3)$$

Therefore,

$$q = C_b \delta V_c \quad \dots(2.4)$$

Hence, it is referred as the apparent charge of a PD pulse, which is the most fundamental quantity of all PD measurements. The word 'apparent' was introduced because this charge again is not equal to the amount of charge locally involved at the site of the discharge or cavity  $C_c$ . This PD quantity is much more realistic than  $\delta V_a$  in Eq-2.2, as the capacitance  $C_a$  of the test object, which is its main part of  $C_t$ , has no influence on it.

In practice, the condition  $C_k \gg C_a (=C_t)$  is not always applicable. Here, either  $C_t$  is quite large or the loading of an A.C. power supply becomes high and the cost of building such a large capacitor without PD is not economical. For a finite value of  $C_k$ , the charge  $q$  or the current  $i(t)$  is reduced, as the voltage across  $C_k$  will also drop during the charge transfer. Designating this voltage drop by  $\delta V_a^*$ , can be computed by assuming that the same charge  $C_b \delta V_c$  has to be transferred in the circuits of Figure-2.1(b) and figure-2.2 Therefore,

$$\delta V_a (C_a + C_b) = \delta V^* (C_a + C_b + C_k) \quad \dots(2.5)$$

Using equation (2.2) and (2.4), it is obtained as

$$\delta V^* = \frac{Cb}{C_a + C_b + C_k} \delta V_c = \frac{q}{C_a + C_b + C_k} \quad \dots(2.6)$$

Again,  $\delta V^*$  is a difficult quantity to be measured. The charge transferred from  $C_k$  to  $C_t$  by the reduced current  $i(t)$  is equal to  $C_k \delta V^*$ . However, it is related to the real value of the apparent charge  $q$ , which can be measured by an integration procedure and referred as  $q_m$  (measured quantity), then

$$q_m = C_k \delta V^* = \frac{C_k}{C_a + C_b + C_k} q \approx \frac{C_k}{C_a + C_k} q$$

$$\frac{q_m}{q} \cong \frac{C_k}{C_a + C_k} \approx \frac{C_k}{C_t + C_k} \quad \dots(2.7)$$

The relationship  $q_m/q$  indicates the difficulties arising in PD measurements for test objects of large capacitance values  $C_t$ . Although  $C_k$  and  $C_t$  may be known, the ability to detect small values of  $q$  will decrease as all instruments capable of integrating the currents  $i(t)$  will have a lower limit for quantifying  $q_m$ . Eq-2.7, therefore sets limits for the recording of ‘pico-coulombs’ in large test objects. During actual measurements, a calibration procedure is needed where artificial apparent charge  $q$  of well-known magnitude is injected to the test object.

## 2.2 THE RECURRENCE OF DISCHARGE (DISCHARGE SEQUENCE) [2,3]

In practice, a cavity in a material is often nearly spherical, and for such cases the internal field strength is

$$E_c = \frac{3\varepsilon_r E}{\varepsilon_{rc} + 2\varepsilon_r} = \frac{3E}{2} \quad \dots(2.8)$$

For,  $\varepsilon_r \gg \varepsilon_{rc}$ .

Here,  $E$  is in the average stress in the dielectric under an applied voltage  $V_a$ . During the operation when  $V_c$  reaches breakdown value  $V^+$  of the gap  $t$  then the cavity may break down. The sequence of breakdown under sinusoidal alternating voltage is illustrated in Figure-2.3. The dotted curve shows the voltage which would appear across the cavity if it does not break down. As  $V_c$  reaches the value  $V^+$ , a discharge takes place, the voltage  $V_c$  collapses and the gap extinguishes. The voltage across the cavity then starts increasing again until it reaches  $V^+$  when a new discharge occurs. Thus, several discharges may take place during the rising part of the applied voltage. Similarly, on decreasing the applied voltage, the cavity discharges as the voltage across it reaches  $V^-$ . In this way, groups of discharges originate from a single cavity and give rise to positive and negative current pulses on increasing and decreasing of the voltage respectively.

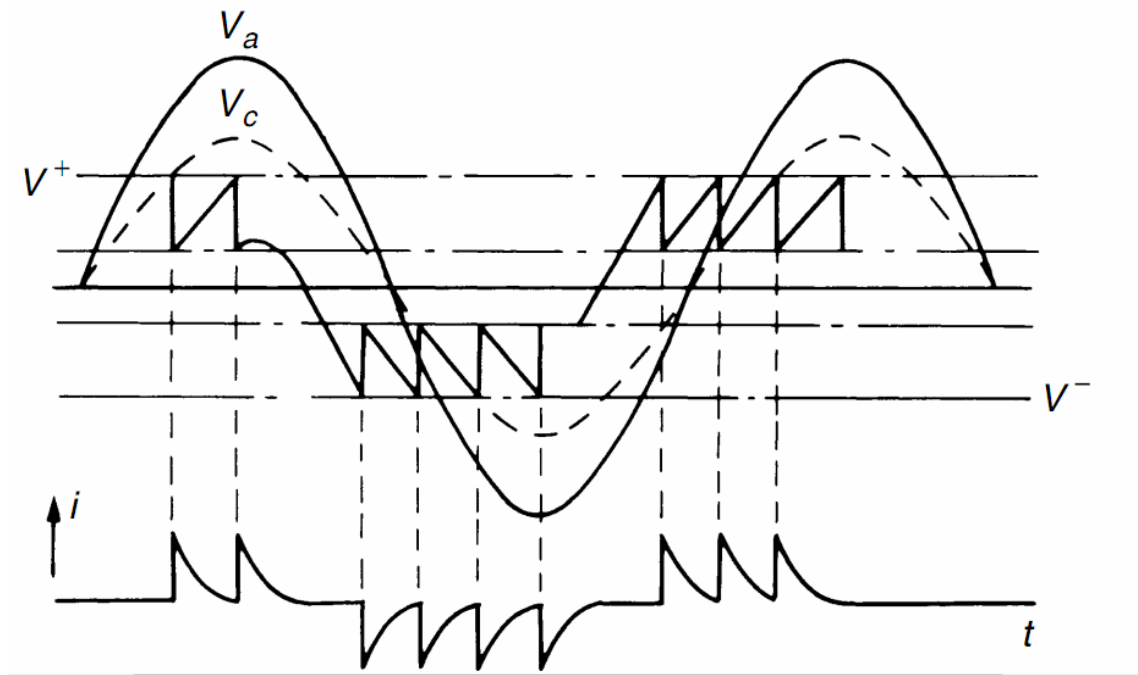


Figure-2.3 Sequence of cavity breakdown under alternating voltages

When the gas in the cavity breaks down, the surface of the insulation, provide instantaneous cathode and anode. Some of the electrons impinge upon the anode are sufficiently energetic to break the chemical bonds of the insulation surface. Similarly, bombardment of the cathode by positive ions may cause damage by increasing the surface temperature and produce local thermal instability. In addition, channels and pits are formed which elongate the insulation by the 'edge mechanism'. Additional chemical degradation may result from active discharge products, and hence the net effect is a slow erosion of the material and a consequent reduction of the breakdown strength of the solid insulation. When the discharge occurs on the insulation surface, the erosion takes place initially over a comparatively large area. The erosion roughens the surface and slowly penetrates the insulation and later on it will increase channel propagation and 'tree-like' growth through the insulation is formed.

For practical application, it is important that the dielectric strength of a system does not deteriorate significantly over a long period of time (years). In practice, however,

because of imperfect manufacturing and/or poor design, the dielectric strength decreases with the time of voltage application (or the life). In many cases, the decrease in dielectric strength ( $E_b$ ) with time ( $t$ ) follows the empirical relationship.

$$tE_b^n = \text{const} \quad \dots(2.9)$$

Where the exponent 'n' is derived from the dielectric material, ambient conditions and the quality of manufacturing.

### 2.3 PD CURRENTS [2]

Before discussing the fundamentals of the measurement of the apparent charge, some remarks concerning the PD currents  $i(t)$  will be helpful, as much of the research work has been still devoted to these currents, which are difficult to measure with high accuracy. The difficulties arise for several reasons.

If  $V$  is an A.C. voltage, the main contribution of the currents flowing within the branches  $C_k$  and  $C_t$  of Figure-2.4 are displacement currents  $C(dV/dt)$ , and both are nearly in phase. If no stray capacitance is in parallel to  $C_k$  were present,  $i(t)$  would be the same in both branches with opposite polarity. For accurate measurements, a shunt resistor with matched coaxial cable may be introduced in the circuit as shown in figure-2.4.

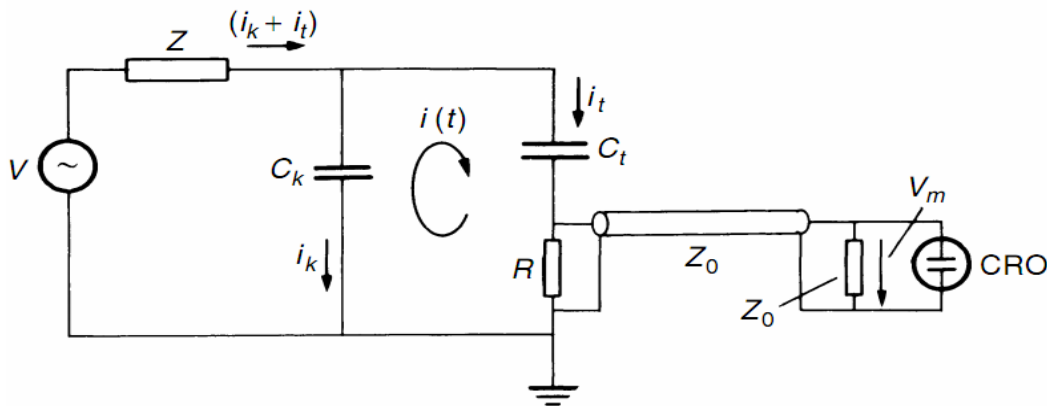


Figure-2.4 Measurement of PD current  $i(t)$  – low sensitivity circuit

The voltage across the CRO input (or transient recorder) is given by,

$$V_m(t) = \frac{(i_r + i)Z_0 R}{(R + Z_0)} \quad \dots(2.10)$$

The test object having small capacitance then the voltages referring to the PD currents  $i(t)$  will be clearly distinguished from the displacement currents  $i_t(t)$ .

Improvements are possible by inserting an amplifier (e.g. active voltage probe) of very high bandwidth at the input end of the signal cable. In this way, the signal cable is electrically disconnected from R. High values of R will introduce measuring errors, which are explained with Figure-2.5. A capacitance C of some 10 pF, which accounts for the lead between  $C_t$  and earth as well as for the input capacitance of the amplifier or other stray capacitances, will shunt the resistance R and thus bypass or delay the very high-frequency components of the current  $i(t)$ . Thus, if  $i(t)$  is a very short current pulse, its shape and crest value are heavily distorted, as C will act as an integrator. Furthermore, with R within the discharge circuit, the current pulse will be lengthened, as the charge transfer even with  $C=0$  will be delayed by a time constant  $RC_tC_k/(C_t + C_k)$ . Both effects are influencing the shape of the original current pulse, and thus the measurement of  $i(t)$  is a complicated task and can be accomplished in future work.

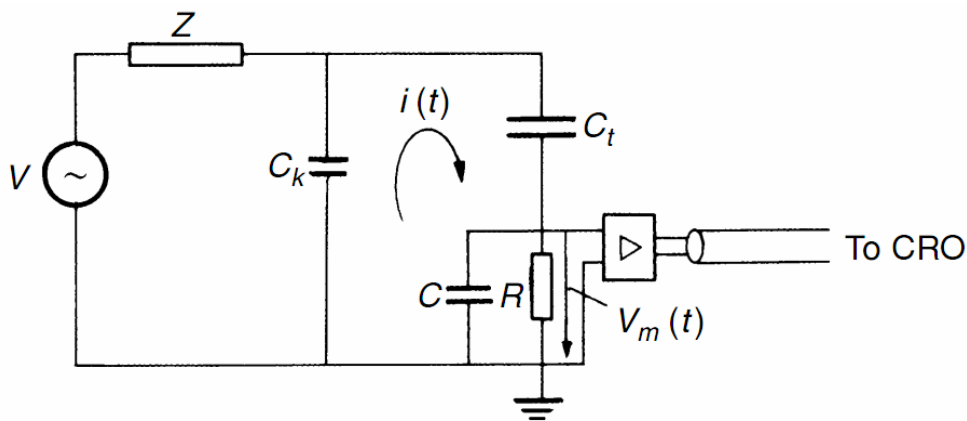


Figure-2.5 Measurement of PD current – high sensitivity circuit

All measured data on current shapes (which is published in many papers) are suffering from this effect. However, the results can be summarized by the following statements. Partial discharge currents originated in voids within solids or liquids are

very short current pulses of less than a few nanoseconds duration. This can be understood, as the gas discharge process within a very limited space is developed in a very short time and is terminated by the limited space for movement of the charge carriers. Discharges within a homogeneous dielectric material, i.e. a gas, produce PD currents with a very short rise time ( $\leq 5$  ns) and a longer tail. Whereas the fast current rise is produced by the fast avalanche processes, the decay of the current can be attributed to the drift velocity of attached electrons and positive ions within the dielectric.

Discharge pulses in atmospheric air provide in general current pulses of less than about 100 nsec duration. Longer current pulses have only been measured for partial discharges in fluids or solid materials without pronounced voids, if a number of consecutive discharges take place within a short time. In most of these cases, the total duration of  $i(t)$  is less than about 1  $\mu$ sec, with only some exceptions e.g. the usual bursts of discharges in insulating fluids.

All these statements refer to test circuits with very low inductance and proper damping effects within the loop  $C_k - C_t$ . However, The current  $i(t)$  may oscillate and oscillations are readily excited by the sudden voltage drop across  $C_t$ . Test objects with inherent inductivity or internal resonant circuits, e.g. transformer or reactor/generator windings, will always cause oscillatory PD current pulses. Such distortions of the PD currents, however, do not change the transferred charge magnitudes, as no discharge resistor is in parallel to  $C_k$  or  $C_t$ . If the displacement currents  $i_t(t)$  or  $i_k(t)$  are suppressed, the distorted PD currents can also be filtered, integrated and displayed.

## 2.4 VARIOUS PD QUANTITIES<sup>[2,3]</sup>

Partial discharge in any test object under given condition may be characterized by different measurable quantities like charge, repetition rate or integrated quantities etc.

Apparent Charge (q):

The apparent charge  $q$  of a partial discharge is that charge which if injected instantaneously between the terminals of the test object, would momentarily change the voltage between its terminals by the same amount as the partial discharge itself and is expressed in pico coulombs. Final note is made with reference to the definition of the apparent charge  $q$  (as given in the new IEC Standard 60270) is not equal to the amount of charge locally involved at the site of the discharge and which cannot be measured directly.

Repetition Rate (n):

It is the average number of partial discharge pulses per second measured over a selected time. In practice, only pulses above a specified magnitude or within a specified range of magnitudes may be considered.

Specified PD Magnitude:

It is the value the PD quantity stated in standards for the given test object at a specified voltage.

Partial Discharge Inception Voltage ( $V_i$ ):

It is the lowest voltage at which PDs are observed in test arrangement, (in practice, lowest value at which PD' magnitude becomes equal to or exceeds a specified low value) when the voltage applied, to the object is gradually increased from a lower value at which no such discharges are observed,'

Partial Discharge Extinction Voltage ( $V_e$ ):

It is the lowest voltage at which no PDs are observed in the test arrangement, (in practice, reduced below a specified value) when the voltage applied to the object is gradually decreased from a higher value at which such discharges are observed.

Partial Discharge Test Voltage:

PD test voltage is a specified voltage, applied in a specified test procedure, during which the test object should not exhibit partial discharges exceeding a specified magnitude.

The Average Discharge Current (I):

It is the sum of the absolute values of the apparent charges during a certain time interval divided by this time interval.

$$I = \frac{1}{T_{ref}} (|q_1| + |q_2| + \dots + |q_i|) \quad \dots(2.12)$$

The Quadratic Rate D:

It is the sum of the squares of the apparent charges during a certain time interval divided by this time interval.

$$D = 1/T_{ref} (q_1^2 + q_2^2 + \dots + q_i^2) \quad \dots(2.13)$$

The Discharge Power p:

It is the average power fed into the terminals of the test object due to partial discharges.

$$D = 1/T_{ref} (q_1 u_1 + q_2 u_2 + \dots + q_i u_i) \quad \dots(2.14)$$

Where  $u_1, u_2, \dots, u_n$  are instantaneous values of the test voltage at the instants of occurrence  $t_i$  of the individual apparent charge magnitudes  $q_i$ .

Additional quantities related to PD pulses, although already mentioned in earlier standards, will be used extensively in the future and thus their definitions are given below with brief comments only:

(a) The phase angle  $\Phi_i$  and time  $t_i$  is the occurrence of a PD pulse is

$$\phi_i = 360 \left( \frac{t_i}{T} \right) \quad \dots(2.15)$$

Where  $t_i$  is the time measured between the preceding positive going transition of the test voltage through zero and the PD pulse. Here  $T$  is the period of the test voltage.

## 2.5 VARIOUS PD MEASUREMENT METHODS <sup>[2,3]</sup>

The detection and measurement of discharges is based on the exchange of energy transform during the discharge. These exchanges include:

- Electrical pulse currents (with some exceptions, i.e. some types of glow discharges)
- Dielectric losses
- Electromagnetic radiation (light)
- Sound (noise)
- Increased gas pressure
- Chemical reactions

Therefore, discharge detection and measuring techniques may be based on the observation of any of the above phenomena.

Non-electrical methods of partial discharge detection include acoustical, optical and chemical methods and also the subsequent observation of the effects of any discharges on the test object. In general, these methods are not suitable for quantitative measurement of partial discharge quantities as defined in the standard by electrical measurement methods, but they are essentially used to detect and/or to locate the discharges.

Acoustic Detection:

Aural observations made in a room with low noise level may be used as a means of detecting partial discharges.

### Visual or Optical Detection:

Visual observations can be carried out in a darkened room, after the eyes have become adapted to the dark and, if necessary, with the aid of binoculars of large aperture.

### Chemical Detection:

The presence of partial discharges in oil or gas insulated apparatus may be detected in some cases by the analysis of the decomposition products dissolved in the oil or in the gas. These products accumulate during prolonged operation, so chemical analysis may be applicable to estimate the degradation, which has been caused by partial discharges.

The oldest and simplest method relies on listening to the acoustic noise from the discharge, the 'hissing test'. This scheme has lower sensitivity and difficulties arise in distinguishing between discharges and extraneous noise sources, particularly when tests are carried out on factory premises. The use of optical techniques is limited to discharges within transparent media and thus not applicable in most of the cases. Latest acoustical detection methods utilize ultrasonic transducers, which can be used to localize the discharges.

The most frequently used and successful detection methods are the electrical ones where new IEC Standard is also related. These methods are aimed to separate the impulse currents linked with partial discharges from any other phenomena. The adequate applications of PD detectors are well defined and presume a fundamental knowledge of the electrical phenomena within the test samples and the test circuits. Electrical PD detection methods are based on the appearance of a 'PD pulse' at the terminals of a test object, which may be either a simple dielectric test specimen for fundamental investigations or even a large HV apparatus which has to undergo a PD test.

## 2.6 PD MEASURING SYSTEM WITHIN THE PD TEST CIRCUIT<sup>[2]</sup>

In above sections the evolution of the PD current pulses and measurement procedures of these pulses have been broadly discussed. To quantify the individual apparent charge magnitudes  $q_i$  for the repeatedly occurring PD pulses; (which may have quite specific statistical distributions) a measuring system must be integrated into the test circuit. Already at this point, it shall be mentioned that under practical environment conditions, quite different kinds of disturbances (background noise) are present, which will be summarized in later section.

Most PD measuring systems applied are integrated into the test circuit in accordance with schemes shown in Figure-2.6(a) and Figure-2.6(b), which are taken from the new IEC Standard. Within these ‘straight detection circuits’, the coupling device ‘CD’ with its input impedance ‘ $Z_{mi}$ ’ forms the input end of the measuring system.

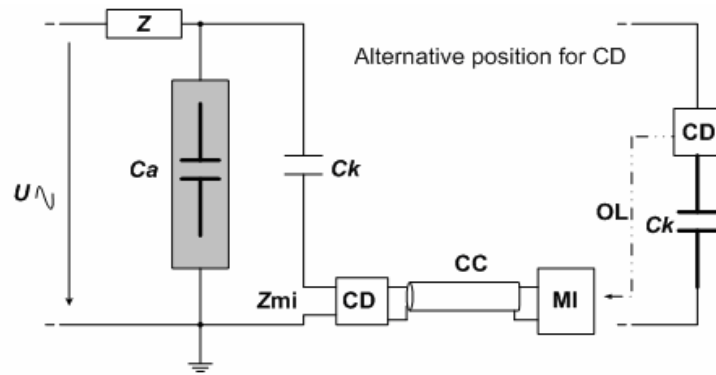
As indicated in Figure-2.6(a), this device may also be placed at the high-voltage terminal side, provided if the test object has one terminal earthed. Optical links are then used to connect the CD with an instrument instead of a connecting cable ‘CC’. Some essential requirements and explanations with reference to these figures as indicated by the standard are cited here:

The coupling capacitor  $C_k$  shall be of low inductance design and should exhibit a sufficiently low level of partial discharges at the specified test voltage to allow the measurement of the specified partial discharge magnitude. A higher level of partial discharges can be tolerated if the measuring system is capable of separating the discharges from the test object and the coupling capacitor and measuring them separately.

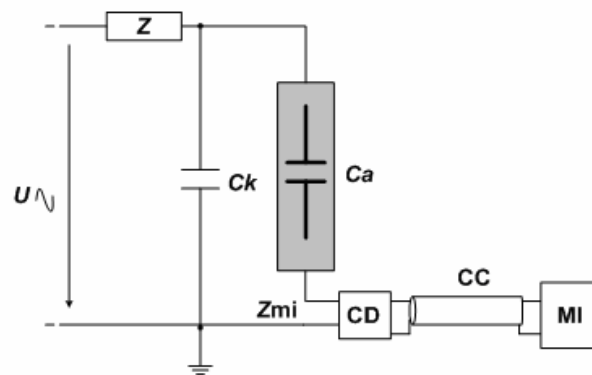
The high voltage supply shall have sufficiently low level of background noise to allow the specified partial discharge magnitude to be measured at the specified test

voltage. Impedance of a filter may be introduced at high voltage to reduce background noise from the power supply.

The main difference between these two types of PD detection circuits is related to the way the measuring system is inserted into the circuit. Figure-2.6(a) shows the CD is at ground potential and in series to the coupling capacitor  $C_k$  as it is usually done in praxis. Figure-2.6(b) shows CD is in series with the test object  $C_a$ .



(a) Coupling device CD in series with the coupling capacitor



(b) Coupling device CD in series with the test object

Figure-2.6 Basic Partial Discharge Detection Test Circuit – Straight Detection

Figure-2.6 refers following notations:

$U_{\sim}$  = High voltage supply

$Z_{mi}$  = Input impedance of measuring system

CC = connecting cable

OL = optical link

C<sub>a</sub> = test object

C<sub>k</sub> = coupling capacitor

CD = coupling device

MI = measuring instrument

Here, the stray capacitances of all elements of the high-voltage side to ground potential will increase the value of C<sub>k</sub> providing a somewhat higher sensitivity for this circuit according to equation-2.7. The disadvantage is the possibility of damage to the PD measuring system, if the test object fails. The transfer impedance Z(f) is the ratio of the output voltage amplitude to a constant input current amplitude, as a function of frequency f, when the input is sinusoidal. This definition is due to the fact that any kind of output signal of a measuring instrument (MI) as used for monitoring PD signals is controlled by a voltage, whereas the input at the CD is a current.

The lower and upper limit frequencies f<sub>1</sub> and f<sub>2</sub> are the frequencies at which the transfer impedance Z(f) has fallen by 6 dB from the peak pass band value. Mid-band frequency f<sub>m</sub> and bandwidth Δf for all kinds of measuring systems, the mid-band frequency is defined by,

$$f_m = \frac{(f_1 + f_2)}{2} \quad \dots(2.16)$$

and the bandwidth by,

$$\Delta f = f_2 - f_1 \quad \dots(2.17)$$

The superposition error is caused by the overlapping of transient output pulse responses when the time interval between input current pulses is less than the duration

of a single output response pulse. Superposition errors may be additive or subtractive depending on the pulse repetition rate ‘n’ of the input pulses. In practical circuits, both types will occur due to the random nature of the pulse repetition rate. This rate ‘n’ is defined as the ratio of total number of PD pulses recorded in a selected time interval to the duration of the time interval.

The pulse resolution time  $T_r$  is the shortest time interval between two consecutive input pulses of very short duration, of same shape, polarity and charge magnitude for which the peak value of the resulting response will change by not more than 10 per cent of that for a single pulse. The pulse resolution time is in general inversely proportional to the bandwidth  $\Delta f$  of the measuring system. It is an indication of the measuring system’s ability to resolve successive PD events.

Figure-2.7 shows correct relationship between amplitude and frequency to minimize integration errors for a wide-band system. The integration error is the error in apparent charge measurement, which occurs when the upper frequency limit of the PD current pulse amplitude spectrum is lower than (i) the upper cut-off frequency of a wideband measuring system or (ii) the mid-band frequency of a narrow-band measuring system.

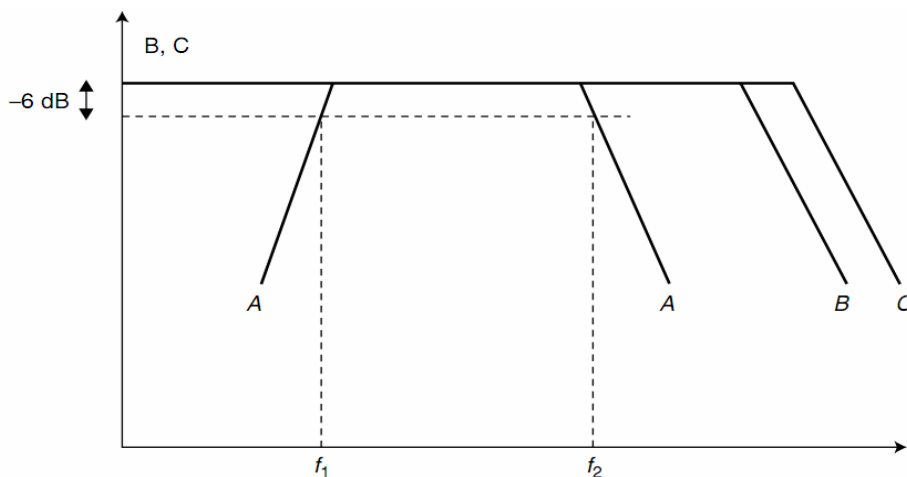


Figure-2.7 Correct Relationship Between Amplitude and Frequency to Minimize Integration Errors for a Wide-band System

As shown in figure-2.7,

A is a band-pass of the measuring system

B is an amplitude frequency spectrum of the PD pulse

C is an amplitude frequency spectrum of calibration pulse

$f_1$  is lower limit frequency

$f_2$  is upper limit frequency

PD measuring systems quantifying apparent charge magnitudes are band-pass systems, which predominantly are able to suppress the high power frequency displacement currents including higher harmonics.

The lower frequency limit of the band-pass  $f_1$  and the kind of 'roll-off' of the bandpass control this ability. Adequate integration can thus only be made if the 'pass-band' of the filter is still within the constant part of the amplitude frequency spectrum of the PD pulse to be measured. Next topic discusses basic types of PD instruments to measure PD.

### **MEASURING SYSTEM FOR APPARENT CHARGE**

The following type of measuring system comprises subsystems like, coupling device (CD), transmission system or connecting cable (CC), and a measuring instrument (MI) as seen in figure-2.6. In general the transmission system, necessary to transmit the output signal of the CD to the input of the MI, does not contribute to the measuring system characteristics as both ends are matched to the characteristics of both elements. The CC will thus not be considered further.

The input impedance  $Z_{mi}$  of the CD or measuring system respectively will have some influence on the waveshape of the PD current pulse  $i(t)$ , which is already mentioned in the figure-2.5 description. The high input impedance will delay the charge transfer between  $C_a$  and  $C_k$  to such an extent that the upper limit frequency of the amplitude frequency spectrum would drop to unacceptable low values. Often, values of  $Z_{mi}$  are in the range of 100  $\Omega$ . In common with the first two measuring systems for apparent charge is a newly defined ‘pulse train response’ of the instruments to quantify the ‘largest repeatedly occurring PD magnitude’, which is taken as a measure of the ‘specified partial discharge magnitude’, permitted in test objects during acceptance tests under specified test conditions.

Sequences of partial discharges follow in general unknown statistical distributions and it would be useless to quantify only one or very few discharges of large magnitude within a large array of much smaller events as a specified PD magnitude. For further information on quantitative requirements about this pulse train response, which was not specified up to now and thus may not be found within in earlier instruments.

### **WIDE BAND PD INSTRUMENTS**

Up to 1999, no specifications or recommendations concerning to permitted response parameters have been available. Now, the following parameters are recommended. In combination with the CD, wide-band PD measuring systems, which are characterized by a transfer impedance  $Z(f)$  having fixed values of the lower and upper limit frequencies  $f_1$  and  $f_2$ , and adequate attenuation below  $f_1$  and above  $f_2$ , shall be designed to have the following values for  $f_1$ ,  $f_2$  and  $\Delta f$ :

$$30 \text{ kHz} \leq f_1 \leq 100 \text{ kHz};$$

$$f_2 \leq 500 \text{ kHz};$$

$$100 \text{ kHz} \leq \Delta f \leq 400 \text{ kHz};$$

The response of these instruments to a (non-oscillating) PD current pulse is in general a well-damped oscillation as shown below. Both the apparent charge  $q$  and with some reservation the polarity of the PD current pulse can be determined from this response. The pulse resolution time  $T_r$  is small and is typically 5–20  $\mu\text{s}$ .

Figure-2.8 shows the typical principle of such a system and Figure-2.8(a) shows simplified equivalent circuit for the CD and amplifier whereas Figure-2.8(b) shows typical time-dependent quantities within (a) ( $T$  = period of power frequency;  $\tau$  = pulse resolution time  $T_r$ )

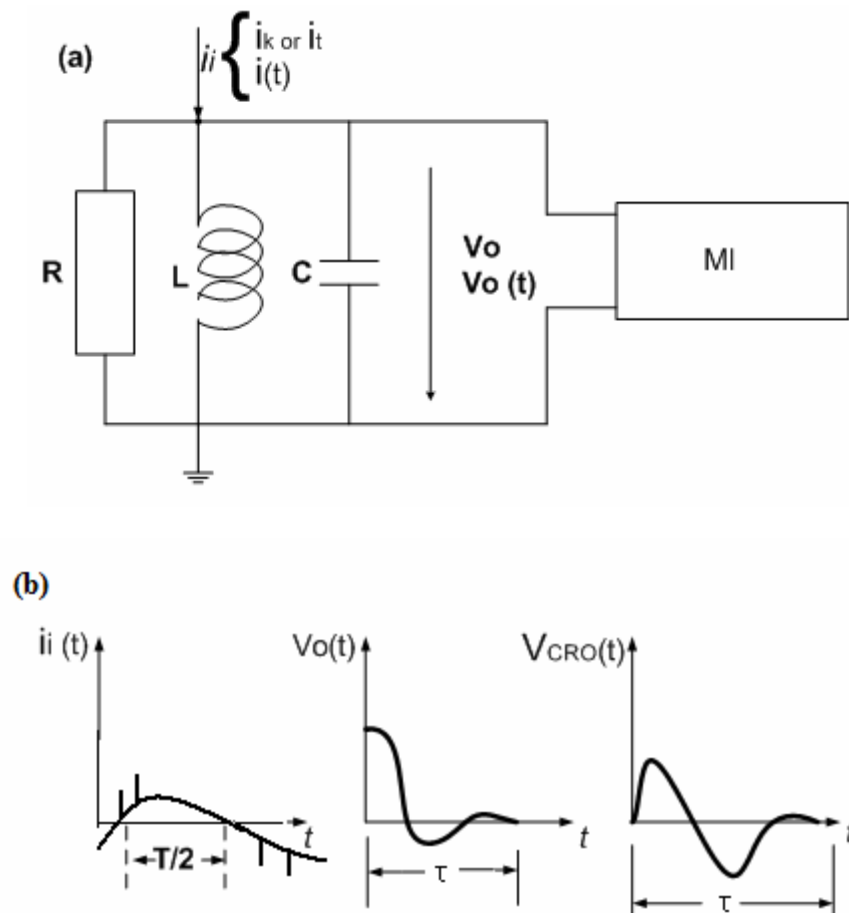


Figure-2.8 Principle of 'Wide-band' PD Measuring System

The coupling devices CD (Figure-2.6) are passive high-pass systems but behave more often as a parallel R-L-C resonance circuit (Figure-2.8(a)) whose quality factor is relatively low. Such coupling impedance provides two important qualities.

At first, a simple calculation, which is the ratio of output voltage  $V_0$  to input current  $I_i$  in dependency of frequency (= transfer impedance  $Z(f)$ ) would readily demonstrate an adequate suppression of low and high frequency currents in the neighborhood of its resonance frequency. For a quality factor of  $Q = 1$ , this attenuation is already  $-20\text{dB/decade}$  and could be greatly increased close to resonance frequency by increasing the values of  $Q$ . Secondly, this parallel circuit also performs an integration of the PD currents  $i(t)$ , as this circuit is already a simple band-pass filter and can be used as an integrating device.

Let us assume that the PD current pulse  $i(t)$  will not be influenced by the test circuit and would be of an extremely short duration pulse, simulated by a Dirac function comprising the apparent charge  $q$ . Then the calculation of the output voltage  $V_0(t)$  according to Figure-2.8(a) results in:

$$V_0(t) = \frac{q}{C} e^{-\alpha t} \left[ \cos \beta t - \frac{\alpha}{\beta} \sin \beta t \right] \quad \dots(2.18)$$

Where,

$$\alpha = \frac{1}{2RC}; \quad \beta = \sqrt{\frac{1}{LC} - \alpha^2} = \omega_0 \sqrt{1 - \alpha^2 LC} \quad \dots(2.19)$$

This equation displays a damped oscillatory output voltage, whose amplitudes are proportional to  $q$ . The integration of  $i(t)$  is thus performed instantaneously ( $t=0$ ) by the capacitance  $C$ , but the oscillations, if not damped, would heavily increase the ‘pulse resolution time  $T_r$ ’ of the measuring circuit and cause ‘superposition errors’ for too short time intervals between consecutive PD events.

With a quality factor of  $Q = 1$ , i.e.  $R = \sqrt{L/C}$ , a very efficient damping can be achieved, since  $\alpha = \omega_{0/2} = \pi f_0$  for a resonance frequency  $f_0$  of typically 100 kHz, and an approximate resolution time of  $T_r \cong t = 3/\alpha$ , this time becomes about 10  $\mu\text{sec}$ .

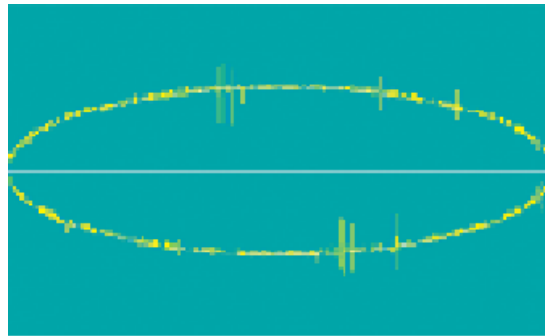
For higher  $Q$  values,  $T_r$  will be longer, but also the filter efficiency will increase and therefore a compromise is necessary. The resonance frequency  $f_0$  is also influenced by the main test circuit elements  $C_k$  and  $C_a$ , as their series connection contributes to  $C$ . Therefore the 'RLC input units' must be changed according to specimen capacitance to achieve a bandwidth or resonance frequency  $f_0$  within certain limits. These limits are postulated by the bandwidth  $\Delta f$  of the additional band-pass amplifier connected to this resonant circuit to increase the sensitivity and thus to provide again an integration.

These amplifiers are typically designed for lower and upper limit frequencies of some 10 kHz and some 100 kHz respectively, and sometimes the lower limit frequency range may also be switched from some 10 kHz up to about 150 kHz to further suppress power frequencies. In general the fixed limit frequencies are thus within a frequency band and are not used by radio stations and higher than the harmonics of the power supply voltages.

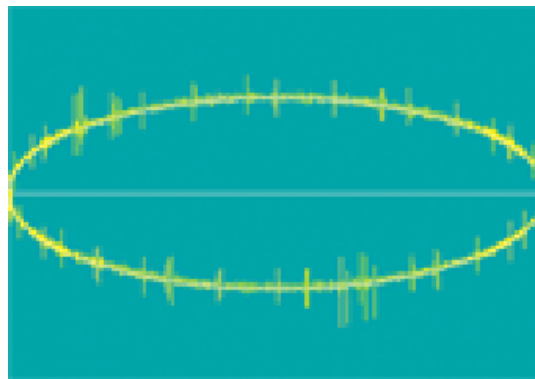
The band-pass amplifier has in general variable amplification to feed the 'CRO' (reading device) following the amplifier with adequate magnitudes during calibration and measurement. Figure-2.8(b) shows the time-dependent quantities (input a.c. current with superimposed PD signals, voltages before and after amplification).

Figure-2.9 shows the amplified discharge pulses are in general displayed by an (analogue or digital) oscilloscope superimposed on a power frequency elliptic time base. The magnitude of the individual PD pulses is then quantified by comparing the pulse crest values with those produced during a calibration procedure. With this type of reading by individual persons it is not possible to quantify the standardized 'pulse

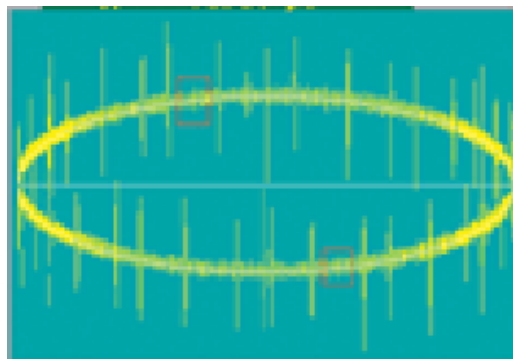
train response' which quantifies the 'largest repeatedly occurring PD magnitude'. Correct readings are, however, possible by applying additional analogue peak detection circuits or digital peak detection software prepared to follow the specified pulse train response. The pattern on the CRO display can often be used to recognize the origin of the PD sources. (Instead of a simple CRO display digital acquisition of PD quantities and up-to-date methods for evaluation are used now).



(a) Point plane ('Trichel pulses')



(b) Void discharges at inception



(c) Void discharges at twice inception voltage

Figure-2.9 Elliptical Display

A typical pattern of Trichel pulses can be seen in figure-2.9(a). Figure-2.9(b), is typical for the case for which the pulse resolution time of the measuring system including the test circuit, which is too large to distinguish between individual PD pulses.

It was clearly shown that even the response of such ‘wide-band PD instruments’ provide no more information about the original shape of the input PD current pulse as indicated in figure-2.8(b) and confirmed by the pattern of the Trichel pulses in figure-2.9(a). Figure-2.10 further confirms this statement. Figure-2.10 shows two recorded responses for two consecutive calibration pulses (‘double pulse’) are shown within a time scale of microseconds.

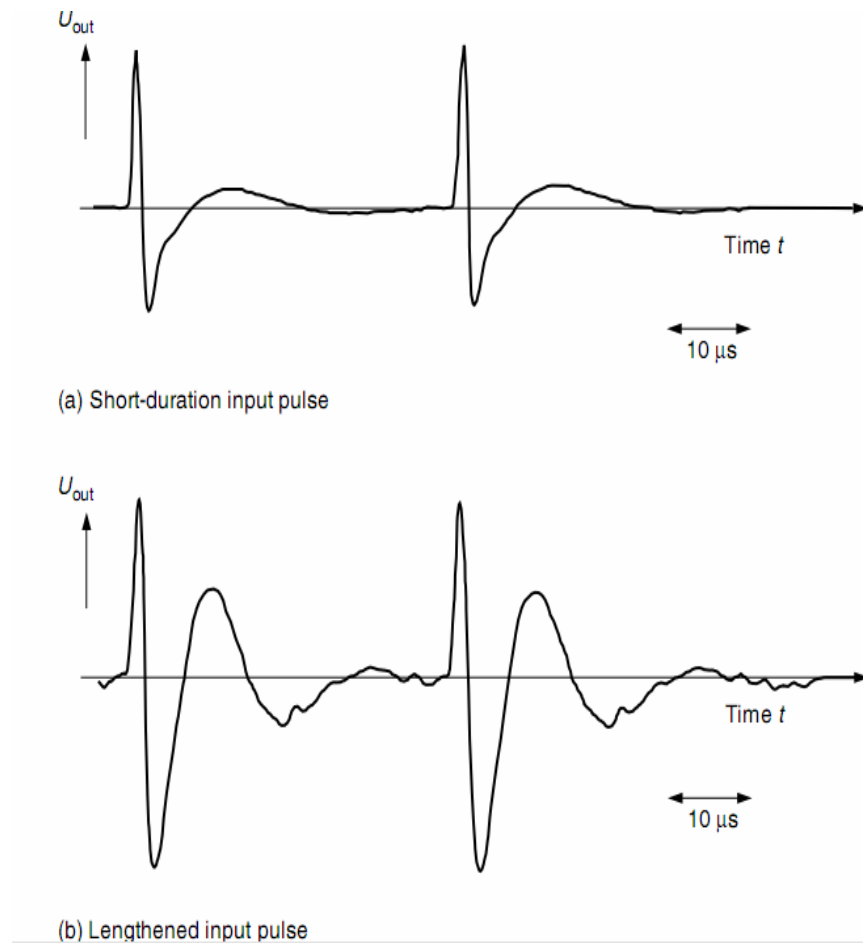


Figure-2.10 Output Voltage Signals  $U_{out}$  of a Wide-band PD Detector with  $\Delta f = 45$  to  $440$  kHz for Two Different Input Pulses

A comparison of both recorded responses shows their differences with respect to a (positive) short and lengthened input pulse, which has some significant influence on the peak value of the undershoot after the first excursion of the response which indicates the polarity of the input signal. Polarity detection by digital PD acquisition systems may thus be difficult.

### **NARROW – BAND PD INSTRUMENTS**

It is well known that radio transmission or radiotelephony may be heavily disturbed by high-frequency interference voltages within the supply mains to which receivers

are connected or by disturbing electromagnetic fields picked up by the aerials. It was also early recognized that corona discharges at HV transmission lines are the source of such disturbances. The measurement of ‘radio noise’ in the vicinity of such transmission lines is thus an old and well-known technique which several decades ago triggered the application of this measurement technique to detect insulation failures, i.e. partial discharges, within HV apparatus of any kind.

The methods for the measurement of radio noise or radio disturbance have been subjected to many modifications during the past decades. Apart from many older national or international recommendations, the latest ‘specifications for radio disturbance and immunity measuring apparatus and methods’ within a frequency range of 10 kHz to 1000 MHz are now described in the CISPR Publication. As defined in this specification, the expression ‘radio disturbance voltage (RDV)’, earlier termed as ‘radio noise’, ‘radio influence’ or ‘radio interference’ voltages, is now used to characterize the measured disturbance quantity.

Narrow-band PD instruments, which are now also specified within the new IEC Standard for the measurement of the apparent charge, are very similar to those RDV meters, which are applied for RDV measurements in the frequency range 100 kHz to 30MHz.

The PD instruments are characterized by a small bandwidth  $\Delta f$  and a mid-band frequency  $f_m$ , which can be varied over a wider frequency range, where the amplitude frequency spectrum of the PD current pulses is in general approximately constant. The recommended values for  $\Delta f$  and  $f_m$  for PD instruments are

$$9 \text{ kHz} \leq \Delta f \leq 30 \text{ kHz}$$

$$50 \text{ kHz} \leq f_m \leq 1 \text{ MHz}$$

It is further recommended that the transfer impedance  $Z(f)$  at frequencies of  $f_m \pm \Delta f$  should already be 20 dB below the peak pass-band value. Commercial instruments of this type may be designed for a larger range of mid-band frequencies; therefore, the standard provides the following note for the user. ‘During actual apparent charge measurements, mid-band frequencies  $f_m > 1\text{MHz}$  should only be applied if the readings for such higher values do not differ from those as monitored for the recommended values of  $f_m$ ’.

This statement denotes that only the constant part of the PD current amplitude\ frequency spectrum is an image of the apparent charge. As shown below in more detail, the response of these instruments to a PD current pulse is a transient oscillation with the positive and negative peak values of its envelope proportional to the apparent charge, independent of the polarity of this charge.

Due to the small values of  $\Delta f$ , the pulse resolution time  $T_r$  will be large, typically above 80  $\mu\text{s}$ . The application of such instruments often causes some confusion for the user. A brief description of their basic working principle and their use in PD measurements will help make things clear. Figure-2.11 displays the relevant situation and results.

In general, such instruments are used together with coupling devices providing high-pass characteristics within the frequency range of the instrument. Power frequency input currents including harmonics are therefore suppressed and assumed that only the PD current pulses converted to PD voltage pulses are at the input of the amplifying instrument, which resembles closely a selective voltmeter of high sensitivity (or a super heterodyne-type receiver) which can be tuned within the frequency range of interest.

Such a narrow-band instrument is again a quasi integration device for input voltage pulses. To demonstrate this behavior, it is assumed that an input voltage  $V_1 = V_0 \cdot e^{-($

$v^T$ ), i. e. an exponentially decaying input pulse which starts suddenly with amplitude  $V_0$  (see Figure-2.11(b)). The integral of this pulse,  $\int_0^{\infty} v_1(t) dt$ , is  $V_0T$  and is thus a quantity proportional to the apparent charge  $q$  of a PD current pulse. The complex frequency spectrum of this impulse is then given by applying the Fourier integral

$$V_1(j\omega) = \int_0^{\infty} v_1(t) \exp(-j\omega t) dt = \frac{V_0T}{1+j\omega T} = \frac{S_0T}{1+j\omega T} \quad \dots(2.20)$$

and the amplitude frequency spectrum  $|V_1(j\omega)|$  by

$$|V_1(j\omega)| = \frac{V_0T}{\sqrt{1+(\omega T)^2}} = \frac{S_0}{\sqrt{1+(\omega T)^2}} \quad \dots(2.21)$$

where  $S_0$  is proportional to  $q$ . From the amplitude frequency spectrum, sketched in Figure-2.11(c), it is obvious that the amplitudes decay already to -3 dB or more than about 30 per cent for the angular frequency of  $\omega c > (1/T)$ . This critical frequency  $f_c$  is for  $T = 0.1 \mu\text{sec}$  only 1.6 MHz, a value which can be assumed for many PD impulses.

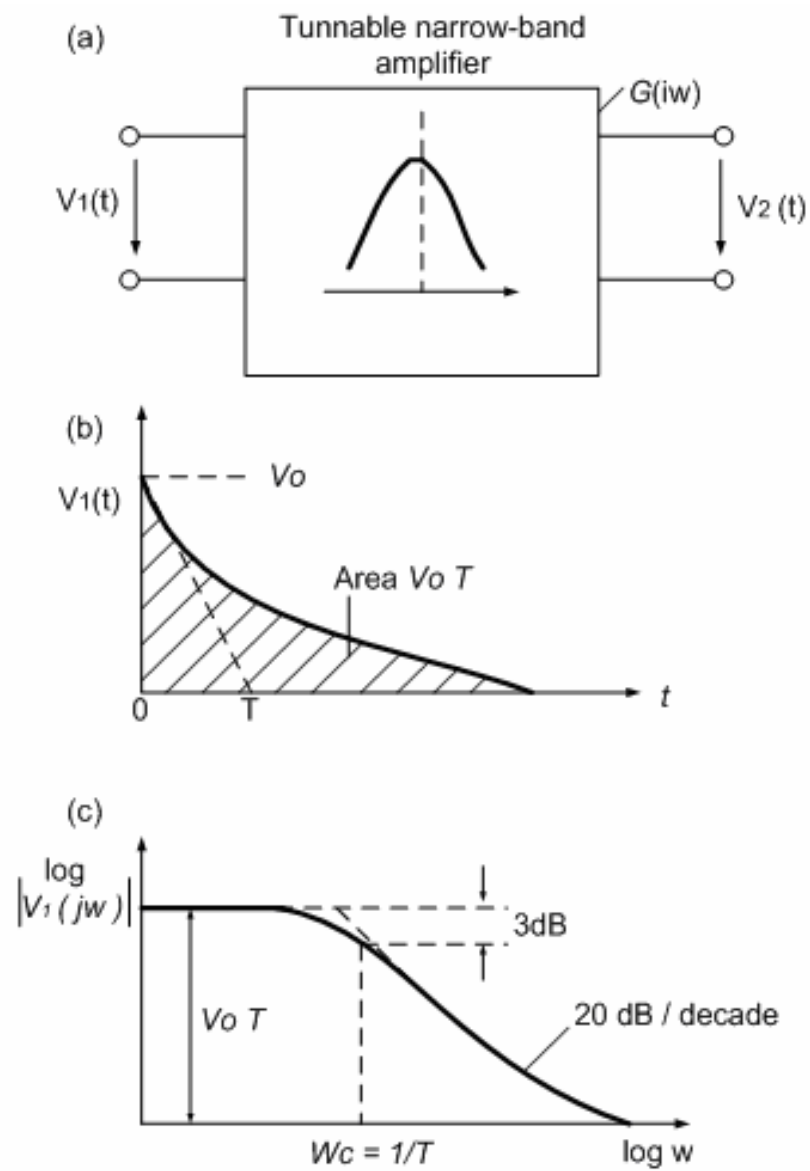


Figure-2.11 Narrow-band Amplifiers Responses (Part-1)

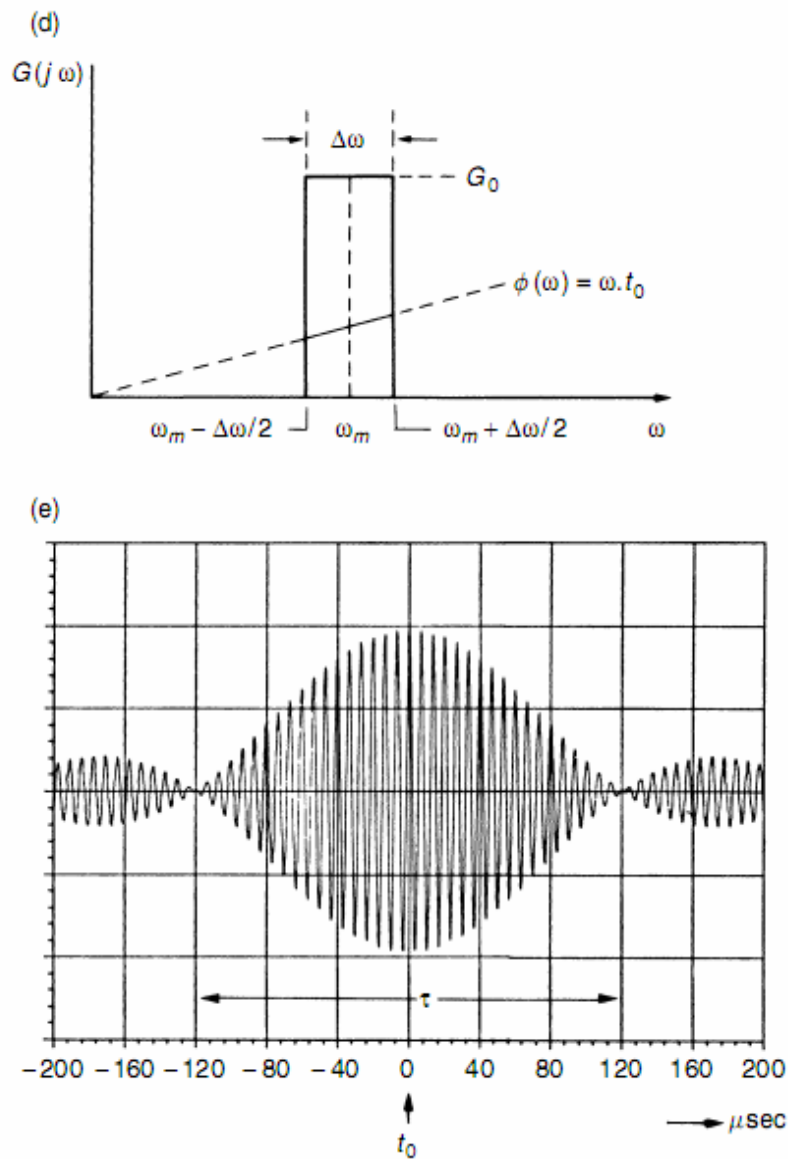


Figure 2.11 Narrow-band Amplifiers Responses (Part-2)

As the indication of a narrow-band instrument, if tuned to  $f_m$ , will be proportional to the relevant amplitude of this spectrum at  $f_m$ , then the recommendations of the new standard can well be understood. If the input PD current pulse were distorted by

oscillations, the amplitude frequency spectrum would also be distorted by maxima and minima, which can then be recorded by tuning  $f_m$ .

If the narrow-band instrument is tuned to the constant part of the spectrum which is proportional to  $q$ , and assumed a Dirac pulse or delta function of magnitude  $V_0T = S_0$  to calculate its output voltage  $V_2(t)$ .

As the spectrum of a Dirac pulse is constant for all frequencies, the response  $V_2(t)$  is then proportional to  $S_0$  at any frequency  $f_m$ . The impulse response of the instrument is then of course dependent upon the exact (output/input voltage) transfer function  $G(j\omega)$  of the system. However, the actual band-pass characteristic by an idealized one as shown in Figure-2.11(d), with a mid-band angular frequency  $\omega_m$ , an angular bandwidth  $\Delta\omega$  and the constant amplitude or 'scale factor'  $G_0$  within  $\omega_m \pm (\Delta\omega/2)$ .

For such ideal band-pass systems and especially narrow-band amplifiers the phase shift  $\Phi(\omega)$  may well be assumed to be linear with frequency as indicated, at least within the band-pass response. With this approximation no phase distortion is assumed, and  $t_0$  (figure-2.11(d)) is equal to the delay time of the system. The impulse response with  $S_0$  as input pulse appearing at  $t = 0$  can then be evaluated from

$$v_2(t) = \frac{1}{\pi} \int_{\omega_m - \Delta\omega/2}^{\omega_m + \Delta\omega/2} S_0 G_0 \cos[\omega(t - t_0)] d\omega \quad \dots(2.22)$$

This integral can easily be solved; the result is

$$v_2(t) = \frac{S_0 G_0 \Delta\omega}{\pi} \text{si} \left[ \frac{\Delta\omega}{2} (t - t_0) \right] \cos \omega_m (t - t_0) \quad \dots(2.23)$$

Where  $\text{si}(x) = \text{Sin}(x) / x$

Equation-2.15 shows an oscillating response whose main frequency is given by  $f_m = \omega_m/2\pi$ , the amplitudes are essentially given by the  $\text{si}(x)$  function, which is the

envelope of the oscillations. A calculated example for such a response is shown in figure-2.11(e). The maximum value will be reached for  $t = t_0$  and is clearly given by

$$V_{2\max} = \frac{S_0 G_0 \Delta \omega}{\pi} = 2 S_0 G_0 \Delta f \quad \dots(2.24)$$

where  $\Delta f$  is the idealized bandwidth of the system.

Here, the two main disadvantages of narrow-band receivers can easily be seen: first, for  $\Delta \omega \ll \omega_m$  the positive and negative peak values of the response are equal and therefore the polarity of the input pulse cannot be detected. The second disadvantage is related to the long duration of the response. Although more realistic narrow band systems will effectively avoid the response amplitudes outside of the first zero values of the  $(\sin x)/x$  function, the full length  $\tau$  of the response, with  $\tau$  as defined by figure-2.11(e), becomes

$$\tau = \frac{2}{(\Delta f)} = \frac{4\pi}{\Delta \omega} \quad \dots(2.25)$$

In above equation  $\tau$  is quite large for small values of  $\Delta f$  and the actual definition of the ‘pulse resolution time  $T_r$ ’ as defined before. This quantity is about 10 % smaller than  $\tau$ , but still much larger than for wide-band PD detectors.

Simple narrow-band detectors use only RLC resonant circuits with high quality factors  $Q$ , the resonance frequency of which cannot be tuned. Although then their responses are still quite similar to the calculated one (equation-2.23), figure-2.12 shown such a response for a ‘double pulse’ taken from a commercial PD instrument.

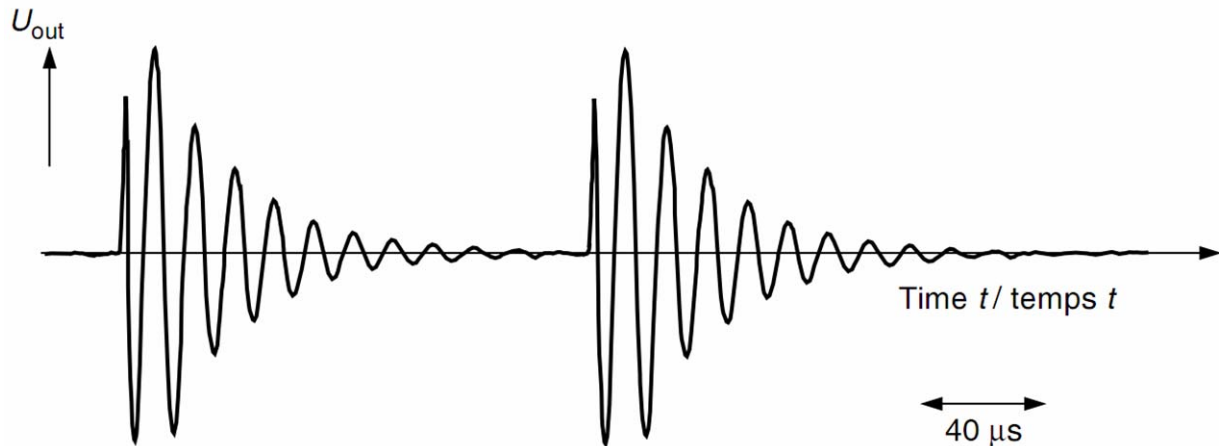


Figure 2.12 Response of a Simple Narrow-band Circuit with  $\Delta f = 10 \text{ kHz}$ ;  $f_m = 75 \text{ kHz}$

### **RADIO DISTURBANCE (INTERFERENCE) METERS FOR THE DETECTION OF PD**

As instruments such as those specified by the International Special Committee on Radio Disturbance or similar organizations are still in common uses for PD detection. The possible application of an ‘RDV’ or ‘RIV’ meter is still mentioned within the new standard.

New types of instruments related to the CISPR Standard are often able to measure ‘radio disturbance voltages, currents and fields’ within a very large frequency range, based on different treatment of the input quantity. Within the PD standard, however, the expression ‘Radio Disturbance Meter’ is only applied for a specific radio disturbance (interference) measuring apparatus, which is specified for a frequency band of 150 kHz to 30MHz (band B) and which fulfils the requirements for a so-called ‘quasi-peak measuring receivers’.

Figure-2.13 shows diagram of such a simple RIV meter, which is compared with the principle of a narrow-band PD instrument as, described and discussed before. The main difference is only the ‘quasi-peak’ or ‘psophometric weighting circuit’ that simulates the physiological noise response of the human ear. As already mentioned within the introduction of this section, forthcoming PD instruments will be equipped

with a similar, but different circuit with a ‘pulse train response’ quantifying the ‘largest repeatedly occurring PD magnitudes’.

Within the figure-2.13, the simplified coupling device as indicated by a resistance shunted by the inductance L forms transfer impedance  $Z_m$  with a high-pass characteristic which for RDV meters are standardized values. Based on the derivations as already made for the calculation equation-2.24 can easily quantify the differences of both types of meter.

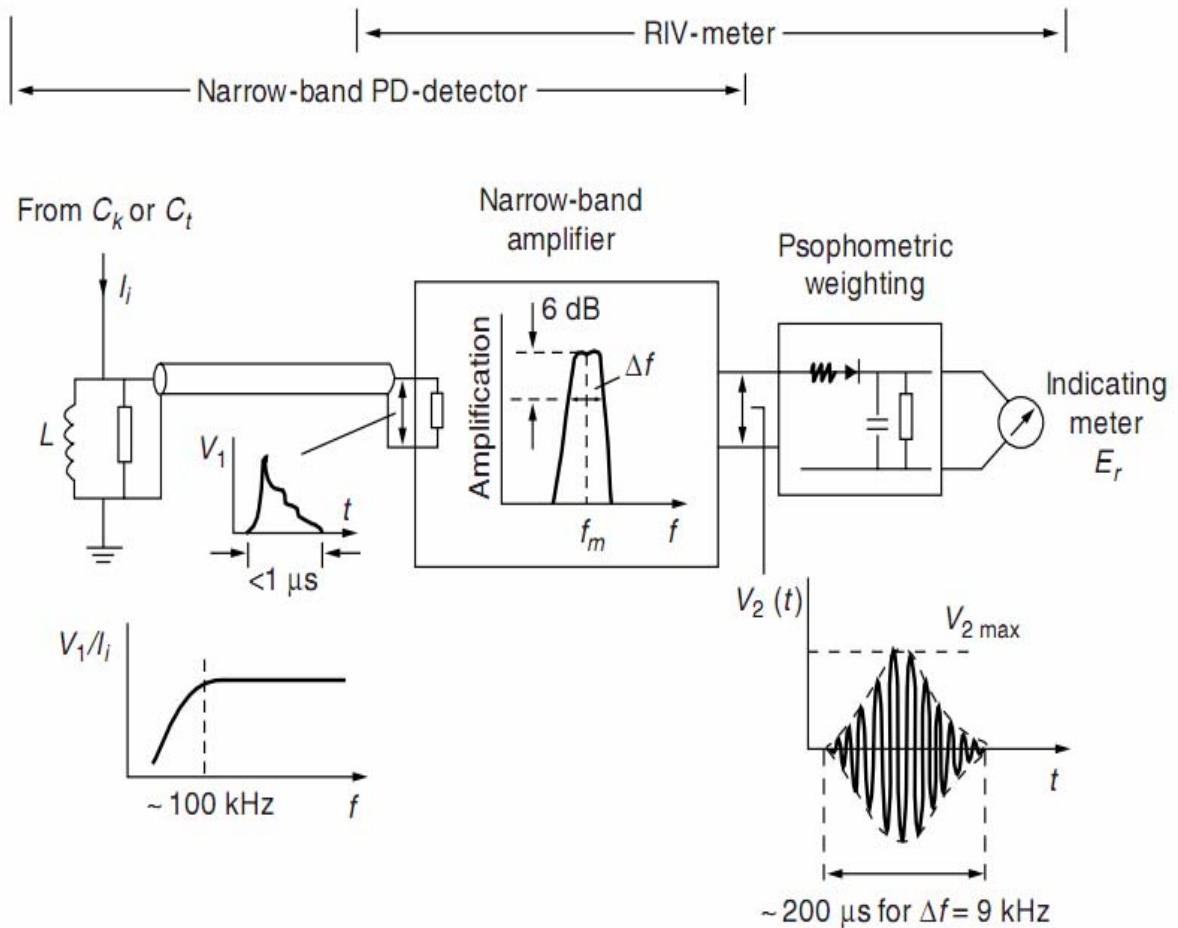


Figure-2.13 Block Diagram of a Quasi-peak RIV Meter Including Weighting Circuit Compared with PD Narrow-band PD Detector

The quasi-peak RDV meters are designed with a very accurately defined overall pass-band characteristic fixed at  $\Delta f = 9$  kHz. They are calibrated in such a way that the response to Dirac type of equidistant input pulses providing each a volt–time area of  $0.316 \mu\text{Vs}$  at a pulse repetition frequency (N) of 100Hz. This is equal to an unmodulated sine-wave signal at the tuned frequency having an e.m.f. of  $2\text{mV}$  r.m.s. as taken from a signal generator driving the same output impedance as the pulse generator and the input impedance of the RIV meter.

By this procedure the impulse voltages as well as the sine-wave signal are halved. As for this repetition frequency of 100Hz the calibration point shall be only 50 per cent of  $V_{2\text{max}}$  in eqn. (2.16), the relevant reading of the RDV meter will be

$$E_{RDV} = \frac{1}{2\sqrt{2}} 2S_0 G_0 \Delta f = \frac{S_0 G_0 \Delta f}{\sqrt{2}} \quad \dots(2.26)$$

As  $G_0 = 1$  for a proper calibration and  $\Delta f = 9\text{kHz}$ ,  $S_0 = 158 \mu\text{Vs}$ , the indicated quantity is  $S_0 \Delta f / \sqrt{2} = 1\text{mV}$  or  $60\text{dB} (\mu\text{V})$ , as the usual reference quantity is  $1 \mu\text{V}$ . RDV meters are thus often called ‘microvolt meters’.

This response is now weighted by the ‘quasi-peak measuring circuit’ with a specified electrical charging time constant  $\tau_1 = 1\text{ms}$ , an electrical discharging time constant  $\tau_2 = 160\text{ms}$  and by an output voltmeter, which, for conventional instruments, is of moving coil type, critically damped and having a mechanical time constant  $\tau_3 = 160\text{ms}$ .

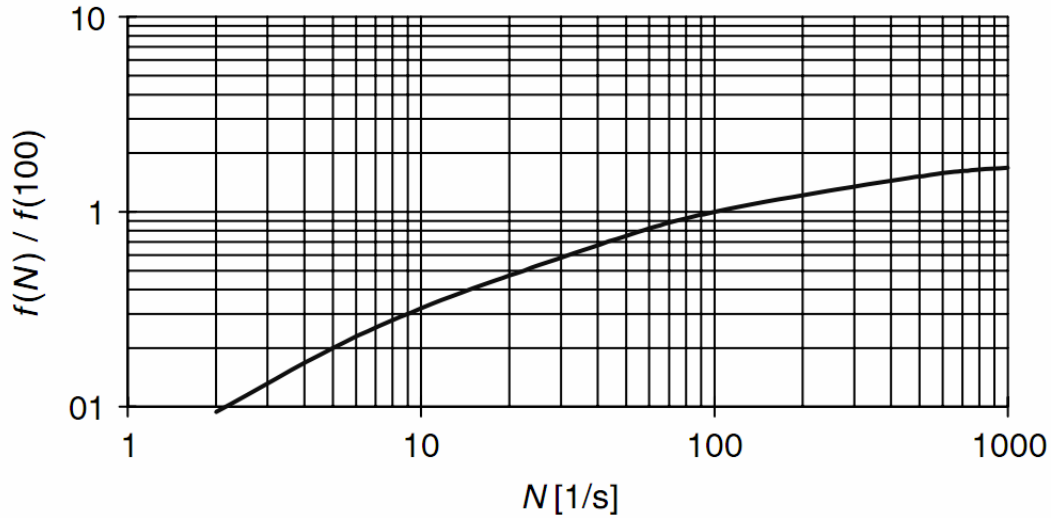


Figure-2.14 Variation of CISPR Radio Interference Meter Reading with Repetition Frequency  $N$ , for Constant Input Pulses

This procedure makes the reading of the output voltmeter dependent on the pulse repetition frequency  $N$ . This non-linear function  $f(N)$  is shown in figure-2.14 and is only accurate if the input pulses are equidistant and of equal amplitudes. It can be seen that for  $N > 1000$  the function  $f(N)$  would saturate to a value of 2, for which, however, superposition errors occur.

With this function  $f(N)$  we can now finalize the reading of an RIV meter by taking the transfer impedance  $Z_m$  of CD in eqn (2.18) into account, which converts input PD currents into input voltages  $v_1(t)$ . For RDV meters, this transfer impedance, the real value of which  $|Z_m|$  is constant for the frequency range under consideration, the quantity  $S_0$  in eqn. (2.18) may then be written as,

$$S_0 = \int v_1(t)dt = |Z_m| \int i_1(t)dt = |Z_m|q \quad \dots(2.27)$$

Where  $q$  is the measured charge quantity for an impulse current  $i_1(t)$ . Here, eq-2.18 can be rewritten as  $E_{RDV} = \frac{Go}{\sqrt{2}} q \Delta f |Z_m| f(N)$  and conversion factors between the

measured charge  $q$  and the indicated voltage by an RDV meter can be calculated. For  $N = 100$  equidistant pulses of equal magnitude  $f(N) = 1$ ,  $\Delta f = 9$  kHz, correct calibration  $G_0 = 1$  and a reading of 1mV ( $E_{RDV}$ ) or 60 dB, charge magnitudes of 1 nC for  $|Z_m| = 150$  (or 60)  $\Omega$  can be calculated. These relationships have also been confirmed experimentally. Instead of eqn (2.19) the new standard displays.

$$U_{RDV} = (q\Delta f Z_m f(N)) / k_i \quad \dots(2.28)$$

where

$N$  = pulse repetition frequency,

$f(N)$  = the non-linear function of  $N$  (see figure-2.14),

$\Delta f$  = instrument bandwidth (at 6 dB),

$Z_m$  = value of a purely resistive measuring input impedance of the instrument,

$k_i$  = the scale factor for the instrument ( $= q / U_{RDV}$ )

As the weighting of the PD pulses is different for narrow-band PD instruments and quasi-peak RDV meters, there is no generally applicable conversion factor between readings of the two instruments. The application of RDV meters is thus not forbidden; but if applied the records of the tests should include the readings obtained in microvolt and the determined apparent charge in pico coulombs together with relevant information concerning their determination.

## **ULTRA-WIDE-BAND INSTRUMENTS FOR PD DETECTION**

The measurement of PD current pulses belongs to this kind of PD detection as well as any similar electrical method to quantify the intensity of PD activities within a test object. Such methods need coupling devices with high-pass characteristics which shall have a pass band up to frequencies of some 100MHz or even higher.

Records of the PD events are then taken by oscilloscopes, transient digitizers or frequency selective voltmeters especially spectrum analyzers. For the location of isolated voids with partial discharges in cables a bandwidth of about some 10MHz only is useful, whereas tests on GIS (gas-insulated substations or apparatus) measuring systems with 'very high' or even 'ultra-high' frequencies (VHF or UHF methods for PD detection) can be applied.

The development of any partial discharge in sulphur hexafluoride is of extremely short duration providing significant amplitude frequency spectra up to the GHz region. More information concerning this technique can be found in the literature..

As none of these methods provides integration capabilities, they cannot quantify apparent charge magnitudes, but may well be used as a diagnostic tool.

## 2.7 CALIBRATION OF PD DETECTORS IN A COMPLETE TEST CIRCUIT<sup>[3]</sup>

The reasons why any PD instrument provides continuously variable sensitivity must be calibrated in the complete test circuit, which has been explained before. Even the definition of the ‘apparent charge  $q$ ’ is based on a routine calibration procedure, which shall be made with each new test object. Calibration procedures for PD detection are thus firmly defined within the standard.

A calibration of measuring systems intended for the measurement of the fundamental quantity  $q$  is made by injecting short duration repetitive current pulses of well-known charge magnitudes  $q_0$  across the test object, subject to any test circuit as shown in Figure-2.15. These current pulses are generally derived from a calibrator which comprises a generator producing step voltage pulses (see ‘G’) of amplitude  $V_0$  in series with a precision capacitor  $C_0$ . If the voltages  $V_0$  also remain stable and are exactly known, repetitive calibration pulses with charge magnitudes of  $q_0 = V_0 C_0$  are injected. A short rise time of 60 ns is now specified for the voltage generator to produce current pulses with amplitude-frequency spectra which fit into the requirements set by the bandwidth of the instruments and avoids integration errors if possible.

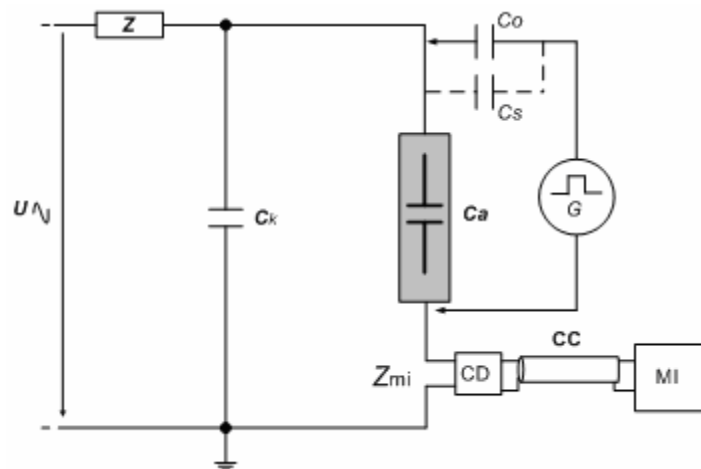


Figure-2.15 The Usual Circuit for the Calibration of a PD Measuring Instrument MI within the Complete Test Circuit.

Whereas further details for the calibration procedures are not discussed here, the new philosophy in reducing measuring errors during PD tests will be presented. It has been known for some time that measuring uncertainties in PD measurements are large. Even today PD tests on identical test objects performed with different types of commercially available systems will provide different results after routine calibration performed with the same calibrator.

The main reasons for this uncertainty are the different transfer impedances (bandwidth) of the measuring systems, which up to 1999 have never been well defined and quantified. The new but not very stringent requirements related to this property will improve the situation; together with other difficulties related to disturbance levels, measures uncertainties of more than about 10 per cent (if exists). The most essential part of the new philosophy concerns the calibrators, for which – up to now – no requirements for their performance exists.

Tests on daily used commercial calibrators sometime display deviations of more than 10 per cent of their nominal values. Therefore routine type and performance tests on calibrators have been introduced with the new standard. At least the first of otherwise periodic performance tests should be traceable to national standards, this means they shall be performed by any accredited calibration laboratory. With the introduction of this requirement it can be assumed that the uncertainty of the calibrator charge magnitudes  $q_0$  can be assessed to remain within  $\pm 5$  per cent or 1 pC, whichever is greater, from its nominal values. Very recently executed inter-comparison tests on calibrators performed by accredited calibration laboratories showed that impulse charges could be measured with an uncertainty of about 3 per cent.

## 2.8 DIGITAL INSTRUMENTS FOR PD MEASUREMENTS <sup>[2]</sup>

Between 1970 and 1980 the state of the art in computer technology and related techniques rendered the first application of digital acquisition and processing of partial discharge magnitudes. Since then this technology was applied in numerous investigations generally made with either instrumentation set up with available components or some commercial instruments equipped with digital techniques.

One task for the working group evaluating the new IEC Standard concerned with implementation of few key requirements for this technology. It is again not the aim of this section to go into details of digital PD instruments, as too many variations in designing such instruments exist.

In general, digital PD instruments are based on analogue measuring systems or instruments for the measurement of the apparent charge  $q$  followed by a digital acquisition and processing system. These digital parts of the system are then used to process analogue signals for further evaluation, to store relevant quantities and to display test results.

It is possible that in the near future a digital PD instrument may also be based on a high-pass coupling device and a digital acquisition system without the analogue signal processing front end. The availability of cheap but extremely fast flash A/D converters and digital signal processors (DSPs) performing signal integration is a prerequisite for such solutions.

The main objective of applying digital techniques to PD measurements is based on recording in real time and most of consecutive PD pulses are within a voltage cycle of the test voltage. These PD pulses are quantified by its apparent charge  $q_i$  (occurring at time instant  $t_i$ ) and its instantaneous values of the test voltage  $u_i$  (occurring at this time instant  $t_i$ ) or for alternating voltages, at phase angle of  $\Phi_i$

As, however, the quality of hardware and software used may limit the accuracy and resolution of the measurement of these parameters, the new standard provides some recommendations and requirements which are relevant for capturing and registration of the discharge sequences. One of the main problems in capturing the output signals from the analogue front end correctly can be seen from Figures-2.12 and Figure-2.14 respectively, in which three output signals of two consecutive PD events are shown.

Although none of the signals is distorted by superposition errors, several peaks of each signal with different polarities are present. For the wideband signals, only the first peak value shall be captured and recorded including polarity, which is not easy to do. For the narrow-band response for which polarity determination is not necessary, only the largest peak is proportional to the apparent charge.

For both types of signals therefore only one peak value shall be quantified, recorded and stored within the pulse resolution time of the analogue measuring system. Additional errors can well be introduced by capturing wrong peak values, which add to the errors of the analogue front end.

Further study of PD instruments is related to post-processing of the recorded values. Firstly; the so-called ' $\varphi_i - q_i - n_i$ ' patterns, available from the recorded and stored data in which  $n_i$  is the number of identical or similar PD magnitudes recorded within short time (or phase) intervals and an adequate total recording duration can be used to identify and localize the origin of the PDs based on earlier experience and/or even to establish physical models for specific PD processes. If recorded raw data are too much obscured by disturbances, quite different numerical methods may also be applied for disturbance level reduction.

This chapter concludes with two records of results from PD tests made with digital PD instrument. Figure-2.16 and figure-2.17, individually, shows typical test results of

phase resolved PD measurement for a moving metal particle within a GIS and on-site PD measurements performed on HV cable (at a terminator).

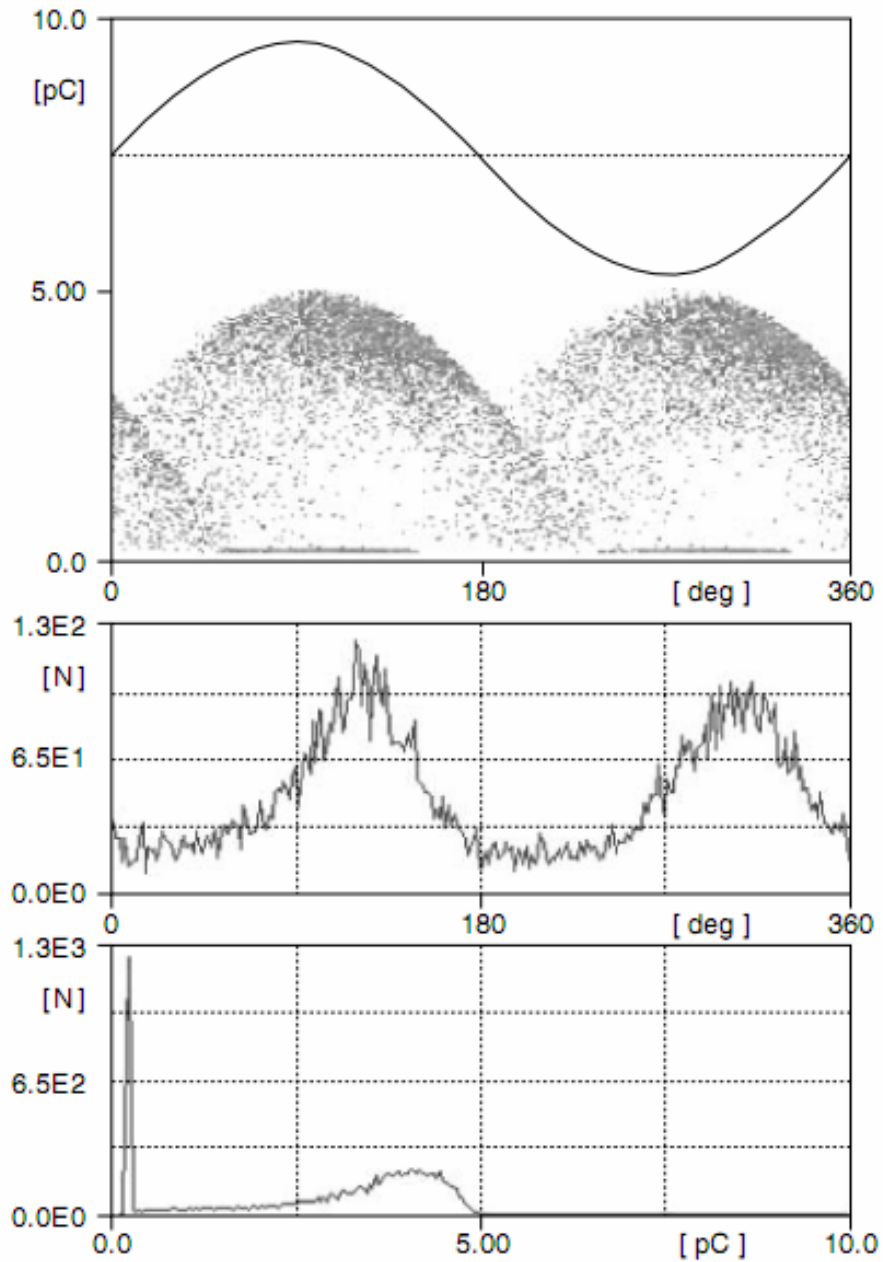


Figure-2.16 The Pattern of a Phase-resolved PD Measurement for a Moving Metal Particle within a GIS.

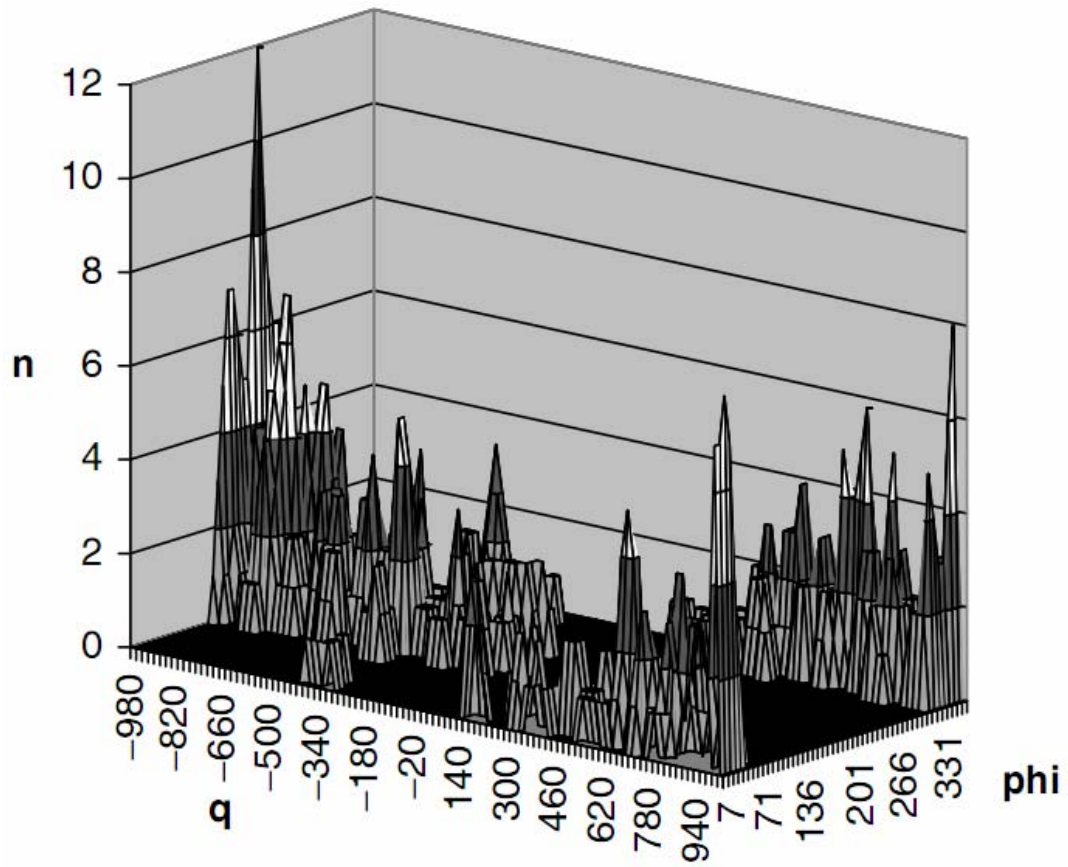


Figure-2.17 An Example of a  $\phi$  - q - n Diagram. On-site PD measurements performed on an HV cable, heavy partial discharges at a terminator

## 2.9 SOURCE OF INTERFERENCE AND REDUCTION OF DISTURBANCES <sup>[2,3]</sup>

One of the most difficult problems that must be coped with in making PD measurements is that of electrical interference (noise) which falls into following categories:

- Disturbances, which occur if test circuit is not energized. They may be caused by switching operations in other circuits, commuting machines, high voltage tests in the vicinity radio transmission etc.
- Disturbances which only occur when the test circuit is energized but which don't occur in the test object, for e.g. PD in testing transformer, HV conductors, bushings, disturbances caused by sparking of imperfectly earthed objects in the vicinity or the loose connections in the area of high voltages.
- Disturbances which may also caused by higher harmonics of test voltage within the band-width of the measuring instruments. These disturbances usually increase with increasing the voltage.

These disturbances can seriously affect the sensitivity of the test circuit and must be controlled and suppressed to minimum and to use detectors equipped with an oscilloscope to give the maximum opportunity for distinguishing spurious signals from the discharges in the test sample.

The following table gives the complete account of different sources of disturbances and their control or remedy for suppression.

All preceding disturbances can be suppressed by using a balance detection method.

TABLE-2.1 DIFFERENT SOURCES OF DISTURBANCES AND THEIR REMEDY FOR SUPPRESSION

Disturbance	Example	Control or remedy
Disturbance in the circuit		
Mains interference		Filter in feeding leads and/or in H.V. Line
H.V. Source		Discharge free H.V. transformer, filter in H.V. line
Coupling Capacitor		Coupling capacitor should be discharge free or two samples should be tested at a time
Terminals	Discharge in cable terminals, bushings etc.	Terminals, bushings etc should be discharge free.

\* All preceding disturbance can be suppressed by using a balanced detector

Pick- up		
Other H.V. tests in the vicinity		Screening, eliminating the cause
Electromagnetic waves	Radio signals	Screening, a detector below about 100KHz can be chosen
Induced discharger		Eliminating the cause, proper earthing, screening samples should be tested at a time

\* Screening is effective in 3-preceding cases.

Contact noise		
Contact noise in circuit		Making good connection and earthing also in variable components in the input circuit
Contact noise in sample	Contact between the foils and terminals in capacitor	Applying current impulses by short circulating.
	Contact noise in bushing, tap changer or earthing of the core in the transformer	Checking contacts before mounting
	Contacts between semi conducting layer and metallic sheath of cable	Choosing smaller time constants (equal to higher resolution) of input circuit

It is obvious that up to now numerous methods to reduce disturbances have been and still are a topic for research and development, which can only be mentioned and summarized here.

The most efficient method to reduce disturbances is screening and filtering, in general only possible for tests within a shielded laboratory where all electrical connections running into the room are equipped with filters. This method is expensive, but inevitable if sensitive measurements are required, i.e. if the PD magnitudes as specified for the test objects are small, e.g. for HV cables.

Straight PD-detection circuits as already shown in Figure-2.6 are very sensitive to disturbances: any discharge within the entire circuit, including HV source, which is not generated in the test specimen itself, will be detected by the coupling device CD. Therefore, such 'external' disturbances are not rejected. Independent of screening and filtering mentioned above, the testing transformer itself should be PD free as far as possible, as HV filters or inductors indicated in figure-2.6 are expensive. It is also difficult to avoid any partial discharges at the HV leads of the test circuit, if the test voltages are very high. A basic improvement of the straight detection circuit may therefore become necessary by applying a 'balanced circuit', which is similar to a Schering bridge.

Figure-2.18 shows the coupling capacitor  $C_k$  and test specimen  $C_t$  form the HV arm of the bridge, and the LV arms are basically analogous to a Schering bridge. As  $C_k$  is not a standard capacitor but should be PD free, the dissipation factor  $\tan \delta_K$  may also be higher than that of  $C_t$ , and therefore the capacitive branch of the LV arm may be switched to any of the two arms. The bridge can then be adjusted for balance for all frequencies at which  $\tan \delta_K = \tan \delta_t$ . This condition is best fulfilled if the same insulation media are used within both capacitors.

The use of a partial discharge-free sample for  $C_k$  of the same type as used in  $C_t$  is thus advantageous. If the frequency dependence of the dissipation factors is different in the two capacitors, a complete balance within a larger frequency range is not possible. Nevertheless, a fairly good balance can be reached and therefore most of the sinusoidal or transient voltages appearing at the input ends of  $C_k$  and  $C_t$  cancel out between the points 1 and 2. A discharge within the test specimen, however, will contribute to voltages of opposite polarity across the LV arms, as the PD current is flowing in opposite directions within  $C_k$  and  $C_t$ .

Polarity discrimination methods take advantage of the effect of opposite polarities of PD pulses within both arms of a PD test circuit.

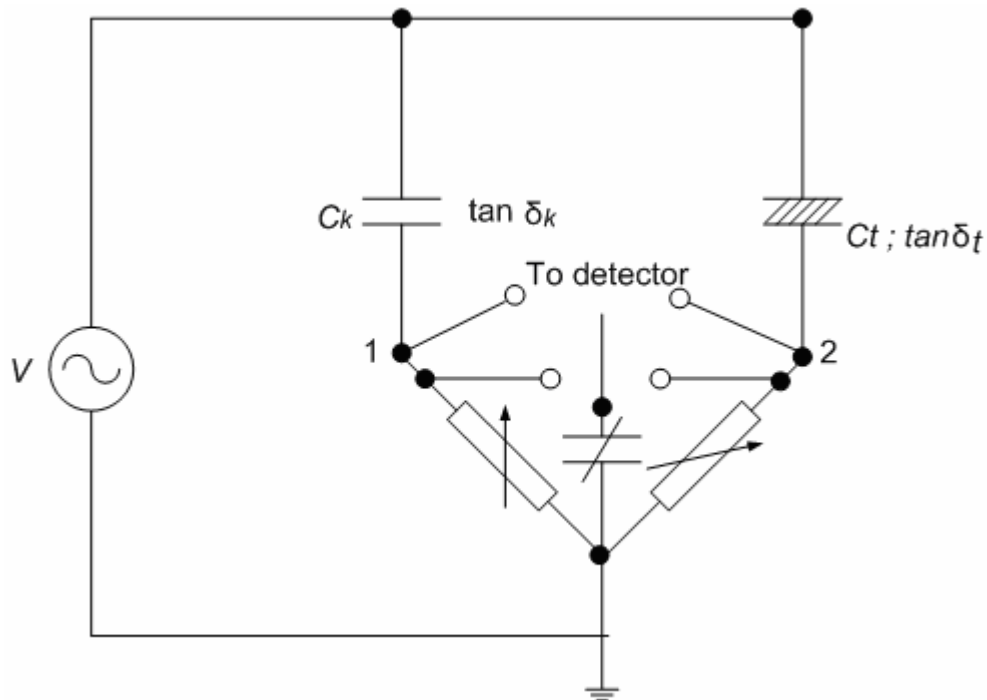


Figure-2.18 Differential PD bridge (Balanced Circuit)

Figure-2.19 shows two coupling devices  $CD$  and  $CD_1$ , which transmits the PD signals to the special measuring instrument  $MI$ , in which a logic system performs the comparison and operates a gate for pulses of correct polarity. Consequently only those

PD pulses which originate from the test object are recorded and quantified. This method was proposed by I.A. Black.

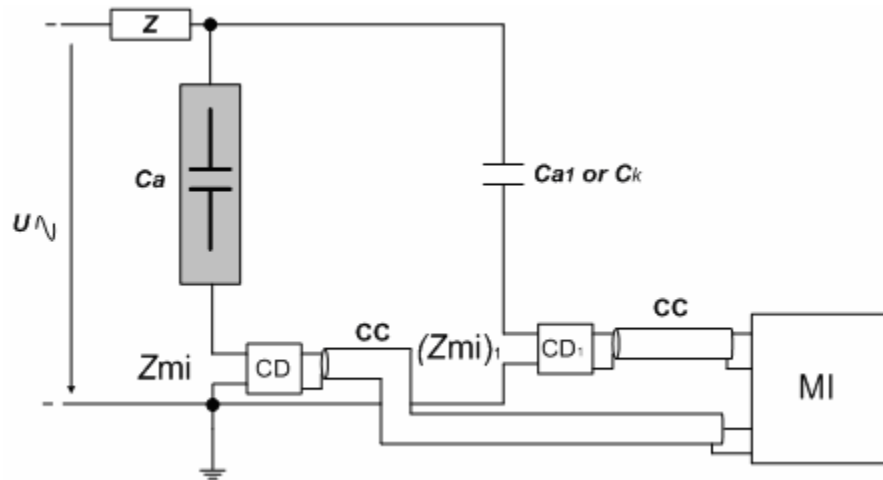


Figure-2.19 Polarity Discrimination Circuit

Another extensively used method is the time window method to suppress interference pulses. All kinds of instruments may be equipped with an electronic gate, which can be opened and closed at preselected moments, thus either passing the input signal or blocking it. If the disturbances occur during regular intervals the gate can be closed during these intervals. In tests with alternating voltage, the real discharge signals often occur only at regularly repeated intervals during the cycles of test voltage. The time window can be phase locked to open the gate only at these intervals.

Some more sophisticated methods are used for digital acquisition of partial discharge quantities.

## 2.10 ORIGIN AND RECOGNITION OF DISCHARGE<sup>[3]</sup>

Oscillographic studies of discharge patterns have been found to be useful in the qualitative investigation of the origins of the discharges. Some of these patterns may be interpreted with the aid of table given below. The table is helpful in interpreting the origins of discharges. The pattern may indicate the type, size and number of discharging source.

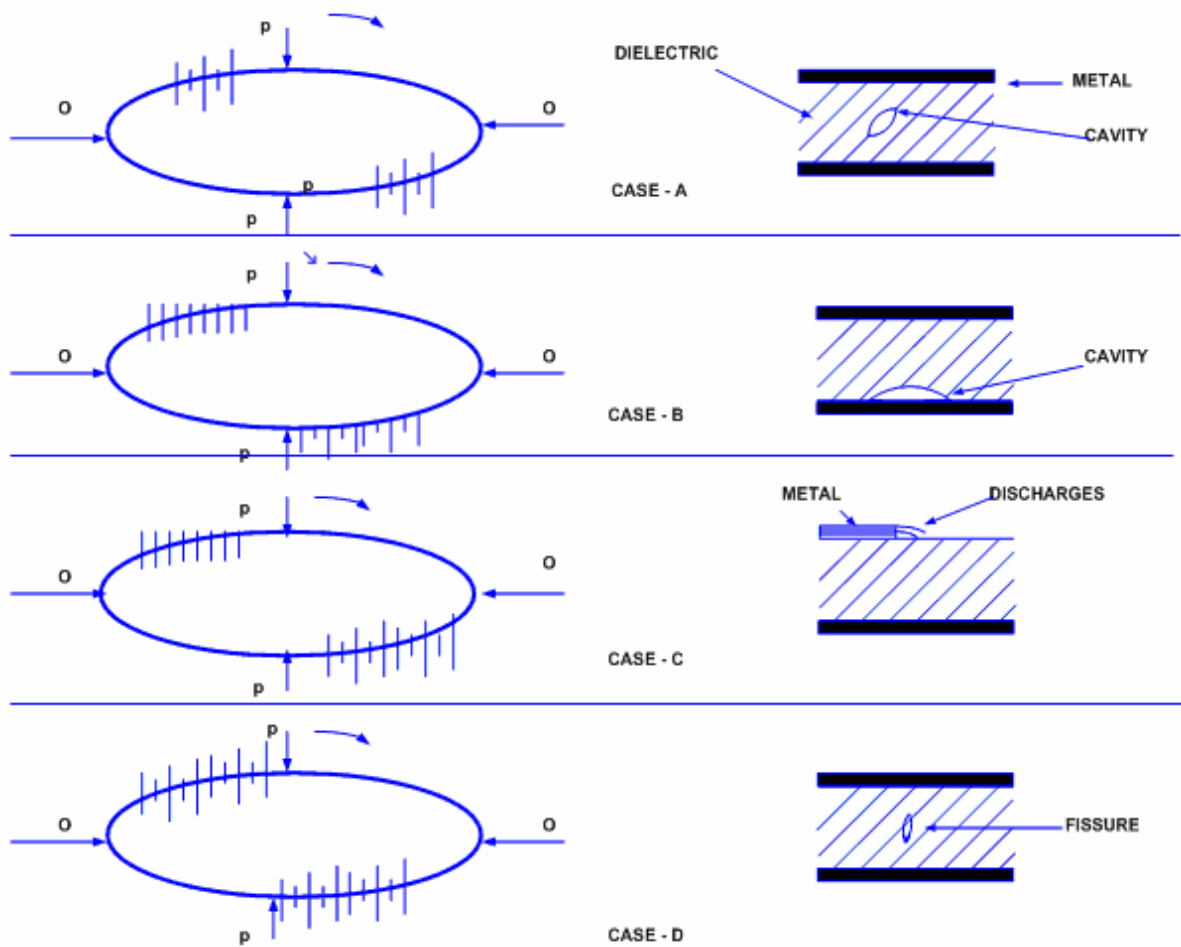


Figure-2.20 Origin and Recognition of Discharges (Part-1)

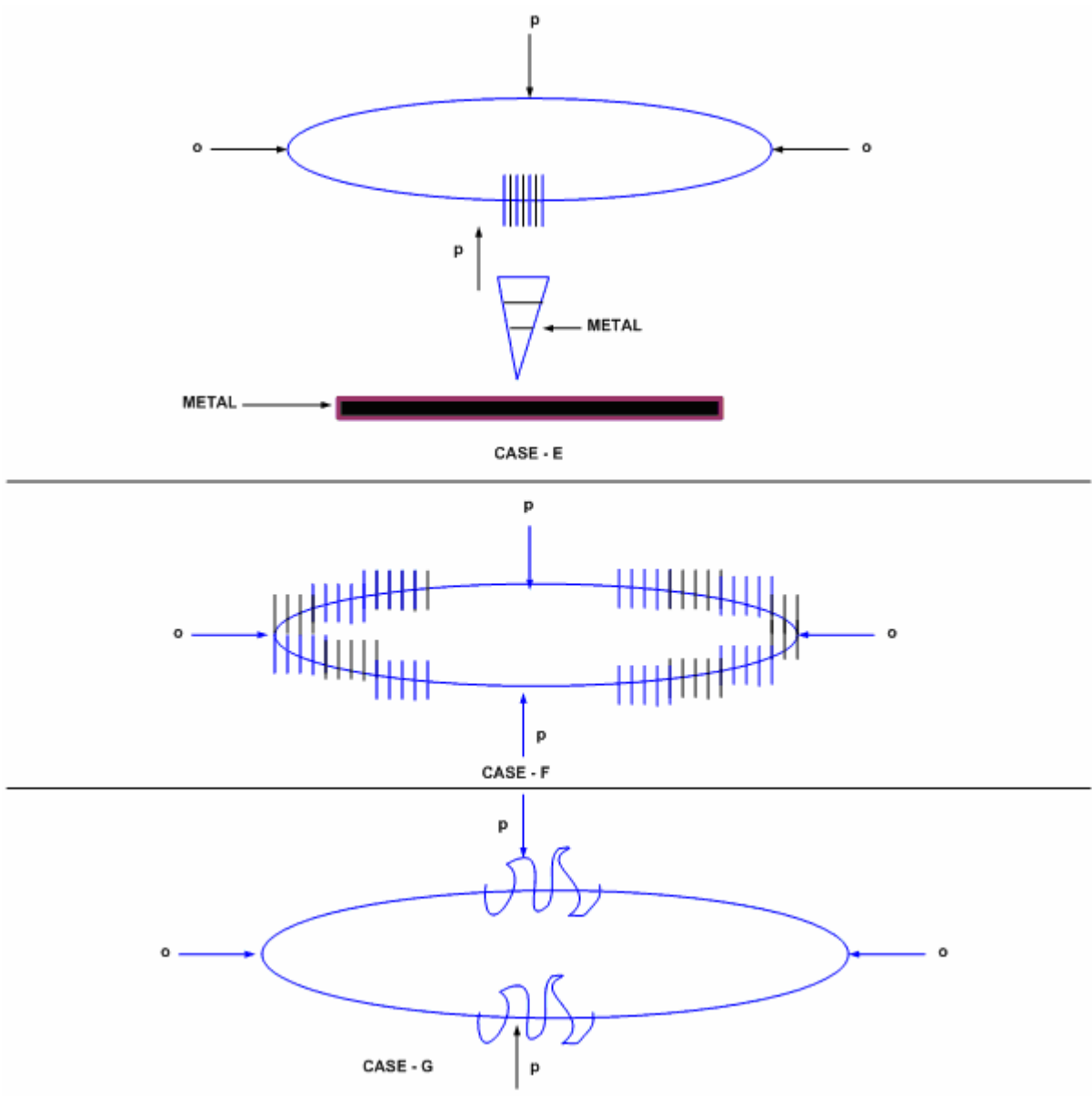


Figure-2.20 Origin and Recognition of Discharges (Part-2)

TABLE-2.1 INTERPRETING THE ORIGIN OF DISCHARGE

Case	Discharge pattern	Effect of voltage	Effect of time	indication	Display on detection & origin
1	The discharges occur symmetrical on the positive and negative halves of test-wave from. The amplitude is sometime nearly the same on both half cycle but different amounting to 3:1 are normal. There is certain degree of random variation in both amplitude and location of discharge in succeeding cycle.	The discharge magnitude inception is clearly above minimum detectable level. There is little or no variation on discharge magnitude as voltage is raised the extinction voltage is equal to or slightly below the inception voltage.	The time of voltage application usually has little effect.	Internal discharge in a dielectric bond cavity. If a response having greater discharge magnitude occurs at a higher voltage this indicates discharge in second cavity. Typical discharges due to voids in cable insulation	Figure-2.20 (a)
2	The discharges occur in advancement of test voltage peaks but are asymmetric. There is a certain degree of random variation in both amplitude and location of discharges in succeeding cycles.	-do-	- do-	Internal discharges between metal and dielectric in a cavity. Typical discharge due to improper adherence of cable insulation with either conductor or screen.	Figure-2.20 (b)

Case	Discharge pattern	Effect of voltage	Effect of time	indication	Display on detection & origin
3	Same as case II except that the number of discharges increase with test voltage.	Same as above except that the discharge magnitude increase steadily as voltage is raised above inception.	-do-	Surface discharges talking place between external metal and dielectric surface typical discharges due to improper end terminations of a cable.	Figure-2.20 (c)
4	Similar as case I response.	If the voltage is raised to its maximum value, then quickly lowered, the characteristic is similar to for cable I discharge.	The discharge magnitude falls with time but the extinction voltage becomes higher.	The behavior describe has been found in cable insulation containing a cavity in form of fissure in the direction of electric field.	Figure-2.20 (d)
5	The discharge occur on one half cycle of the test wave form only asymmetrically disposed about the voltage peak and all of them are equal in magnitude and are equally spaced in time.	There is no change in discharge magnitude as the voltage is raised and the magnitude remains constant as the voltage lowered. The extinction voltage coincides with inception voltage	The response is normally unaffected by the time for which the test voltage is applied.	External corona discharge from sharp metal points.	Figure-2.20 (e)

Case	Discharge pattern	Effect of voltage	Effect of time	indication	Display on detection & origin
6	Coarse and irregular usually unresolved symmetrically distributed about test voltage zeros, but the amplitude is zero near the test voltage peaks.	The magnitude usually increases slowly and proportionally with voltage. It is also observed that it may disappear completely at a particular voltage level and be absent for all voltages above that level.	The response is normally unaffected by the time for which the test voltage is applied.	Contact noise due to imperfect metal to metal joints.	Figure-2.20 (f)
7	Groups of low frequency oscillations located on the test voltages peaks.	The response is usually undetectable in lower range of voltage & grows rapidly as voltage approaches highest rated voltage of the test transformer	-do-	Harmonics generated by test transformer core.	Figure-2.20 (g)

## **Chapter-3**

# **Measurement and Analysis of Solid Insulating material Ageing Test Under the Effect of Temperature on Partial Discharges**

### 3.1 INTRODUCTION

During the last thirty years, a large amount of research has been done on new dielectric materials to study their endurance for electrical, mechanical, thermal and other stresses. <sup>[4]</sup> Also, both the users and manufacturers of electrical power equipment are interested in multi-factor functional testing of the related insulation systems in order to validate the assessment of their service performance. Indeed, there is not much literature available concerning to this subject and that's why many researchers study the dielectric ageing phenomena on elementary insulation systems under multi stress conditions in accelerated ageing tests. <sup>[4, 8]</sup> It should be emphasized that the degree of insulation deterioration is actually dependent on the applied stress factors or factors of influence (voltage, temperature, pressure and so on) and on their interaction as well, that could in principle, accelerate or slow down the ageing rate due to the nonlinear phenomena involved with respect to a single applied stress. This matter is widely emphasized in the IEC publication 792-1 <sup>[58]</sup> in terms of 'the realistic modeling of service aging in a functional test, and the concern that tests be as simple and practical as possible.'

The ageing of insulating materials due to electrical field and thermal multistress has been extensively studied and modeled, <sup>[8, 11]</sup> but when a defect is present then partial discharge (PD) inception generally increases the degradation rate. In this case, even if the PD phenomenon can be considered as an effect of the applied voltage or electric field (primary stress), the temperature was found to assume the function of an indirect ageing factor mostly in changing the PD activity. <sup>[12-16]</sup> Furthermore, when an epoxy material is considered, a thermal stress which is lower than its material glass transition temperature should be considered for practical purposes, in order to keep its mechanical consistency as requested in service conditions. Here thermal stress which is higher than its material glass transition temperature is also considered for research purpose.

Studies on PDs have been generally approached by means of digital measurement systems <sup>[17-19]</sup>, mainly in order to post-process the data acquired. Making use of these technologies, it was evidenced that PD ageing mechanisms in epoxy resins as well as their related degradation effects in a simple dielectric configuration test, radically change at temperatures higher than the ambient. <sup>[20 21]</sup> Taking into account this basic concept, the purpose of this thesis is to define a life modeling procedure for the material lifetime estimation with stress conditions (which can deteriorate its performance). This goal has been pursued by observing the variation of PD (by varying quantities like voltage and temperature) with the use of digital measurement techniques.

The first step is to study and model the interaction between temperature and PD activity, in order to give an in-depth description of the model formulation that is in agreement with inverse power law. It is describes ‘a function  $S$  of the applied stress and the lifetime  $D$  (here expressed in hours).

$$D = \frac{k}{S^n} \quad \dots (3.1)$$

Where  $k$  and  $n$  are constants, which depend on the particular material under test. Following the idea that all degradation phenomena are always linked to the wasted energy, a model has been produced and it makes clear that energy dissipated inside the specimen under test is primary stress function, contrary to the case where the applied voltage ( $V$ ) is assumed in the same role. <sup>[25]</sup>

### 3.2 PD MEASUREMENTS FOR SOLID INSULATING MATERIALS AT DIFFERENT TEMPERATURES

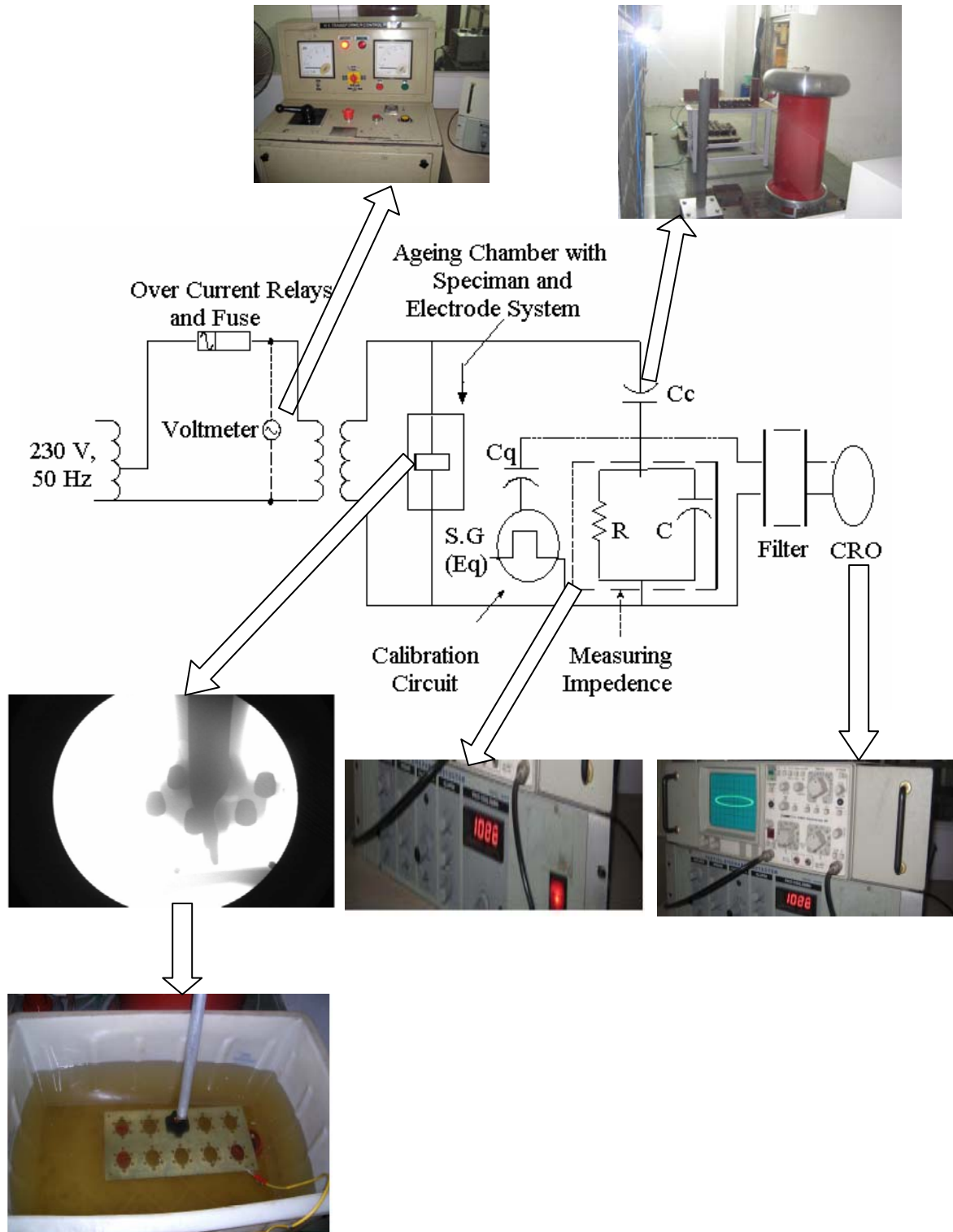


Figure-3.1 Electrical set up for PD Measurements

Electrical set up of partial discharge measurement is shown in figure-3.1 which follows IEC Standard No 60137 and IS 2099. A feeder silica Flore C epoxy resin: CY 225, Hy 925, generally used for bushing as switch gear of electrical power system manufacture, is used for investigation. This epoxy resin has its glass transition temperature in the range between 105°C and 120°C<sup>[22]</sup>. Each specimen (epoxy resin bushing) is passed through x-ray unit to observe its pin hole (cavity) size. Each specimen was connected to the test voltage by a mechanical connection as shown in Figure-3.1. To avoid air flashover the test cell was immersed in a silicon oil bath and temperature uniformity was ensured by an external pump arrangement. The testing procedure was based on 11 kV specimens under 50 Hz sinusoidal voltages, for four voltage values are inception voltage, extinction voltage, 15kV and 20 kV. Furthermore for each voltage, six temperatures  $T$  were applied, e.g. - 05°C, 30°C, 60°C, 100°C, 120°C and 150°C. Thus given twenty four test conditions for various combinations of the above thermal and electrical stresses. Also there were six specimen used for the testing purpose. Before PD testing, calibration of measuring circuit was performed according to section 4 of IS: 6209-1982. An experimental result gives PD values at different combination of voltage and temperatures stresses. Discharge pulses appearing at  $RLC$  impedance (180 kHz resonance frequency), were first filtered to remove any power frequency component. Then they were amplified by a wideband three-stage amplifier (30–800 kHz) and amplification factor was adjusted to provide wanted dynamic range which has sensitivity of 1 pC. At the end of the acquisition phase, further PD modeling and analysis was carried out.

### 3.3 PD MODELING <sup>[24-26]</sup>

To model the material life performance, varying applied voltage, for at particular temperature as previously outlined, a suitable stress function  $S$  imposed on the material must be chosen. Here,  $S$  is function of either the effect of PD or the indirect effect of temperature  $T$ . Furthermore, this should be performed by a mathematical formulation that  $S$  equivalent values able to reproduce lifetime  $D$  in agreement with equation (3.1) e.g. when  $S$  increases,  $D$  should decrease. Therefore, for modeling purposes, the first step consists of identifying the primary stress for the material that may be directly linked to the presence of PD at applied voltage  $V$  or the material constant  $k$  and  $n$ . Then the different temperature's effect can be quantified by a suitable mathematical function of the epoxy under test. The data distinction can be put forward between the temperature, applied voltage and lifetime. Now all the data depends only on  $T$  and leaves the voltage appearing as invariant parameter. The resulting curve can be fitted by the following parabolic function in order to consider the increasing & decreasing life trend below & above 0.7–0.8 of  $T_g$  Respectively. <sup>[25]</sup>

$$C\left(\frac{T}{T_g}\right) = \frac{D(T)}{D(30)} = k_1\left(\frac{T}{T_g}\right)^2 + k_2\left(\frac{T}{T_g}\right) + k_3$$
$$C\left(\frac{T}{T_g}\right) = \frac{D(T)}{D(30)} = -0.69\left(\frac{T}{T_g}\right)^2 + 1.00\left(\frac{T}{T_g}\right) + 0.83 \quad \dots(3.2)$$

Where,  $k_1$ ,  $k_2$  and  $k_3$  are parameters depending on the epoxy material under test, and are obtained by a linear regression method.

## Experimental life data modeling

Voltage stress:

If a function of the equivalent stress imposed on the material is

$$S(V, T) = V/C (T/T_g)$$

Then it is possible to see that various data sets are now well approximated by a straight line in a log–log plot, where the y-axis stands for  $\log[S(V, T)]$  and the x-axis for  $\log[D]$  with  $D$  expressed in hours. The validity of the ‘inverse power law’ is inferred<sup>[25-26]</sup> and applying the linear regression techniques, the following numerical model was obtained.

$$D = k \left( \frac{V}{k_1 \left( \frac{T}{T_g} \right)^2 + k_2 \left( \frac{T}{T_g} \right) + k_3} \right)^{-n} = 2.72E + 8S^{-1.44} \quad \dots(3.3)$$

Therefore, it could be pointed out that the ‘inverse power model’, most widely employed for single stress,<sup>[24]</sup> can be applied in the multi-stress ageing studied here, by choosing a suitable function of the stress imposed, but the constants to be experimentally determined are five, viz.  $k$ ,  $k_1$ ,  $k_2$ ,  $k_3$  and  $n$ . Six life tests data have been obtained at six temperatures. This fact may be the result of the exponential form of the chosen function of the voltage (e.g. the ratio of  $V$  with  $C (T/T_g)$ ), while usually only one value of  $V$  is used.

### 3.4 RESULTS AND ANALYSIS

During experiments, several results were acquired and used in developed model.

#### LABORATORY EXPERIMENTS FOR DIFFERENT TEMPERATURE

The tendency of the lifetime variance with different temperature (each temperature with different voltage and vice versa) was observed. Variation in stress for other different epoxy resin systems <sup>[11-21]</sup> was also observed and this gives idea of the characteristic performance of such epoxy materials. Therefore, it could be inferred that under PD stress, the application of temperatures higher than the ambient and lower than a fraction of related  $T_g$  appears not to be detrimental conditions for the material's lifetime, <sup>[25]</sup> i.e.  $T/T_g$  is 0.7 to 0.8. This could probably be explained with a major epoxy softening that reduces the related erosion action of the PD impinging on the epoxy surface. <sup>[21]</sup> In contrast, the use of a temperature higher than above fraction of  $T_g$  would reverse this tendency because the resin becomes less homogeneous and loses its mechanical characteristics especially in the proximity of its  $T_g$ . The results reported <sup>[11, 19]</sup> were experimentally demonstrated that a maximum stress exists for the lifetimes when the ratio between the testing temperature  $T$  and the material glass transition temperature  $T_g$  is around 0.70–0.80. It infers a parabolic dependence between the applied voltage and  $T/T_g$ . Present experimental work is carried out 0.25-0.6 and 0.8-1.25 range of  $T/T_g$ . The off-line analysis of the acquired PD data gives some information regarding the ageing processes that take place in the resin. At different temperature PD increases with applied voltage <sup>[22]</sup> is shown figure-3.2. Around temperature 60°C PD magnitude increases drastically due to the may be rapid change in internal structure of the insulator. Sample data of practical observations are shown in Table-3.1. It is also shown that PD increment is proportional to applied voltage in range of 100°C to 150°C. This peculiarity was ascribed to an increase of the material work function with temperature and it could probably be generalized for epoxy materials. Behavior of PD with different temperature is shown in figure-3.2.

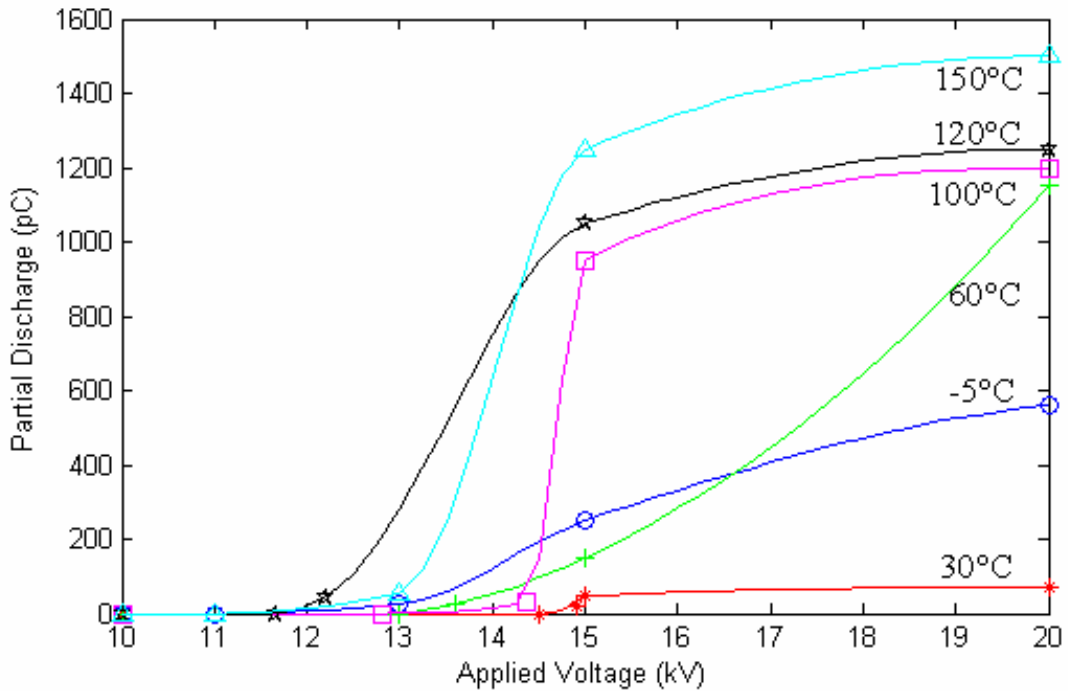


Figure-3.2 PD vs. Applied Voltage (kV) at Different Temperatures.

TABLE-3.1 APPLIED VOLTAGE AND PARTIAL DIACHARGE MEASUREMENTS

		Inception Voltage	Reading-1	Reading-2	Extinction Voltage
Temperature 30°C	Applied Voltage (kV)	14.9	15	20	14.5
	Partial Discharge (pC)	17	47	70	0
Temperature 60°C	Applied Voltage (kV)	13.6	15	20	13
	Partial Discharge (pC)	25	150	1150	0
Temperature 100°C	Applied Voltage (kV)	14.36	15	20	12.8
	Partial Discharge (pC)	30	950	1200	0
Temperature 120°C	Applied Voltage (kV)	12.2	15	20	11.65
	Partial Discharge (pC)	45	1050	1250	0
Temperature 150°C	Applied Voltage (kV)	13	15	20	11
	Partial Discharge (pC)	55	1250	1500	0
Temperature -5°C	Applied Voltage (kV)	13	15	20	11
	Partial Discharge (pC)	25	250	560	0

## EXPERIMENTAL LIFE DATA MODELING

The deterministic proposed model describes the ageing behaviors of insulation systems; because it is actually characterized by a random nature of the lifetime  $D$ . Figure-3.3 to figure-3.8 shows stress - life at different temperatures. Table 3.2 shows value of life and stress at different temperatures.

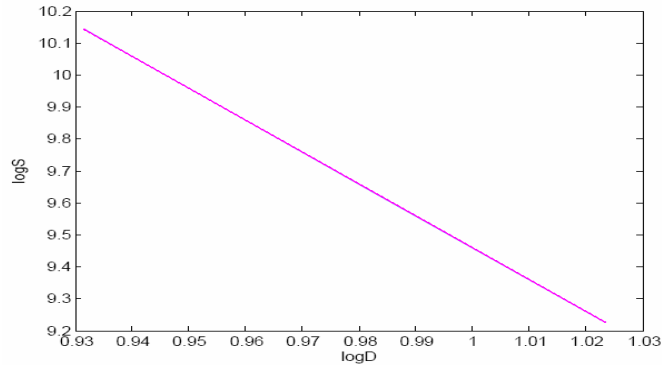


Figure 3.3- Stress Vs life at -5° C Temperature

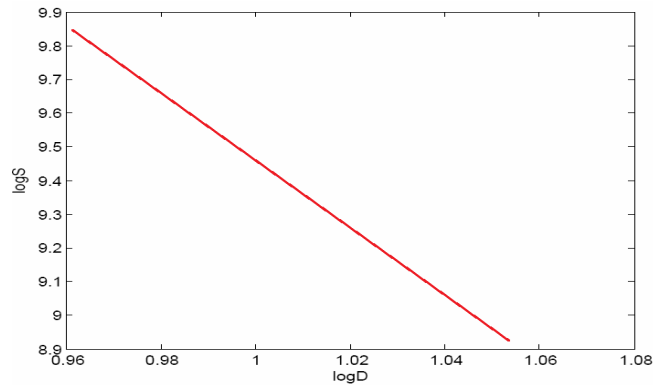


Figure-3.4 Stress Vs life at 30 ° C Temperature

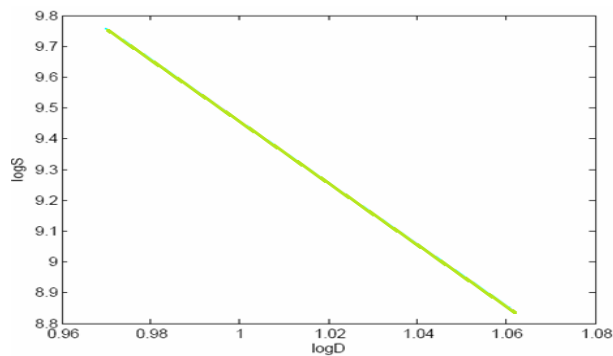


Figure-3.5 Stress Vs life at 60° C Temperature

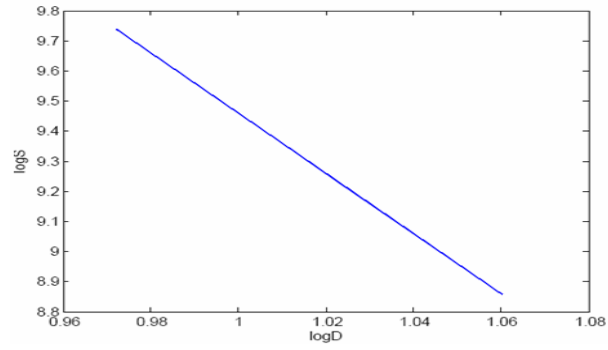


Figure-3.6 Stress Vs life at 100 ° C Temperature

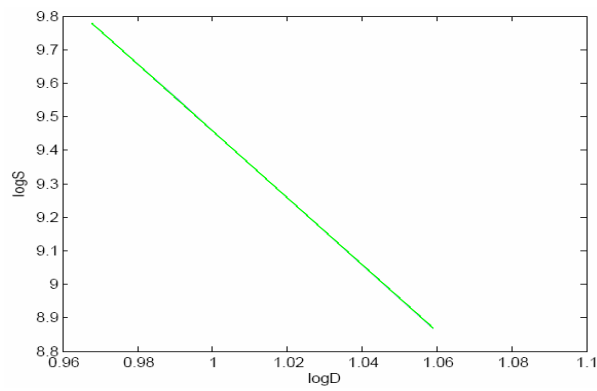


Figure-3.7 Stress Vs life at 120 ° C Temperature

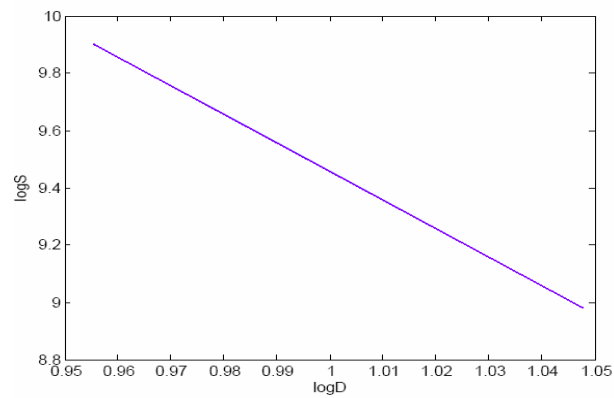


Figure-3.8 Stress Vs life at 150 ° C Temperature

TABLE-3.2 STRESS AND LIFE AT DIFFERENT TEMPRATURES

Temperature	Stress at constant voltage (log S)	Life (log D)
30° C	9.85	1.055
60° C	9.9	1.063
100° C	9.92	1.061
120° C	9.94	1.059
150° C	9.95	1.044
-5° C	10.15	1.025

### 3.4 CONCLUSION

The present work introduces an experimental approach to obtain phenomenological and statistical life models based on the inverse power law, which has been defined and discussed in this thesis. The main goal is to describe the life behavior of epoxy resin systems subjected to partial discharge activity under varying temperature from -5 °C to 150 °C. These different ratios of  $T/T_g$  are examined, even if PD phenomenon could be considered as an effect of the applied voltage, the temperature is assumed as the function of an indirect factor of ageing which attributes mostly to changing the PD activity. The basic modeling concept was to choose a suitable quantity to be assumed as the stress function and that is most indicative of the real working conditions for the materials. After modeling the interaction between the temperature and PD activity, the conclusions is derived that stress increases and life decreases with respect to ratio of  $T/T_g$  equal to 0.8 to 1.25. Also, the average life increases when ratio of  $T/T_g$  is 0.25 to 0.6. It has an almost linear trend with ageing time and that fruitfully can be used for modeling purposes. The major feature of this model is that it provides a means of connecting the physics and statistics of the breakdown process. Obviously, the results reported here cannot be extrapolated directly to complex insulating systems, but it could be considered as a useful and necessary starting point again for future research work to be explored in epoxy embedded electrical components.

## **Chapter-4**

# **Wavelet Transform**

## 4.1 INTRODUCTION <sup>[27]</sup>

The most common representation of signals and waveforms is in the time domain. However the most signal analysis techniques work only in the frequency domain. The concept of the frequency domain representation of a signal is quite difficult to understand when anyone is first introduced to it. The following section attempts to explain the frequency domain representation of signals.

### TIME AND FREQUENCY DOMAIN

The frequency domain is simply another way of representing a signal. For example, consider a simple sinusoid as shown in Figure 4.1.

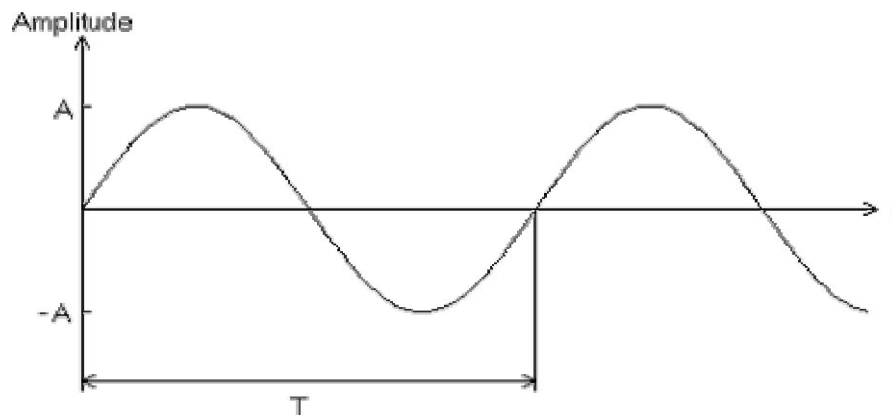


Figure-4.1 A Simple Sinusoidal Function

The time – amplitude axes on which the sinusoid is shown define the time plane. If an extra axis is added to represent frequency, then the sinusoid would be as illustrated in Figure-4.2.

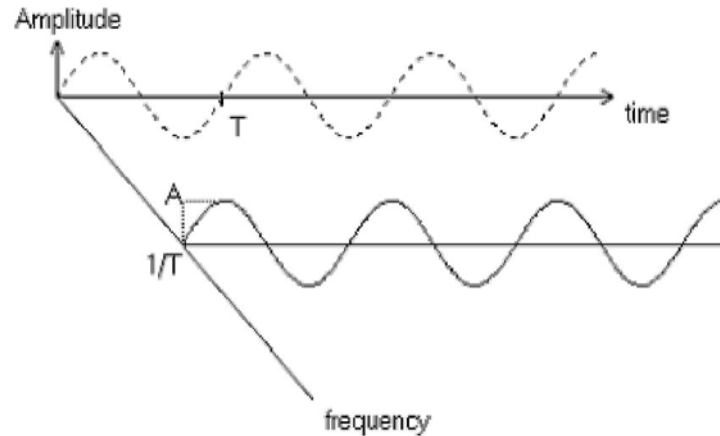


Fig.4.2 Time – Frequency Representation of a Sinusoidal Function

The frequency – amplitude axes define the frequency plane in a similar manner to the way the time plane is defined by the time – amplitude axes. This frequency plane represents the frequency spectrum of the original signal with respect to time. The frequency plane is orthogonal to the time plane, and intersects with a line which is the amplitude axis itself. Note that the time signal can be considered to be the projection of the sinusoid onto the time plane (time – amplitude axes). The actual sinusoid can be considered as existing some distance along the frequency axis away from the time plane. This distance along the frequency axis is the frequency of the sinusoid, equal to the inverse of the period of the sinusoid.

The waveform also has a projection onto the frequency plane. If you imagine yourself standing on the frequency axis, looking toward the sinusoid, you would see the sinusoid as simply a line. This line will have a height equal to the amplitude of the sinusoid. So, the projection of the sinusoid onto the frequency plane is simply a line equal to the amplitude of the sinusoid.

These two projections means that the sinusoid appears as a sinusoid in the time plane (time –amplitude axes), and as a line in the frequency plane (frequency – amplitude axes) going up from the frequency of the sinusoid to a height equal to the amplitude of the sinusoid.

It should be noted very carefully that all the information about the sinusoid (frequency, amplitude and phase) is represented in the time plane projection, but phase information is lost in the projection onto the frequency plane. If the full signal is to be reconstructed from the frequency representation then an additional graph called the phase diagram is needed. The phase diagram is simply a graph of the phase versus frequency, similar to the amplitude versus frequency graph obtained from the frequency plane.

## 4.2 DISCRETE FOURIER TRANSFORM (DFT) AND FAST FOURIER TRANSFORM (FFT) [28-44]

### INTRODUCTION

The Fourier Transform provides the means of transforming a signal defined in the time domain into in the frequency domain. When a function is evaluated by numerical procedures, it is always necessary to sample it in some fashion. This means that in order to fully evaluate a Fourier transform with digital operations, it is necessary that the time and frequency functions be sampled in some form or another. Thus the digital or Discrete Fourier Transform (DFT) is of primary interest.

### THE FOURIER TRANSFORM

The Fourier transform is used to transform a continuous time signal into the frequency domain. It describes the continuous spectrum of a non-periodic time signal. The Fourier transform  $X(f)$  of a continuous time function  $x(t)$  can be expressed as :

$$X(f) = \int_{-\infty}^{+\infty} x(t) (e^{-i2\pi ft}) dt \quad \dots(4.1)$$

The Inverse transform is:

$$X(t) = \int_{-\infty}^{+\infty} X(f) (e^{i2\pi ft}) df \quad \dots(4.2)$$

### THE DISCRETE FOURIER TRANSFORM (DFT)

This is used in the case where both the time and the frequency variables are discrete (where digital computers are being used to perform the analysis). Let  $x(nT)$  represent the discrete time signal, and let  $X(mF)$  represent the discrete frequency transform function. The Discrete Fourier Transform (DFT) is given by

$$X(mF) = \sum_n x(nT) e^{-inm2\pi FT} \quad \dots(4.3)$$

Where

$$x(nT) = \frac{1}{N} \sum_m (mF) e^{inm2\pi FT} \quad \dots(4.4)$$

## **THE FAST FOURIER TRANSFORM (FFT)**

The fast Fourier transform (FFT) is simply a class of special algorithms which implement the discrete Fourier transform with considerable savings in computational time. It must be pointed out that the FFT is not a different transform from the DFT, but rather just a means of computing the DFT with a considerable reduction in the number of calculations required.

Since this section is intended as an introduction to the Fourier transform, a rigorous development of the underlying theory of the FFT will not be attempted here. While it is possible to develop FFT algorithms that work with any number of points, maximum efficiency of computation is obtained by constraining the number of time points to be an integer power of two, e.g. 1024 or 2048.

## **APPLICATIONS OF FFT**

Once the waveform has been acquired and digitized, it can be Fast-Fourier-Transformed to the frequency domain. The FFT results can be either real and imaginary, or magnitude and phase, functions of frequency. The choice of output format belongs to the user. Since the FFT generates the frequency spectrum for a time domain waveform, some fairly simple applications, e.g., harmonic analysis, distortion analysis, vibration analysis, and modulation measurements, might suggest themselves immediately. Another important area is that of frequency response estimation. A linear, time-invariant system can be stimulated with an impulse function. Its output,

the impulse response, then can be acquired and converted it into to the frequency domain. The FFT of the impulse response, referred to as the frequency response function, completely characterizes the system. Once a system's frequency response function is known, one can predict how that system will react to any waveform. This is done by Convolution. An important aspect of the FFT is that convolution can easily be performed through frequency-domain multiplication. For instance, a system's impulse response is given by  $h(t)$ , and an input waveform is given by  $x(t)$ . The output, say  $y(t)$ , caused by  $x(t)$ , can be computed in the classical manner by the convolution integral. But this is tedious and slow. An easier and faster approach is to FFT  $x(t)$  and  $h(t)$  to the frequency domain. Then the product of their frequency domain functions can be formed, giving  $Y(f) = X(f) \cdot H(f)$ . This product corresponds to time domain convolution, and the convolution result can be obtained by Inverse-Fourier-Transform (IFT) of  $Y(f)$ .

Correlation is another useful operation that the FFT makes easier. Mathematically, correlation looks and is performed in a manner similar to convolution. The difference is that one of the frequency domain functions is conjugated before the frequency domain product is formed.

Although the operations of convolution and correlation may look similar, their applications are not. Correlation is a sort of searching or looking for similarities between two waveforms. When two waveforms are different, like uncorrelated noise, their correlation function is zero. On the other hand, correlation of two waveforms that is exactly alike will produce a perfect correlation function.

This property of finding similarities makes correlation a useful tool for detecting signals that are hidden or masked by other signals.

Another useful property of correlation is its ability to indicate delay. This is particularly useful in measuring things like path delay, path diversity, and echo return times.

### **4.3 INTRODUCTION TO WAVELET TRANSFORMS** <sup>[28-41]</sup>

The wavelet transform is a mathematical tool that cuts up data, functions or operators into different frequency components, and then studies each component with a resolution matched to its scale. For example, in signal analysis, the wavelet transform allows us to view a time history in terms of its frequency components, which means it maps a one-dimensional signal of time,  $f(t)$ , into a two dimensional signal function of time and frequency. The wavelet transform represents the signal as a sum of wavelets at different locations (positions) and scales (frequency bands). The wavelet coefficient essentially shows the strength of the contribution of the wavelets at these locations and scales.

Next section of this chapter is devoted to the general introduction of wavelet transform and its applications in the PD. Wavelet types, conditions, efficiency, basic mathematics and applications to partial discharges are illustrated.

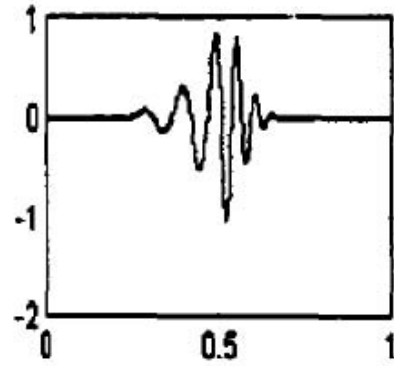
#### **WAVELET AND MULTI-RESOLUTION**

A wavelet is a small wave, which has its energy concentrated in time to give a tool for analyzing the transient, non-stationary, or time-varying phenomena. A wavelet still has oscillating wave-like characteristics but has the ability to allow simultaneous time and frequency analysis with a flexible mathematical foundation. Different wavelets are shown in Figure-4.3.

The wavelet transform can be accomplished in three different ways namely as: the Continuous Wavelet Transform (CWT), the Wavelet Series (WS) and Discrete Wavelet Transform (DWT).



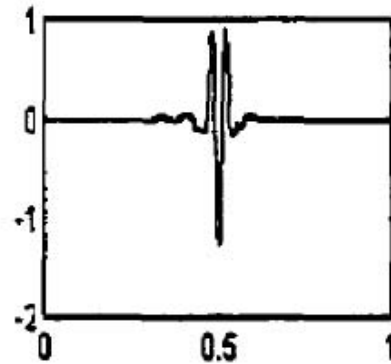
***Daubechies-4***



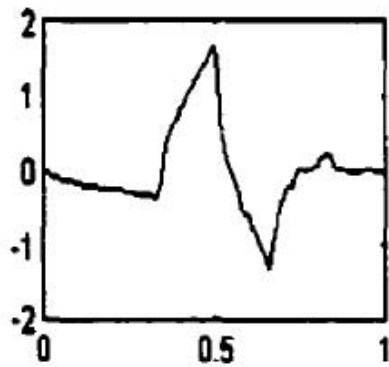
***Daubechies-10***



***coiflet-2***



***coiflet-5***



***symlet-2***



***symlet-8***

Figure-4.3 Examples of Different Wavelet Functions

The discrete wavelet transform (DWT) is sufficient for most practical applications in de-noising the signal and for reconstruction of the PD signal. It provides enough

information, and offers an enormous reduction in the computation time. It is considerably easier to implement when compared to the continuous wavelet transform. The discrete wavelet coefficients measure the similarity between the signal and the scaled and translated versions of a scaled wavelet  $\Psi_{a,b}$ .

On the other hand, Multi-Resolution Analysis (MRA) is used to analyze a signal at different frequencies with different resolutions. The goal of MRA is to develop representations of a complicated signal  $f(t)$  in terms of several simpler ones and study them separately. This goal will help to achieve two important properties. The first is the localization property in time of any high frequency signal, and the second is the presence of specific frequencies at different resolution levels.

The DWT uses selected wavelets as digital Filters with different cutoff frequencies to analyze a signal at different scales. In MRA, the signal is passed through a series of discrete filters “selected mother wavelet” to analyze and localize the high and the low frequencies that embedded in the signal.

## **WAVELET PROPERTIES**

Wavelet has three main properties:

- They build blocks to decompose and reconstruct signals. This means complicated signals can be decomposed and represented as simple building blocks in terms of the selected wavelets.
- The wavelet expansion gives a Time-frequency localization of the signal. This means most of the energy of the signal is well represented by a few expansion coefficients that are localized in the time and frequency domains.
- The calculation of the wavelet coefficients from the signal can be done efficiently. This means that by using orthogonal wavelets, the distorted signal coefficients in the wavelet domain are simply given as the inner product of the

signal with the wavelet function, which greatly simplifies the transform algorithm<sup>[24-30]</sup>

## **WAVELET EFFICIENCY**

Wavelet transforms have been proven to be very efficient in signal analysis. With reference to above mentioned properties of the wavelet transform, the following advantages can be gained:

- Wavelet expansion coefficients represent a component that is itself local and are easier to interpret. Therefore, the location of these coefficients can be used to detect and localize any sudden change in the PD signal due to noise or abnormal system condition. Furthermore, the energy of these coefficients will assist in extracting features that can classify such transient signal in terms of its magnitude, frequency components and duration.
- MRA that decomposes a signal at different resolution levels will allow a separation of components that overlap in both time and frequency. This property will be useful in detecting and classifying multiple transient events that may take place in the same monitored window.
- The wavelet transform coefficients represent the energy of the transient signal. These coefficients will be used to measure the magnitude of the transient signal and quantify the transient events.
- The rapidly drop off in the size of the coefficients, with increasing translation and scaling factors, will assist in representing the transient event by using only small number of coefficients. This will help in designing an automated recognition system that has the ability to store a large number of transient events using a small number of coefficients.

- MRA and DWT calculations are efficiently performed by digital computers. Discrete wavelet transform (DWT) computation relies on convolution and decimation or interpolation. These operations depend on addition and multiplication. Furthermore, the number of mathematical operations for DWT is in the order of  $(N)$  Which is lower than that for the Fast Fourier Transform (FFT) algorithm which needs  $(N \log(N))$ operations. This computational speed feature of the DWT will help in implementing the automated recognition system on-line and for real time applications.

## **4.4 WAVELET AND MULTI-RESOLUTION ANALYSIS MATHEMATICAL REPRESENTATION<sup>[27, 42-44]</sup>**

### **GENERAL INTRODUCTION**

The Wavelet transform will be proposed in this thesis as a tool to remove noise and detect PD pulses from the acquired data. Using wavelet properties, detection, discrimination, localization and classification of any unwanted signal like noise occurrences in the PD signal can be removed.

#### **General Mathematical Preliminaries**

The purpose of this section is to introduce to the mathematical notations and tools which are useful to present Wavelet Transform theory. Some definitions of vector spaces and related mathematical relations are introduced.

### **VECTOR SPACES**

The totality of vectors that can be constructed by scalar multiplication and vector addition from vectors in a given set is called a vector space. A set of vectors that is capable of generating the totality of vectors by these operations is said to span the space. If the set consist of the least number of vectors that span the space, the set is called a Basis of the space. The number of vectors in the basis is called the dimension of the space. N-basis vectors generate an n-dimensional space. Any subset of r-basis vectors from the basis of an r-dimensional subspace.

### **NORMS**

The concept of the distance is generalized in the case of vectors through the use of norms. The norm of a vector  $x$ ,  $\|x\|$  is a real non negative number such that:

$$\|x\| = 0 \text{ if and only if } x = 0$$

$$\|Cx\| = |C|\|x\| \text{ For all scalars } c \text{ and vectors } x \quad \dots(4.5)$$

$$\|x_1 + x_2\| \leq \|x_1\| + \|x_2\| \text{ For all } x_1 \text{ and } x_2 \quad \dots(4.6)$$

There exist many norms for vectors. Three of the commonly used ones are:

$$\|x_1\| = \sum x_i$$

$$\|x_2\| = \sqrt{\sum |x_i|^2}$$

$$\|x\|_\infty = \max |x_i| \quad \dots(4.7)$$

## INNER PRODUCT

It is a scalar “a” obtained from two vectors  $f(t)$  and  $g(t)$ , by an integral. It is denoted as:

$$a = \langle f(t), g(t) \rangle = \int f(t)g(t)dt \quad \dots(4.8)$$

The length of a vector “norm” can be defined in terms of the inner product as:

$$\|f(t)\| = \sqrt{|\langle f(t), g(t) \rangle|} \quad \dots(4.9)$$

## HILBERT SPACES

It is a complete inner product space with orthogonal basis, where any signal

$f(t) \in L^2(\mathbb{R})$  satisfies the following condition:

$$\int_{-\infty}^{\infty} |f(t)|^2 dt < \infty \quad \dots(4.10)$$

This means that the signal  $f(t)$  has finite energy.

## **BASIS**

A set of vectors  $\Phi_k(t)$  spans a vector space  $F$ . If any element  $f(t)$  in that space can be expressed as a linear combination of members of that set. This means that  $f(t)$  can be written as:

$$f(t) = \sum_k a_k \phi_k(t). \quad \dots(4.11)$$

With  $k \in Z$  the set of integers and  $a, t \in R$ .  $\Phi_k(t)$  is known as the expansion set and  $a_k$  is known as the expansion coefficients. The expansion set  $\Phi_k(t)$  forms a basis set or basis if the set of expansion coefficients  $\{a_k\}$  are unique for any particular  $f(t) \in F$ . There may be more than one basis for a vector space. However, all of them have the same number of vectors, and this number is known as the dimension of the vector space.

The expansion set  $\Phi_k(t)$  forms an orthogonal basis if its inner product is zero:

$$\langle \phi_k(t), \phi_l(t) \rangle = 0 \text{ For all } k \neq l \quad \dots(4.12)$$

The expansion set  $\Phi_k(t)$  forms an orthogonal basis if the inner product can be represented as:

$$\langle \phi_k(t), \phi_l(t) \rangle = \delta(k-l) = \begin{cases} 0 & k \neq l \\ 1 & k = l \end{cases} \quad \dots(4.13)$$

This means that in addition of being orthogonal, the basis is normalized to unity norm.

$$\|\phi_k(t)\| = 1 \text{ for all } k \quad \dots(4.14)$$

For an orthonormal basis, the set of expansion coefficients  $\{ a_k \}$  can be calculated using the inner product,

$$a_k = \langle \phi_k(t), f(t) \rangle \quad \dots(4.15)$$

Therefore, having an orthonormal basis, any element in the vector space  $f(t) \in F$ , can be

written as:

$$f(t) = \sum_k \langle \phi_k(t), f(t) \rangle \phi_k(t). \quad \dots(4.16)$$

This expansion formulation is extremely valuable. The inner product of  $f(t)$  and  $\Phi_k(t)$  produce the set of coefficients  $a_k$ . This set of coefficients  $a_k$ , can be used linearly with the basis vectors  $\Phi_k(t)$  to give back the original signal  $f(t)$ .

## 4.5 WAVELET TRANSFORM AND MULTILEVEL REPRESENTATION <sup>[27, 45-46]</sup>

The Wavelet Transform is a tool that can cut any signal into different frequency components and then study each component at a certain resolution level. The WT depends on two sets of functions known as scaling functions and wavelet functions. In order to implement a multi-level presentation of a signal, first define the scaling function and then use it to represent the wavelet function.

### THE SCALING FUNCTION

The scaling function  $\Phi(t)$  is a function that belongs to the Hilbert space. The scaling set  $\Phi_k(t)$  is defined as a set of integer translations of a basis scaling function  $\Phi(t)$ , where:

$$\phi_k(t) = \phi(t - k) \text{ for all } k \in Z; \phi_k \in L^2(R) \quad \dots(4.17)$$

and  $L^2(R)$  is the Hilbert space, which can be represented by a set of subspaces  $(V_j \{j \in Z\})$ , where  $Z$  is the set of integers.

The set of scaling functions  $\Phi_k(t)$  span the subspace  $V_0$  defined as:

$$V_0 = \text{span}[\phi_k(t)] = \text{span}_k \{\phi(t - k), k \in Z \} \quad \dots(4.18)$$

if  $f(t)$  is a finite energy signal  $\{f(t) \in L^2(R)\}$ , then an approximated version of  $f(t) \in V_0$ , can be represented in terms of the scaling function as shown in Figure-4.4 and can be expressed according to Equation 4.19 as:

$$f(t) = \sum_k a_k \phi_k(t) \quad \dots(4.19)$$

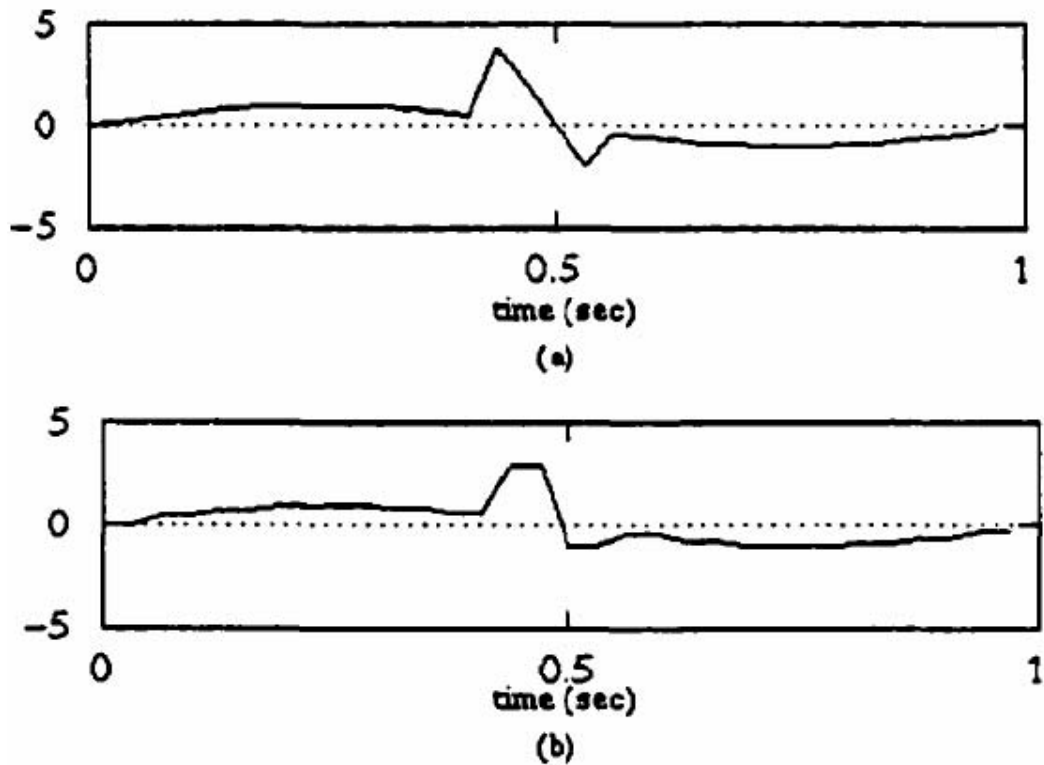


Figure-4.4 Approximation of (a) the Input Signal and (b) Approximation of the Input Signal using Haar Scaling Function

By contemplating the containment property, the scaling function  $\Phi(t)$  can be expressed in terms of a weighted sum of shifted  $\Phi(2t)$ :

$$\phi(t) = \sum h(n)\sqrt{2}\phi(2t-n), n \in Z \quad \dots(4.20)$$

Where the coefficients  $h(n)$  are a sequence of real or complex number called the scaling function coefficients (or the scaling filter coefficients) and the  $\sqrt{2}$  maintains the unity norm of the scaling function with the scale of two. This equation is called the multi-resolution analysis equation. It can be utilized to represent the signal at different resolution levels. This is presented in the following subsection.

## MULTILEVEL REPRESENTATION USING SCALING FUNCTION

In order to represent a signal  $f(t)$  at different resolution levels, the used scaling function  $\Phi(t)$  must be translated and scaled. Therefore, the two dimensional family of scaling function  $\Phi_{j,k}(t)$  is presented as:

$$\phi_{j,k}(t) = 2^{jl^2} \phi(2^j t - k) \quad \dots(4.21)$$

where,  $j$  is the scaling factor and  $k$  is the translation factor. This two dimensional family can span different subspaces ( $V_j \{j \in Z\}$ ) as:

$$V_j = \text{span}_k \{ \phi_{j,k}(t) \} = \text{span}_k \{ 2^{jl^2} \phi(2^j t - k) \} \quad \dots(4.22)$$

for all integers  $k$ .

This means that any signal  $f(t) \in L^2(\mathbb{R})$  can be approximated and represented at different resolution levels ( $f(t) \in V_j$ ), as:

$$f(t) = \sum_k a_k 2^{jl^2} \phi(2^j t - k) \quad \dots(4.23)$$

The multi-level representation of the signal  $f(t)$  is shown in Figure-4.5. The Haar scaling function is scaled and translated to represent the input signal at five resolution levels. As the scale  $j$  changes in Equation 4.23 changes, more details are added to the approximated version and a more similar version of the original signal can be achieved. These details, which exist in between each of the two approximated versions of the signal, are very important in analyzing and monitoring the original signal. These details can be extracted by using the wavelet function.

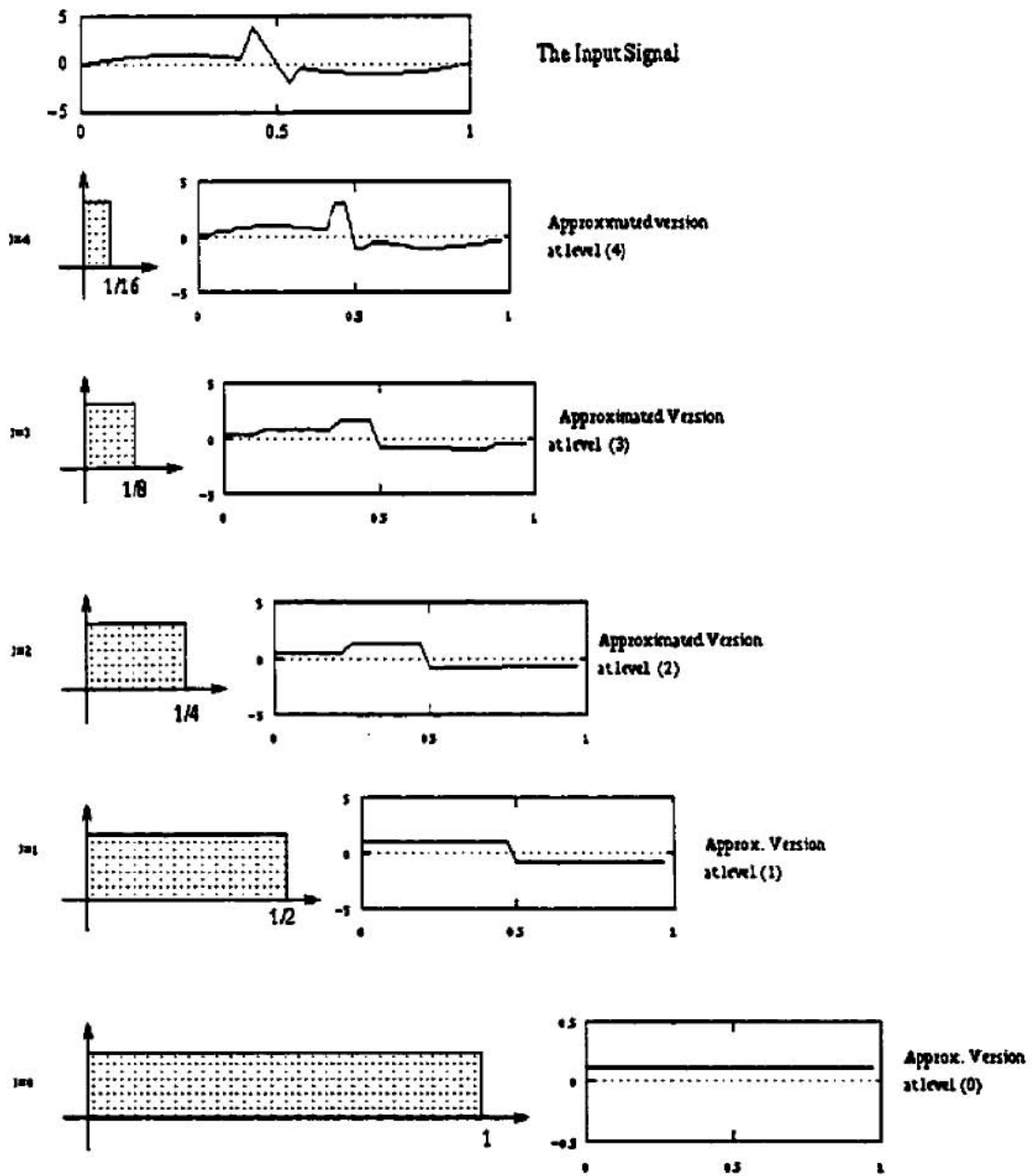


Figure-4.5 Multilevel Representation of an Input Signal using the Haar scaling function

## THE WAVELET FUNCTION

More important features of a signal can be extracted by using a function that spans the difference between various approximated versions obtained using the scaling function  $\Phi_{j,k}(t)$ . This can be achieved by using the wavelet function  $\Psi_{j,k}(t)$ . As indicated by the containment property, the subspace  $V_0$ , is embedded in the subspace  $V_1$ ,  $V_0 \subset V_1$ . In order to move to a finer subspace  $V_1$ , from a coarser subspace  $V_0$ , one must add another subspace in between, which is known as the complement subspace  $W_0$ . This is illustrated clearly in Figure-4.6. Since this wavelet resides in the space spanned by the next narrower scaling function, they can be represented by a weighted sum of shifted scaling functions at that space. For example  $\Psi(t)$  resides in the space  $W_0$ , and  $W_0 \subset V_1$ . Therefore,  $\Psi(t)$  can be represented by a weighted sum of shifted scaling function  $\Phi(2t)$ . This is illustrated in Figure-4.6 and mathematically can be presented by:

$$\psi(t) = \sum_n h_1(n) \sqrt{2} \phi(2t - n), \quad n \in \mathbb{Z} \quad \dots(4.24)$$

for some set of wavelet coefficients (wavelet Filter coefficients)  $h_1(n)$ , where.

$$h_1(n) = (-1)^n h(1 - n) \quad \dots(4.25)$$

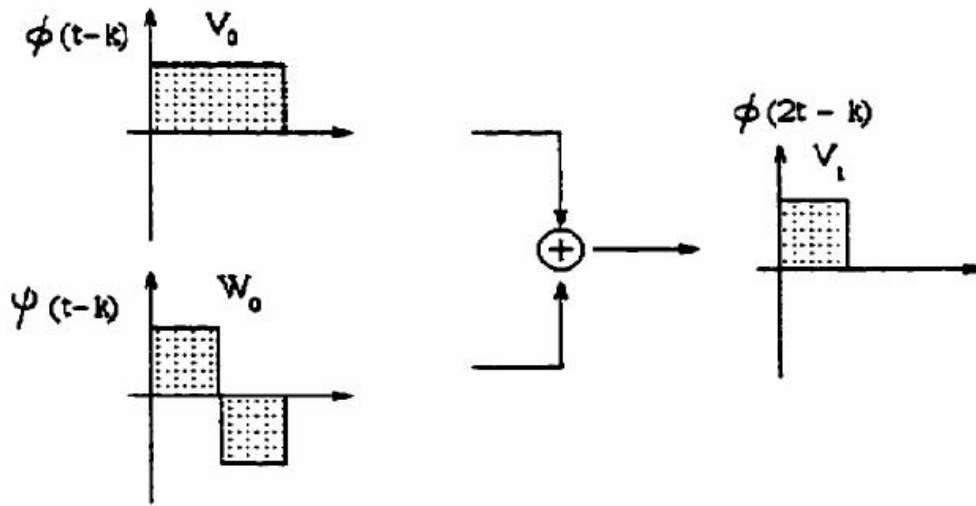


Figure-4.6 Moving to a Finer Space using the Wavelet,  $\Psi_{j,k}(t)$  and Scaling Function,  $\Phi_{j,k}(t)$   
 Again, the scaled wavelet function can be utilized to extract different details that reside in between different approximated versions of the signal. This will be discussed in the following subsection.

### MULTILEVEL REPRESENTATION USING THE WAVELET FUNCTION

As the scaling function  $\Phi_{j,k}(t)$  spans  $V_0$ , and  $\Phi_{l,k}(t)$  spans  $V_l$ , there are particular functions which spans  $W_0$ , and  $W_l$ . Therefore, as the scaling function  $\Phi_{j,k}(t)$  spans  $V_j$ , the wavelet function  $\Psi_{j,k}(t)$  spans  $W_j$ , Where  $W_j$  is the orthogonal complement of  $V_j$ . This means that all members of  $V_j$  are orthogonal to all members of  $W_j$ , ( $V_j \perp W_j$ ).

Therefore, the space  $V_j$  can be represented in terms of a set of subspaces where each subspace can be spanned using the scaling and wavelet functions. This is mathematically represented as:

$$V_j = V_{j-1} \oplus W_{j-1} = V_0 \oplus W_0 \oplus W_1 \oplus W_2 \oplus \dots \oplus W_{j-1} \quad \dots(4.26)$$

Therefore, any signal  $f(t) \in L^2(\mathbb{R})$  can be represented as a series expansion by using a combination of the scaling function and wavelets function:

$$f(t) = \sum_{k=-\infty} c_k \varphi(t-k) + \sum_{k=-\infty} \sum_{j=0} d_{j,k} \psi(2^j t - k) \quad \dots(4.27)$$

Where  $C_k$  is the approximated coefficient of the last approximated version and  $d_{j,k}$  is the detail coefficient at different scales.

Equation 4.27 represents the signal  $f(t)$  at different resolution levels in terms of one approximated version and different details that exist in between different approximated versions. The first summation gives the approximated version of the signal  $f(t)$  in terms of the scaling function. The second summation gives different details that can be extracted in terms of the wavelet function at different scales. The summation of the approximated version and the different detail versions will represent the original signals  $f(t)$ .

Figure-4.7 shows the details of the input signal at different resolution levels by using the Haar wavelet function. It is clear from the figure-4.7 that as the scale changes more resolution is achieved.

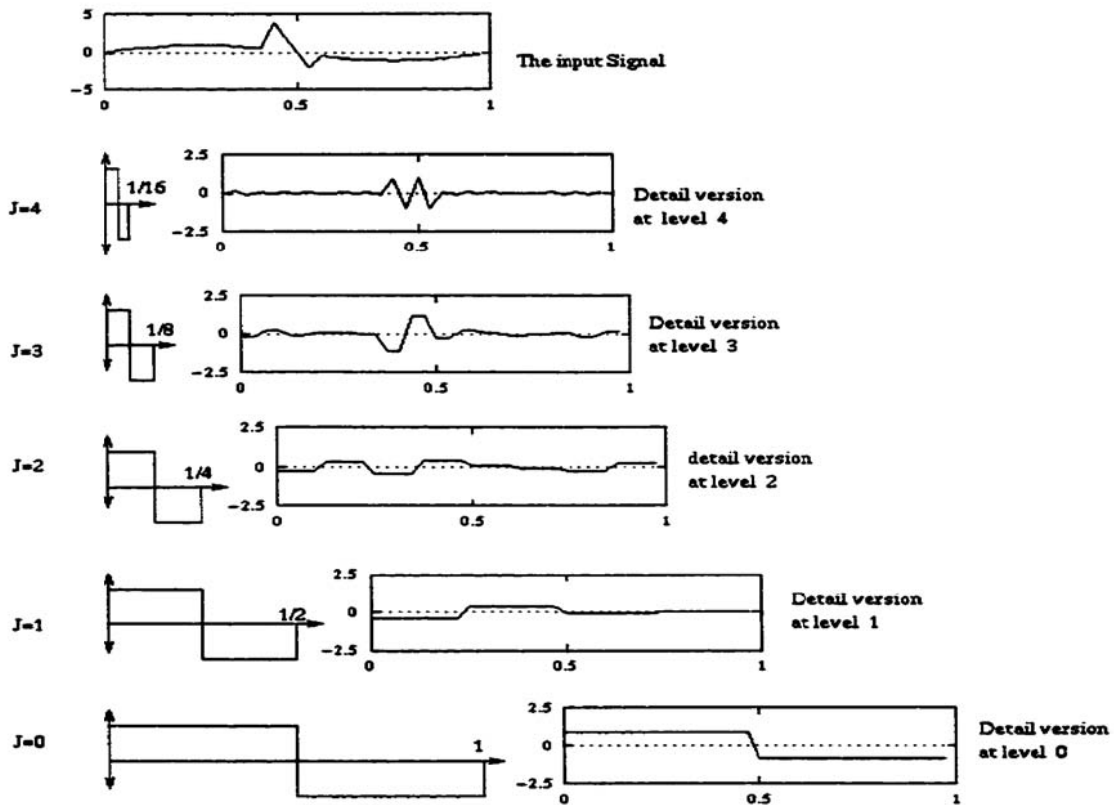


Figure-4.7 Multilevel Representation of an Input Signal using Wavelet Function

## MULTI RESOLUTION ANALYSIS

Multi-resolution analysis (MRA) is used to decompose any signal and represent it at different resolution levels. The goal of multi-resolution analysis (MRA) is to develop representations of a complicated signal  $f(t)$  in terms of several simpler ones and study them separately. This goal will help in achieving two important properties. The first is the localization property in time of any transient phenomena. And the second is the presence of specific frequencies at different resolution levels. In multi-resolution analysis, the signal is decomposed to find a time-frequency picture of the signal and then reconstructed to get back the original signal.

In MRA, the first stage divides the spectrum into two equal frequency bands; the second stage subdivides the lower frequency band into quarters, and so on. In other words, the Discrete Wavelet Transform (DWT) coefficients for any signal, periodic or non-periodic, can be computed by using a multi-rate filter bank. The total number of the resolutions that can be achieved depends on the number of sampling points, which can be controlled by the sampling frequency and the window size of the data. This is best explained by Figure-4.8.

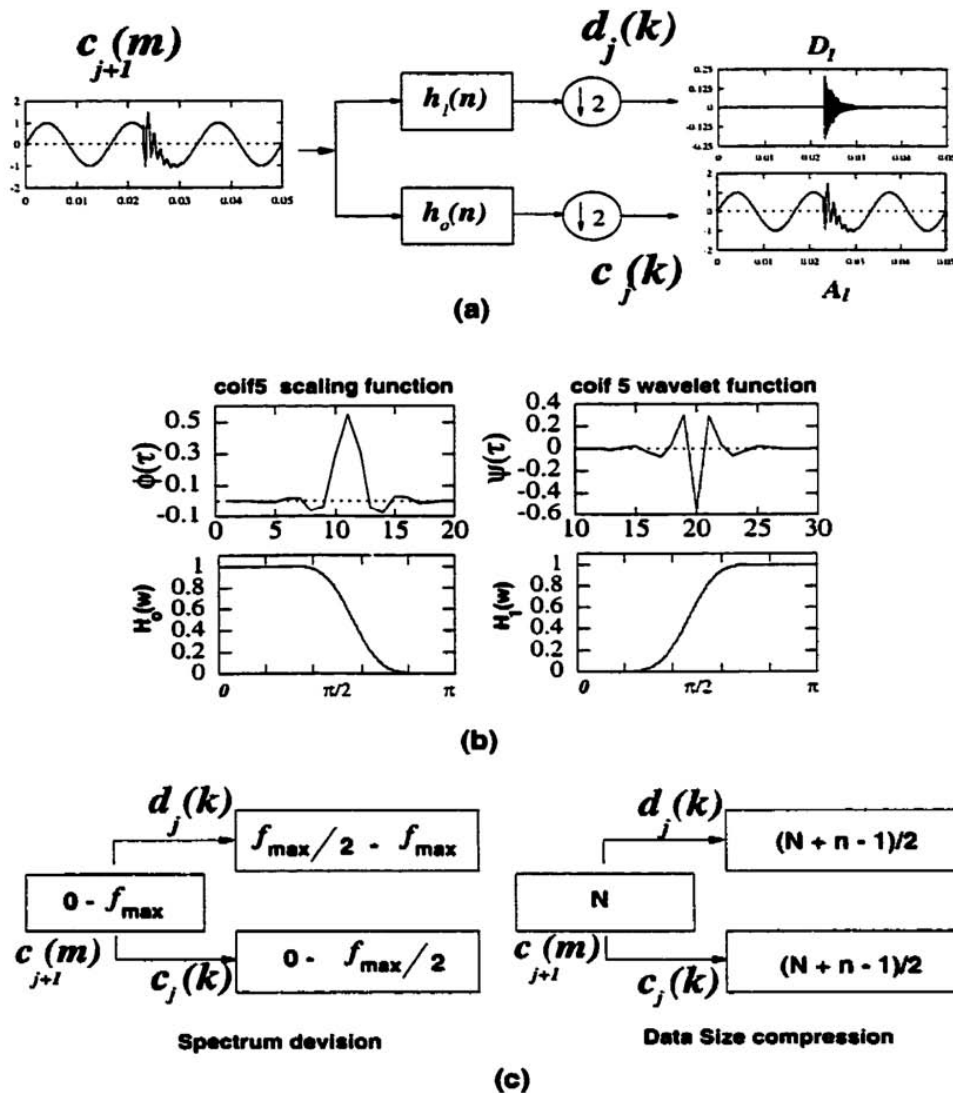


Figure-4.8 One Stage MRA and Wavelet Filters – (a) decomposing into detail and approximated version,(b) Coif-5 scaling and wavelet function and their frequency response,(c) Spectrum division and data size compression

In other words, an analysis filter bank efficiently calculates the discrete wavelet transform (DWT) using banks of digital filters and down-samplers, and the synthesis filter bank calculates the inverse discrete wavelet transform (IDWT) to reconstruct the signal from the transform. Figure-4.9 shows five-levels of multi-resolution signal decomposition using the Haar scaling and wavelet functions.

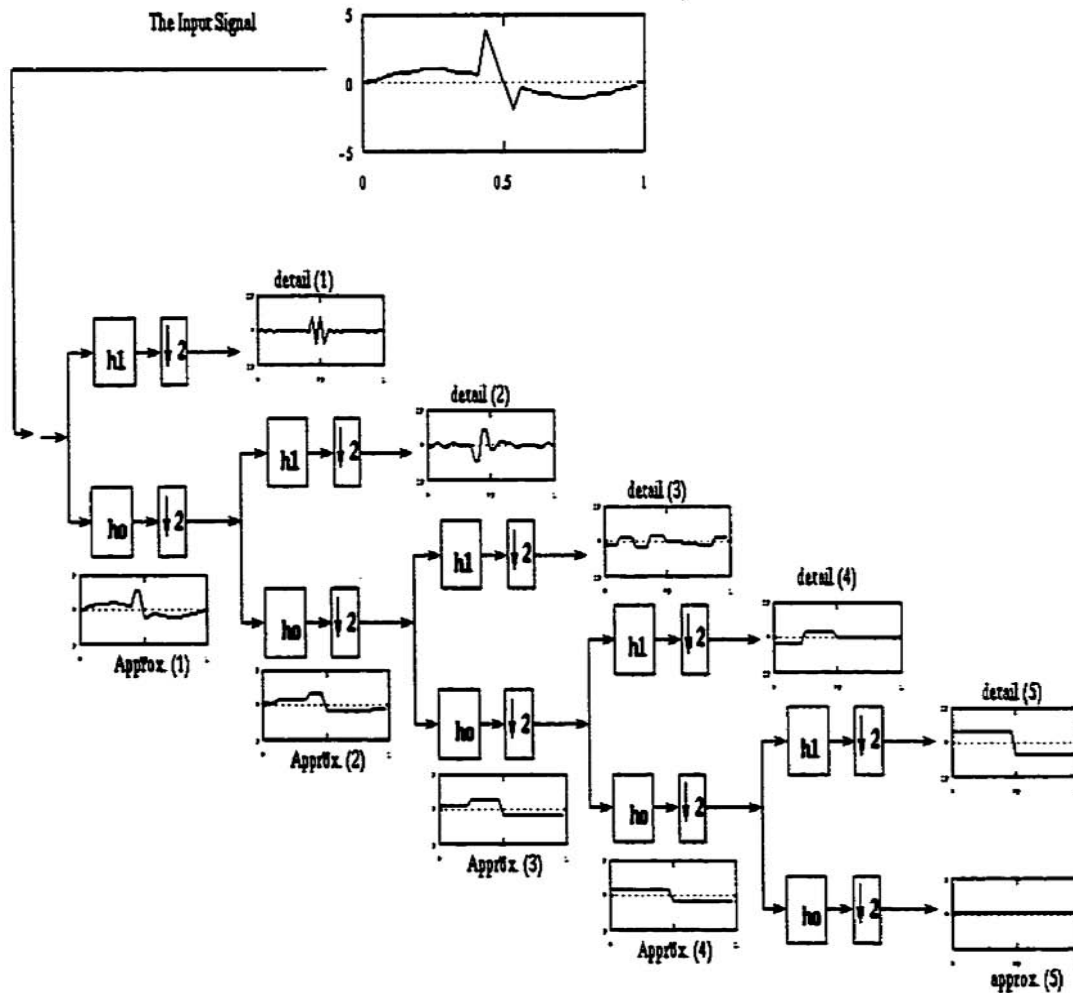


Figure-4.9 Five Level Multi-Resolution Signal Decomposition

#### 4.6 REVIEW OF WAVELET APPLICATIONS <sup>[45, 46]</sup>

Several works have been developed in many areas with the help of this tool, especially in the last ten years, the potential benefits of applying WT to power systems analysis and processing the voltage-current signals in order to make a real time identification of transients in fast and accurate way.

The aim of the following subsection is to provide a descriptive overview of the wavelet transform applications in power system especially to those who are novice in this subject study. For this purpose, the main publication carried out in this field have been analyzed and classified by application areas.

In the mainstream literature, wavelets were first applied to power system in 1994 by Robertson <sup>[45]</sup> and Ribeiro <sup>[46]</sup>. Since then, the number of publications in this area has been increasing substantially as shown in Figure-4.10.

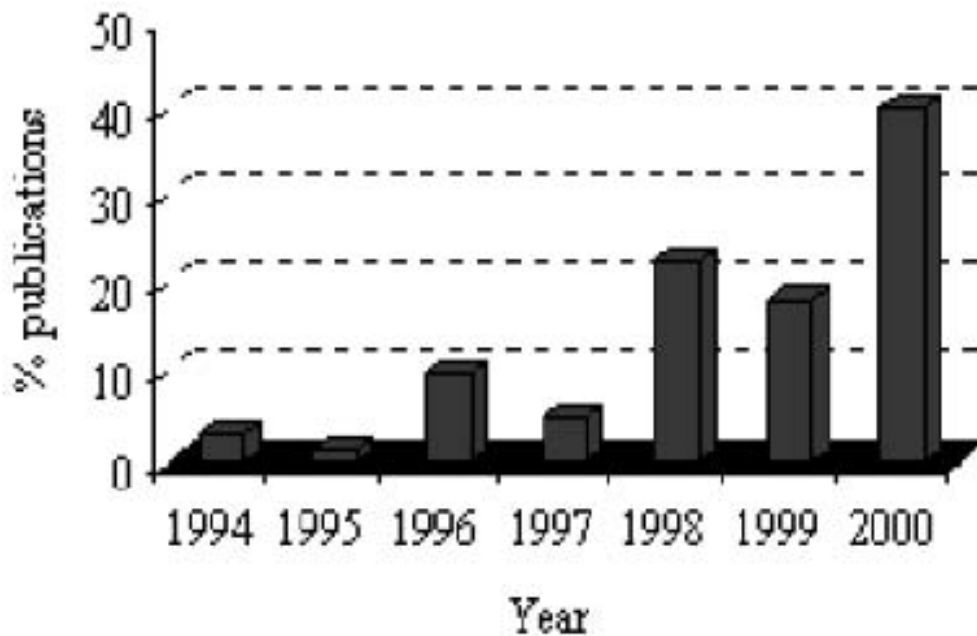


Figure-4.10 Evolution of Wavelet Publication in Power System

The main focus in the subsection has been on the identification and the classification methods from the measured signals analysis stand point. However, few works have been using wavelet transform as an analysis technique for the solution of voltages and currents which propagate throughout the system for example, a transient disturbance.

The most popular wavelet transform applications in power systems are:

- Power system protection
- Power quality
- Power system transients
- Partial discharges
- Load forecasting
- Power system measurement

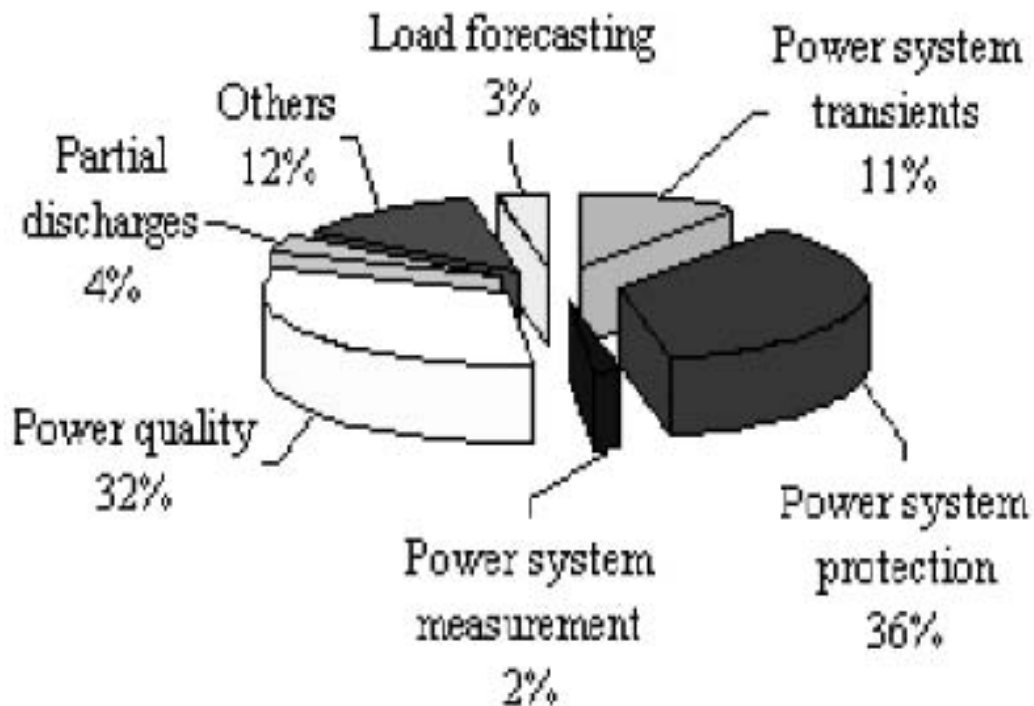


Figure-4.11 Percentage Usage of Wavelet publications in different power system areas

As shown in the PI chart of figure-4.11, wavelet transform is used in various areas of electrical engineering particularly related to the core work; wavelet transform is used for partial discharge analysis. Around 4% wavelet transform algorithms are used in partial discharge analysis.

#### **4.7 WAVELET TRANSFORM (WT) AS APPLIED TO PD ANALYSIS <sup>[47-49]</sup>**

The well-known Fourier analysis decomposes a signal into constituent sinusoids of different frequencies. During signal transformation Fourier Transformation lose time information. This is undesirable particularly when the signal is non-stationary. This kind of signals has great importance for their transitory characteristics. Short-Time Fourier Transform (STFT) is a method which can overcome such problems, which analyses the signal over a short time window. It maps signal into a two dimensional function, one is time and another is frequency. But, STFT has problem of resolution. Narrow window gives good time resolution, but poor frequency resolution whereas wide window gives good frequency resolution, but poor time resolution. Also, wide windows may violate the condition of non-stationary signal because time information is lost. Finally, the problem with STFT is to select appropriate window function which is to be used for all. In our case, low frequency and unknown repeatability rate PD pulses are merged with noise components. Hence, STFT does not solve problem for detecting PD pulses from mixed signal.

The WT is already developed to overcome some resolution related problems of the STFT. Wavelet analysis is an extension of STFT which allows variable-sized window and produces a time-scale view of the signal (instead of time-frequency). In essence, this technique decomposes a signal into shifted and scaled versions of an original (or mother) wavelet. It is capable of providing the time and frequency information simultaneously.

Wavelet Transforms have been successively applied to wide variety of research areas. Recently, wavelet analysis techniques have been proposed extensively in the literature as a new tool to be implemented in different power engineering areas. The wavelet transform analysis is proposed as a new tool for monitoring power system related problems.

The scaling property of the selected wavelet function is to be used in decomposing the signal, will assure the ability of the MRA technique to detect any transient event and localize it in the time and frequency domains. Selecting Ortho-normal wavelets, multi-resolution analysis will have the ability to distribute the energy of the distorted signal in terms of the expansion coefficients of the wavelet domain. Therefore both the expansion approximated and detail coefficients will give an indication about the energy content of the distorted signal in certain time and frequency bands. This feature can be used to classify different PD measuring system related problems. In contrast, the energy of the wavelet coefficients can be combined with the localization property to give a measure of the transient events like initiation of PD occurrence which may further deteriorate the system. The small value of the expansion coefficients will give an indication about the resolution levels that contains low energy of the transient signal and hence can be ignored for data compression purposes. This can reduce the large volume of transient's data to a manageable size. It will provide a higher quality of information about the PD events to be analyzed by power system engineers. Furthermore, the expansion coefficients of the highest resolution levels can be ignored for de-noising purposes.

WT has combination of high pass and low passes filters, which filters out either high frequency or low frequency components of the signal and there are many such filter stages. In WT, the time domain signal pass through various filters. At each stage some portion of the signal corresponding to some frequencies being removed from the signal. Wavelet has two basic prosperities shifting and scaling. Shifting a wavelet means delaying or hastening its onset. Scaling of a wavelet means stretching or compressing it. There is a correspondence between scaling and frequency. Low scale produces a compressed wavelet suitable for rapidly changing details and thus corresponds to high frequency. Similarly, high scale gives a stretched wavelet which characterizes slowly changing features and thus corresponds to low frequency.

Wavelet analysis is one of the techniques which efficiently removes random background noise and detect PD pulses. Wavelet decomposition is used to remove the high-frequency noise from the signal. Successive approximations become less noisy as more high frequency information is filtered out. Thus, this provides a simple method to de-noise the signal.

Signal decomposition can be achieved by various thresholding methods. It includes threshold value determination and threshold function selection.

There are four common methods used for threshold value determination. These methods are (1) Universal threshold rule; (2) Minimax threshold rule,(3) Stein unbiased risk threshold rule and (4) Level-dependent threshold rule.

There are two threshold functions available: Hard thresholding and Soft thresholding.

Hard thresholding processes data in such a way that those wavelets coefficients whose absolute values are greater than the threshold are kept while those less than the threshold are set to zero. Derived hard threshold function value  $\delta_{\lambda}^H$  is shown in equation-4.28.

$$\delta_{\lambda}^H(x) = \begin{cases} x, & \text{if } |x| > \lambda \\ 0, & \text{otherwise} \end{cases} \quad \dots(4.28)$$

Here, x is input value and  $\lambda$  shows threshold value. In Soft thresholding, the wavelet coefficients below the threshold normalized to zero and the coefficients greater than threshold are kept and then shrunk towards zero. Derived Soft threshold function value  $\delta_{\lambda}^S$  is shown in equation-4.29.

$$\delta_{\lambda}^S(x) = \begin{cases} x - \lambda, & \text{if } x > \lambda, \\ 0, & \text{if } |x| \leq \lambda, \\ x + \lambda, & \text{if } x < -\lambda, \end{cases} \quad \dots(4.29)$$

Hard and soft threshold values can be shown in figure-4.12.

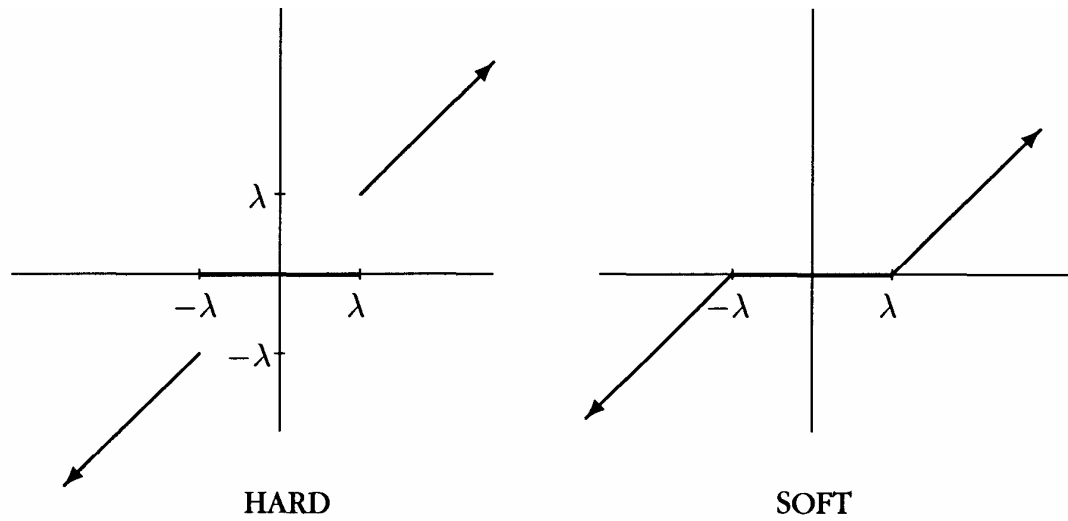


Figure-4.12 The Hard and Soft Threshold Function

Hard and Soft threshold functions are extensively used in practice, resulting in good effect. Hard threshold function can preserve PD energy and characteristic but results in unsmooth PD de-noised signal. Soft threshold function can achieve smooth PD signal but has energy loss.

## **Chapter-5**

# **Practical Application of Wavelet Transform for PD Detection and Analysis**

## 5.1 INTRODUCTION <sup>[50-55]</sup>

As discussed in the previous chapter, WT can be applied for any data extraction. The WT is mainly used to detect specified interested signals from the noisy signal that are PD pulses in current application. It is carried out with data acquisition, WT applicability check, WT analysis for different threshold methods and time domain signal analysis. WT analysis is carried out for both threshold value and threshold

function determination. During analysis, it is observed that original time-domain signal analysis can be used for some kind of WT parameter selection. So, this is also covered in the thesis.

During data acquisition phase, data is acquired by Mtronics made PD data acquisition system. The Mtronics system software gives the sampled time-stamped values, which are used for further analysis.

WT suitability is checked by different type of pulses (with different time width and amplitude) with noise addition. The simulation restores PD signals from noisy simulated signal.

The signal is analyzed in two phases (1) original signal (define below) analysis and (2) WT analysis. The receiving signal during extensive testing of transformer is referred as original signal. In original signal analysis phase, the signal is separated in positive/negative samples and then analyzed separately. In WT analysis phase, the original signal is transformed to WT domain and is analyzed for WT threshold function selection method. Finally, a comparison is carried out between two analyses and relation is envisaged for WT threshold function selection based on original signal.

## 5.2 EXPERIMENTAL DATA ACQUISITION AT LABORATORY <sup>[57]</sup>

Block diagram of on line PD measurement is shown in figure-5.1. The PD measurements are carried out using Mtronix made Advanced Partial Discharge Measuring System MPD540.

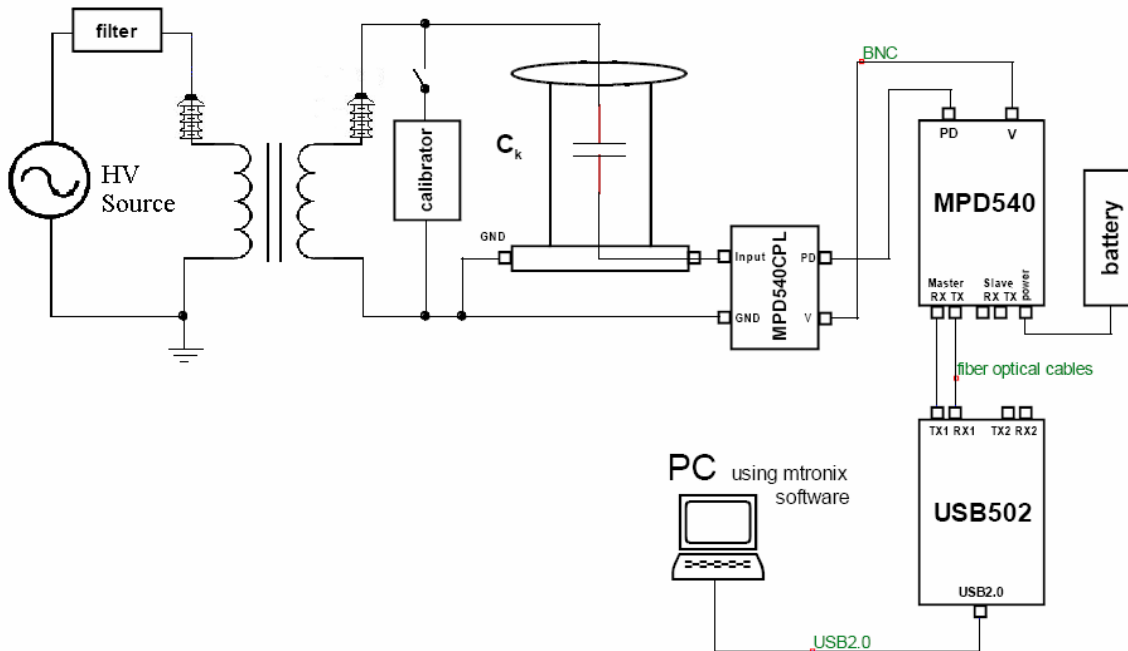


Figure-5.1 Block diagram of PD Measurement Setup

This unit comprises of data acquisition unit (MPD540) and fiber optics controller (USB502). Former consist a Coupling unit (MPD540CPL) and data acquisition unit whereas later is USB based data transfer unit. MPD540CPL is connected to a high voltage coupling unit CPL542, also referred to as “quadripole”, which is connected to high voltage coupling capacitor. Figure-5.2 and Figure-5.3 show the practical PD measurement set up for 100 MVA, 220/132 kV transformer. The measured waveforms are stored in computer (at different time instance). The Mtronics software has data export feature, which converts recorded signal values to time stamped signal

samples. Also, the extracted samples are stored in text file and further analysis is carried out.

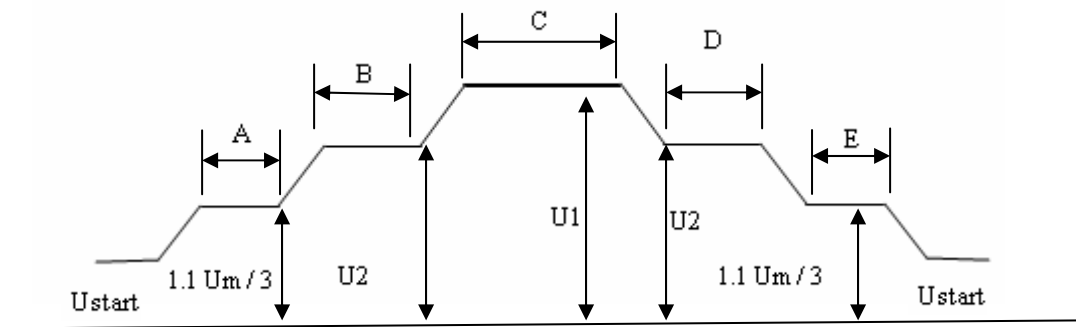


Figure-5.2 Data acquisition Setup for PD Measurement



Figure-5.3 Power Transformer Setup as a Test Object

This text file data (reference data) is given to develop the program and further WT analysis is carried out to get PD pulses. WT has removed noise samples and has estimated PD pulses. PD test bandwidth is kept 300 KHz with PD test maximum voltage 245 KV as per IS standard. PD pulse & measurement value is obtained at different range of voltages with respect to time schedule on each phase of transformer. The test is performed as per standard IEC 60270 method. Before starting the measurement, the set-up is calibrated for 500 pC (as per the calibration criteria). Measurements are carried out at various voltages and durations as given in figure-5.4. Both quantities (PD and PD test voltage) are measured and set of data is recorded with software. This recorded data is used for WT analysis. PD measurements results (at various voltage and duration) during the experiment are recorded in Table-5.1.



A= 5 min., B=5min., C= test time, D= 30 min., E= 5 min.

Figure-5.4 Measure Record Diagram

TABLE-5.1 MEASURED PD AT DIFFERENT CONDITIONS AS PER STANDARD

Voltage →	212.18 kV	245 kV	212.18 kV
No of Samples→	5	1	10
Duration→	1 minute	5 second	3 minute
Sample No.	(pC)		
1	260	505	450
2	280	-	500
3	290	-	600
4	280	-	1000
5	270	-	1500
6	-	-	2480
7	-	-	3484
8	-	-	5480
9	-	-	6000
10	-	-	6282

### 5.3 WT SUITABILITY CHECK FOR PD MEASUREMENT <sup>[55-56]</sup>

PDs are small electrical sparks resulting from the electrical breakdown of a gas contained within a void. If the void is within a solid or liquid, the PD will degrade the material and may eventually cause the failure of the insulation. The discharge in small void in insulation is extremely rapid event. In literature analysis of the PD events, it is found that PD events can occur from 1ns to few  $\mu$ s. S. N. Hettiwatte et al. has reported the propagation of PD pulse duration varying from 100ns-10 $\mu$ s. It is also reported that one PD pulse can be discriminated within 100 $\mu$ s for a 50Hz voltage and can be extensively analyzed on PD pulse pattern. Considering these references, it is necessary to carryout PD data acquisition, WT modeling (for suitability check) and WT analysis on acquired data.

Based on above reference, the simulation is carried out for four different PD pulse widths with two different amplitudes. So, total eight PD pulses are simulated and Gaussian noise is added in it. Finally, generated stream is applied for WT and PD pulses extraction. Block diagram of this Simulation is shown in figure-5.5.

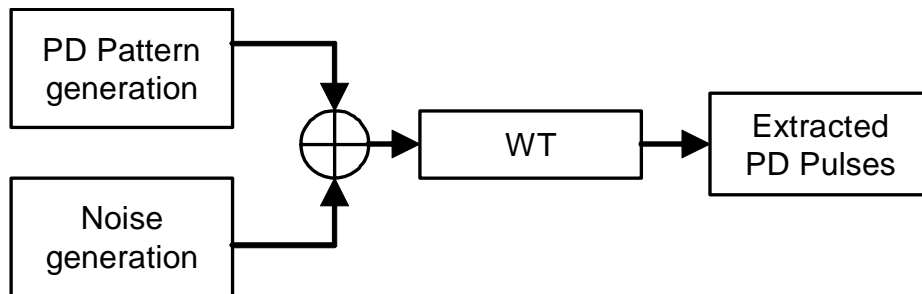


Figure-5.5 Block Diagram for PD Simulated Data

## 5.4 METHOD FOR ESTIMATING WT THRESHOLD FUNCTION <sup>[48, 51]</sup>

As discussed in earlier sections; PD data is acquired and analysis is carried out on various measurements. The analysis is carried out as per flow-5.6 given below. The work is carried out in two phases (1) Measurement and (2) signal acquisition and analysis.

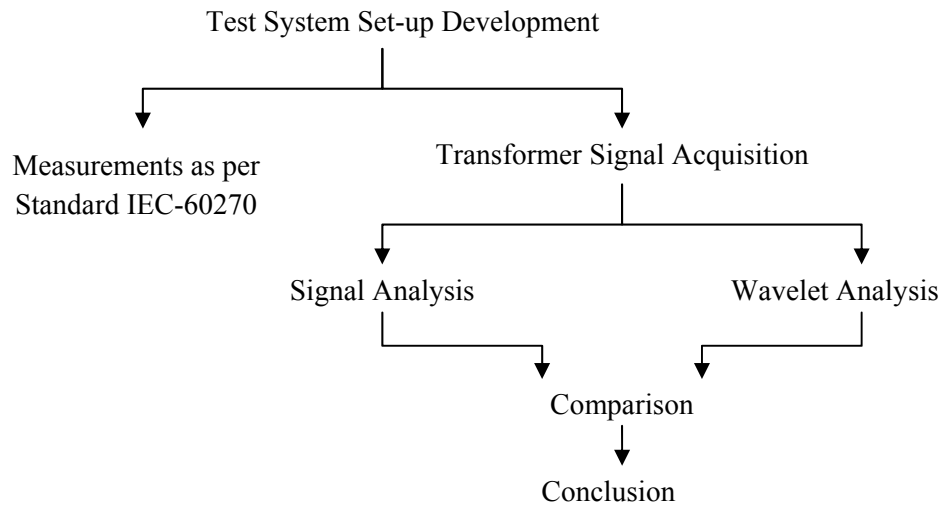


Figure-5.6 Flow of the Analysis

Figure-5.7 shows block diagram of acquired signal analysis. Partial discharge signals are bidirectional in nature. Also, standard deviation and other statistical methods cannot be directly useful for signal analysis. So, the direct analysis is not viable for this signal and therefore signal has to separate between positive and negative samples. Further analysis is done separately on positive and negative samples & obtained result is compared with WT analysis signal.

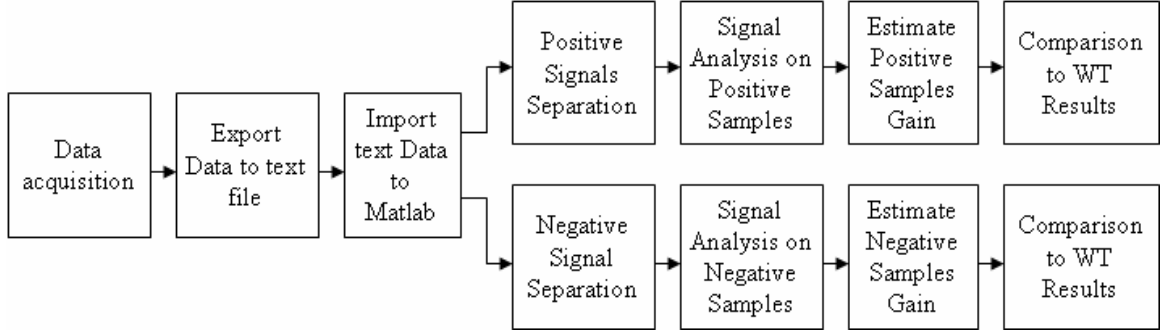


Figure-5.7 Block Diagram for Acquired Signal Analysis

Let  $S_n$  is a signal having PD pulses. The sampled signal can be expressed as

$$S_n = S_{n_{pos}} + S_{n_{neg}} \quad \dots (5.1)$$

Where  $S_{n_{pos}}$  is total positive samples and  $S_{n_{neg}}$  is total negative samples. A developed program separates positive and negative samples and their average is found out as

$$Avg_{pos} = (\sum S_{n_{pos}}) / N_{pos} \quad \dots (5.2)$$

$$Avg_{neg} = (\sum S_{n_{neg}}) / N_{neg} \quad \dots (5.3)$$

where,  $Avg_{pos}$  and  $Avg_{neg}$  are positive & negative samples' average respectively and Similarly,  $N_{pos}$  and  $N_{neg}$  are the numbers for positive and negative samples individually. PD pulses estimation is carried out as per given below.

$$\begin{aligned}
 Avg_{est\_pos\_PD} &= \sum (S_{n_{pos}} - Avg_{pos}) / N_{est\_pos\_PD}, \text{ if } S_{n_{pos}} > (p^* Avg_{pos}) \\
 &= 0, \quad \text{if } S_{n_{pos}} \leq (p^* Avg_{pos}) \dots (5.4)
 \end{aligned}$$

$$\begin{aligned}
 Avg_{est\_neg\_PD} &= \sum (S_{n_{neg}} - Avg_{neg}) / N_{est\_neg\_PD}, \text{ if } S_{n_{neg}} < (p^* Avg_{neg}) \\
 &= 0, \quad \text{if } S_{n_{neg}} \geq (p^* Avg_{neg}) \dots (5.5)
 \end{aligned}$$

where,  $Avg_{est\_pos\_PD}$  is average of pulses which are above  $Avg_{pos}$ ,  $N_{est\_pos\_PD}$  is number of pulses whose value is above  $p * Avg_{pos}$ ,  $Avg_{est\_neg\_PD}$  is average of pulses which are below  $Avg_{neg}$ ,  $N_{est\_neg\_PD}$  is number of pulses whose value is below  $p * Avg_{neg}$  and  $p$  is the number which is used to estimate PD pulse amplitude. This analysis is carried out for different values of  $p$  that are 1, 1.5, 2 and 3. Here,  $p$  selects the signal level of comparison with respect to  $Avg_{pos}$  or  $Avg_{neg}$ . However, for  $p=2$  best result is achieved among all 13 data set files (each data set has more than 5000 samples).

A positive pulse ratio of estimated positive pulses and average positive signal samples determines positive PD pulse intensity and vice versa. These ratios are indicated by

$$R_{pos} = Avg_{est\_pos\_PD} / Avg_{pos} \quad \dots(5.6)$$

$$R_{neg} = Avg_{est\_neg\_PD} / Avg_{neg} \quad \dots(5.7)$$

Where  $R_{pos}$  and  $R_{neg}$  are ratios for positive and negative estimated PD pulses respectively. This ratio estimates PD pulses intensity on actual signal.  $R_{pos}$  high indicates that the signal has low noise contribution and high PD amplitude and vice versa. During the experiment,  $R_{pos}$  and  $R_{neg}$  ratios are found normally equal. Figure-5.8 and Figure-5.9 shows analysis results on data sets-1 and data set-13, respectively. This confirms that the signal is PD signal. Therefore these ratios are used for comparison by WT analysis.

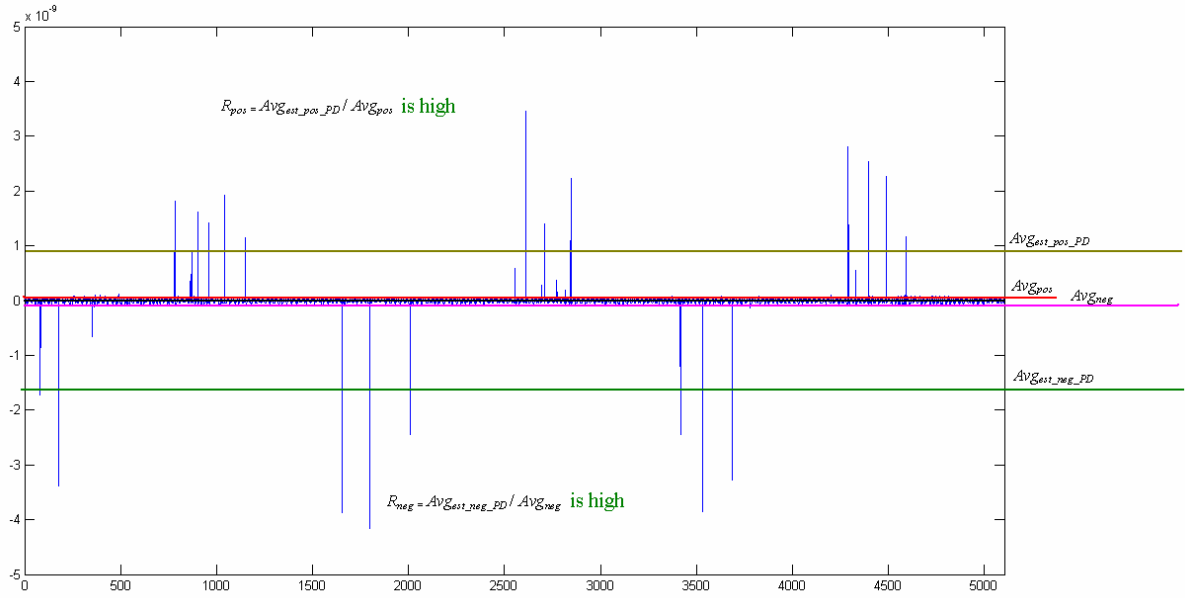


Figure-5.8 Signal Analysis on Data Set-1 ( $R_{pos}$  and  $R_{neg}$  are High)

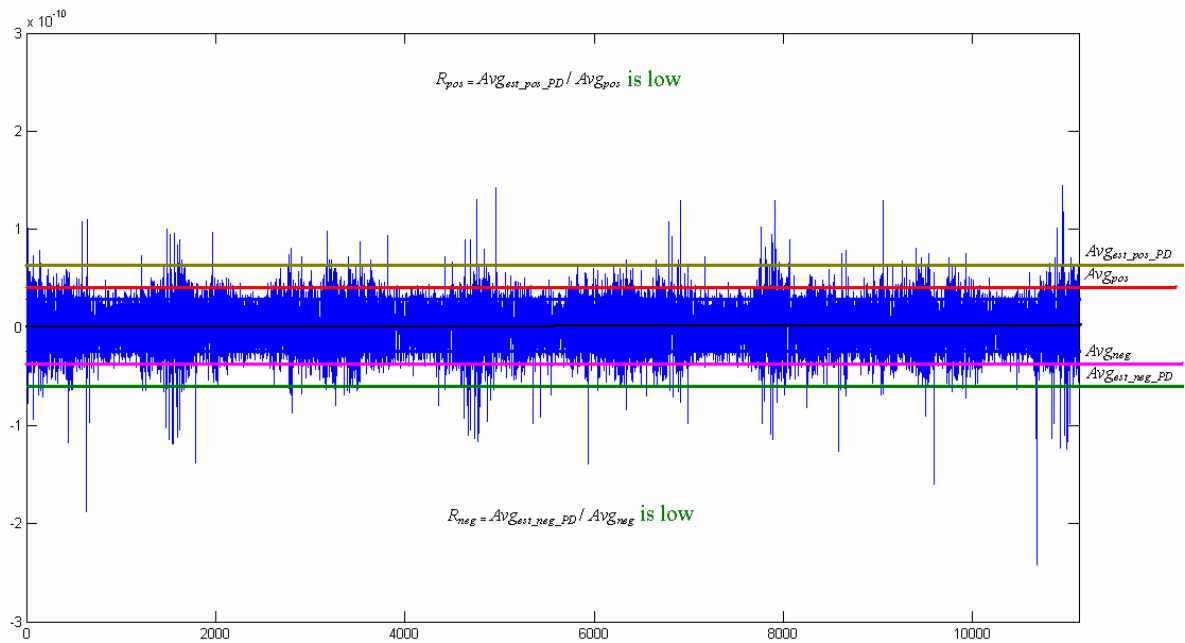


Figure-5.9 Analysis on Data Set-13 ( $R_{pos}$  and  $R_{neg}$  are Low)

Figure-5.10 shows block diagram for WT analysis to determine hard threshold function gain over soft threshold function. As discussed earlier, universal threshold

method decides threshold value for present analyses. WT is applied on signal with universal threshold value for hard and soft threshold function.

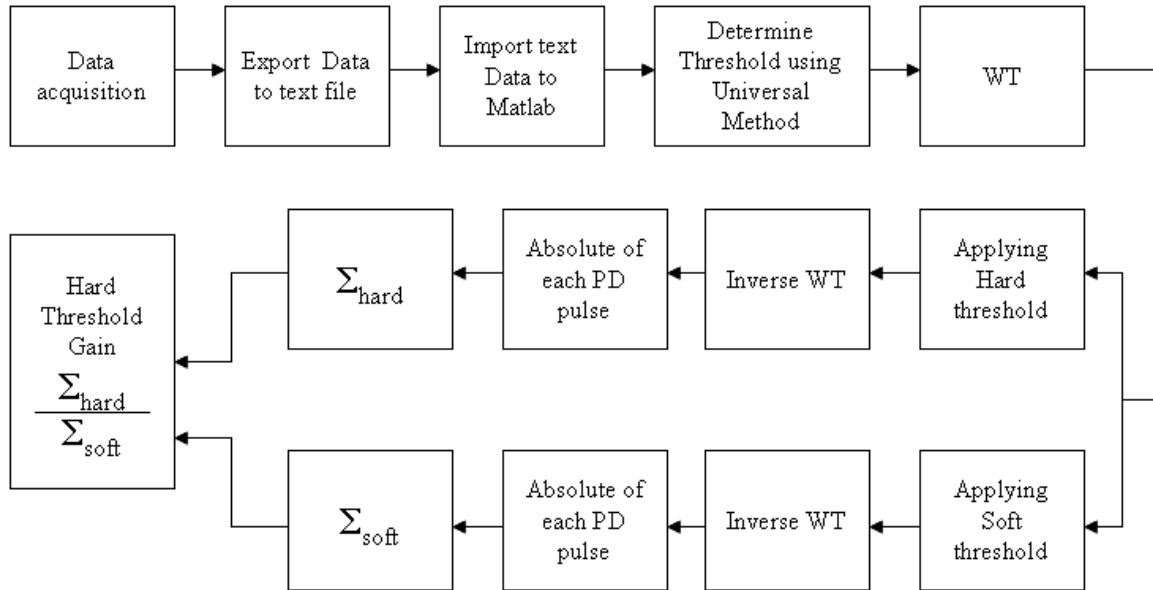


Figure-5.10 Block Diagram for WT analysis

Flow chart for combing both the analyses (with different involved phases) and complete process is shown in figure-5.11.

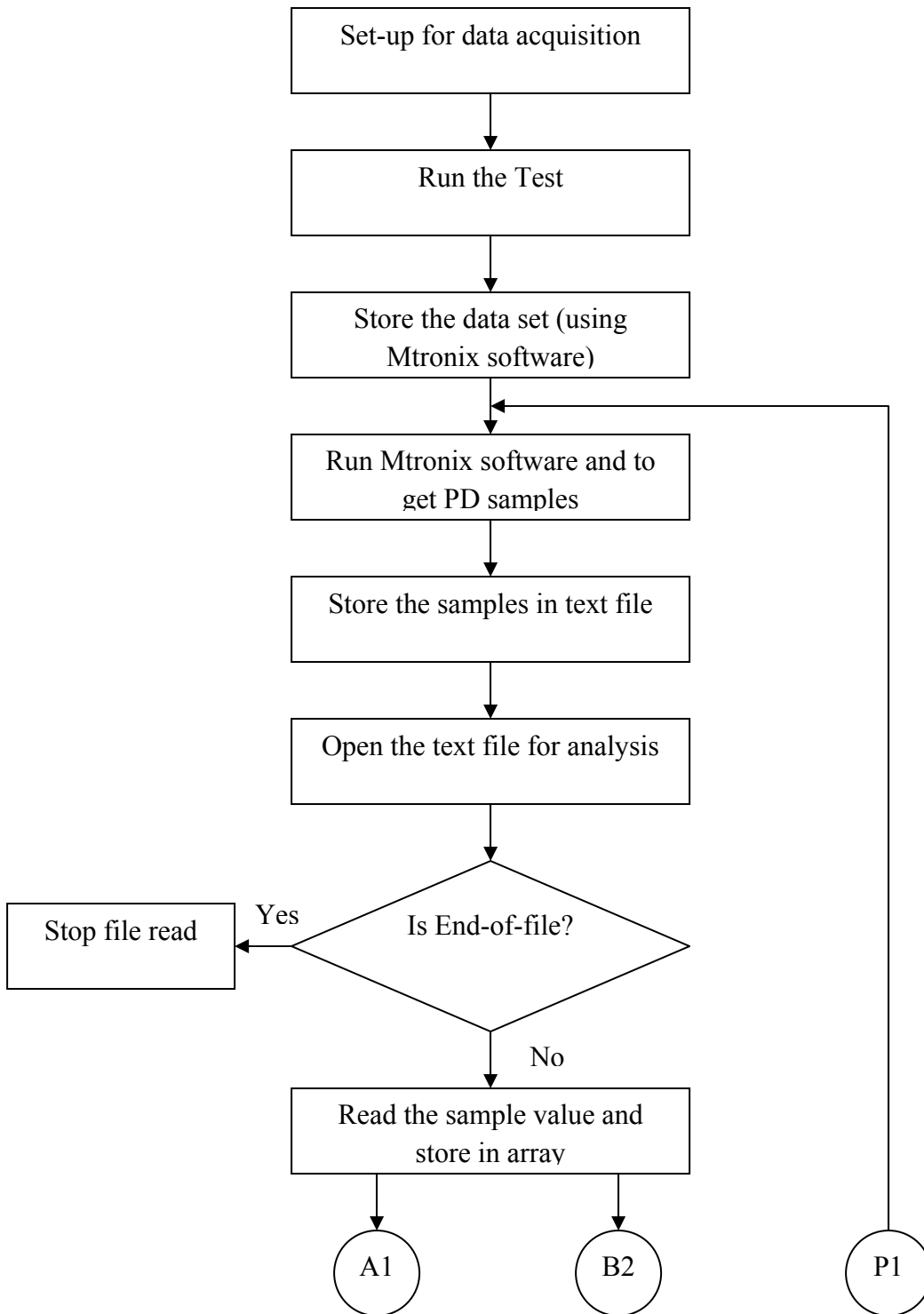


Figure-5.11 Flowchart of signal analyses Contd...

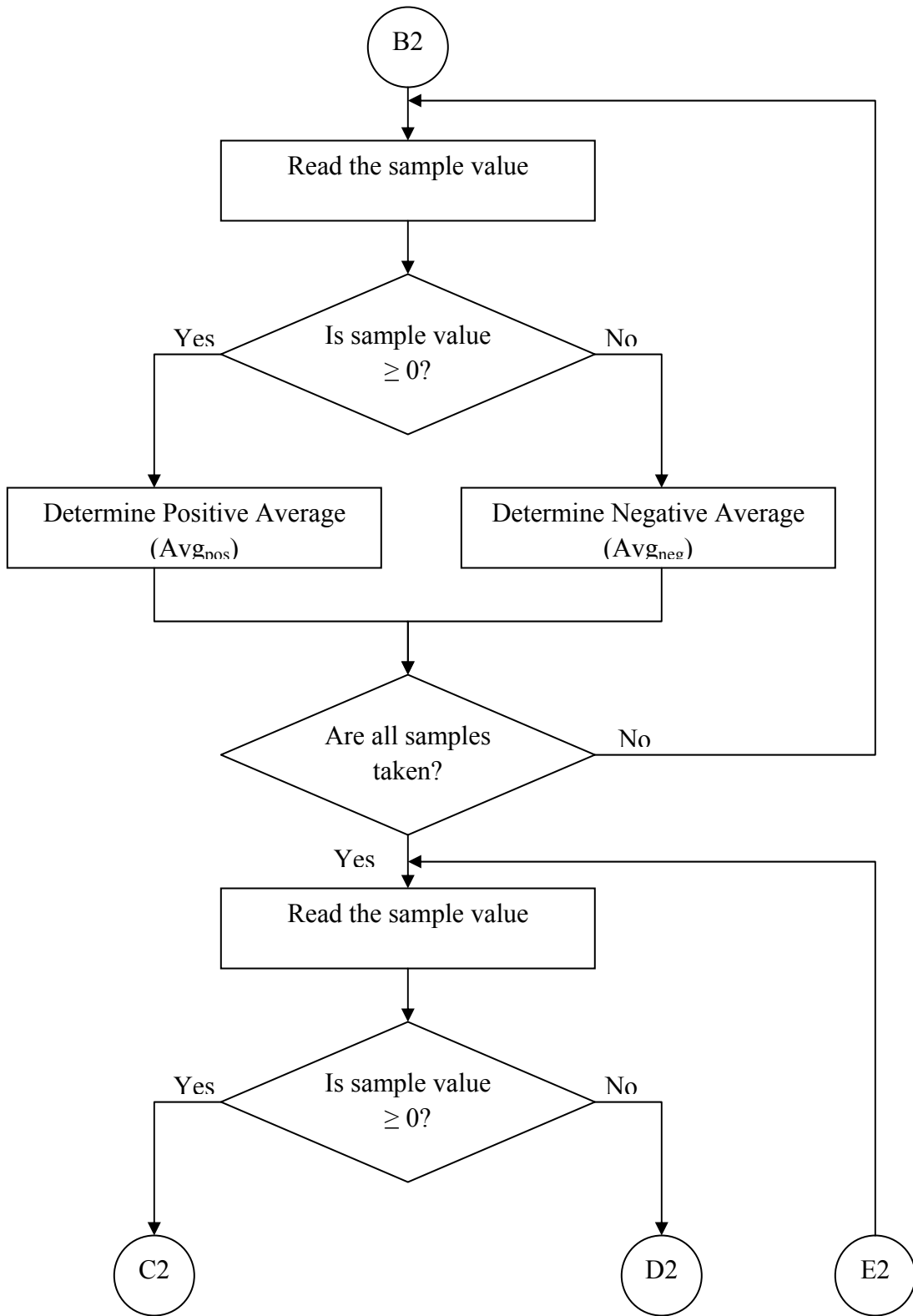


Figure-5.11 Flowchart of signal analyses Contd.

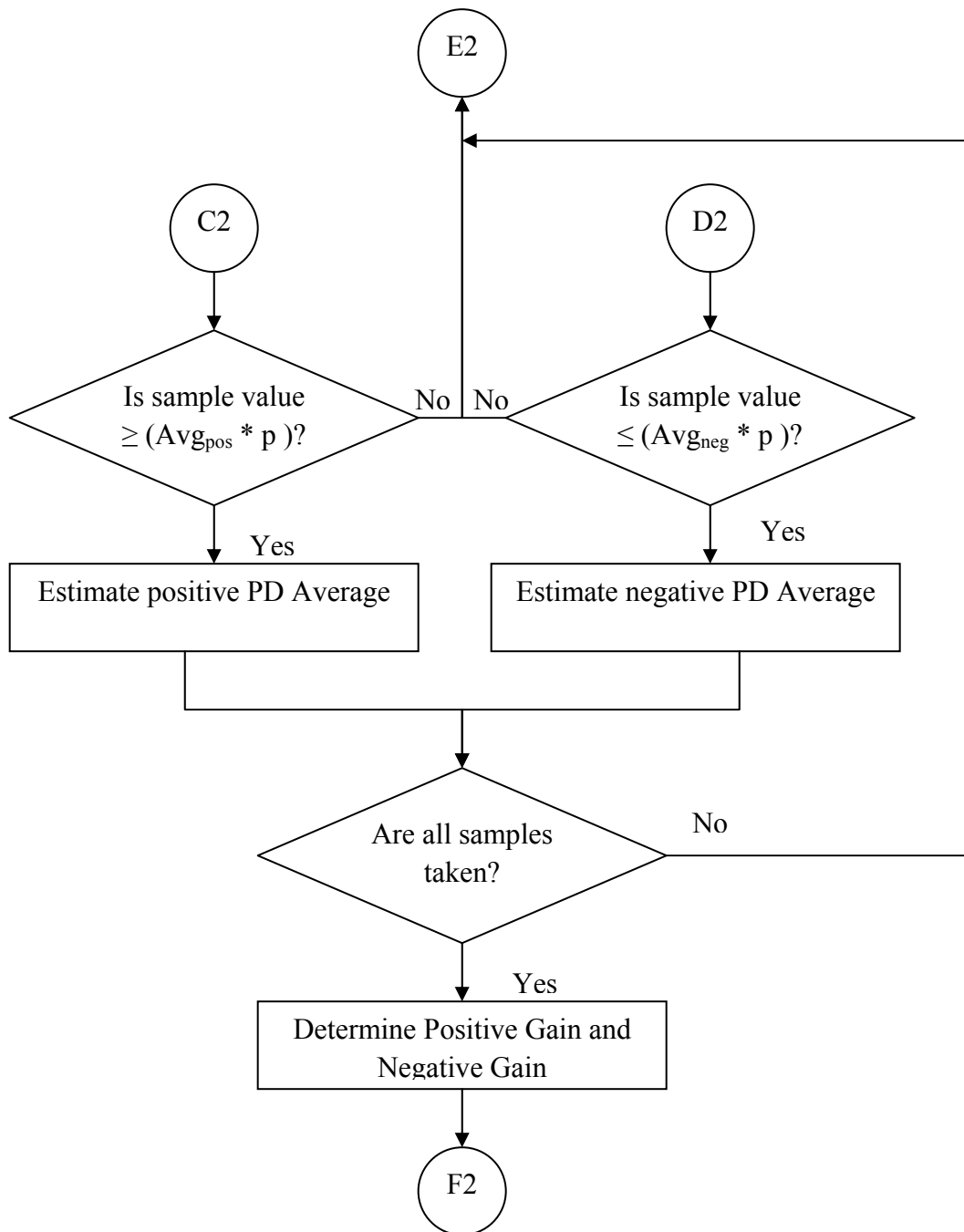


Figure-5.11 Flowchart of signal analyses Contd.

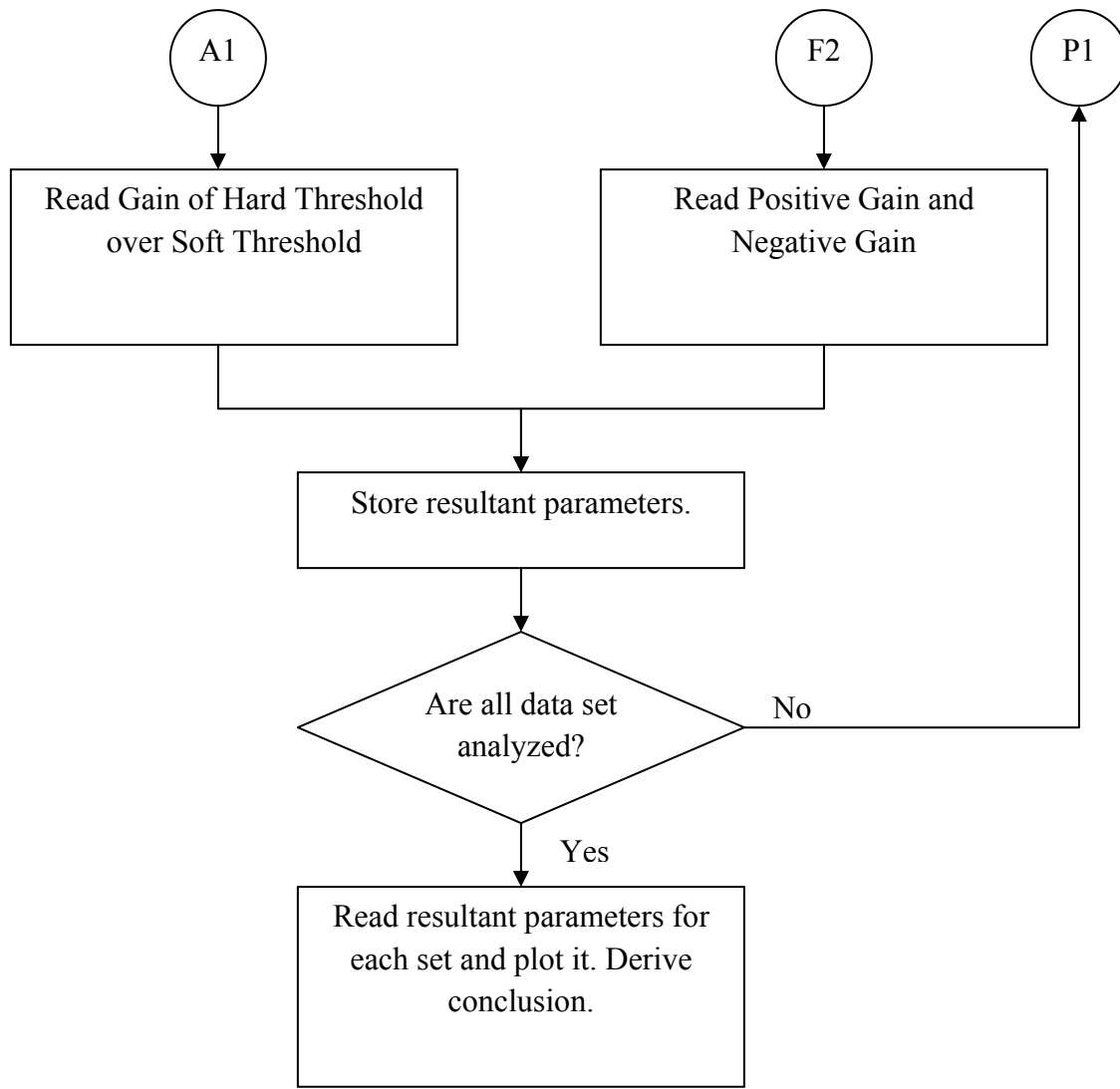


Figure-5.11 Flowchart of signal analyses

## 5.5 RESULTS

### PD MODELING FOR SUITABILITY CHECK USING WT

This simulation is carried out with two amplitude sets with four varying pulse widths. Hence, total eight pulses are generated. Noise is also added with consideration of Gaussian in nature. Table-5.2 shows characteristics of simulated pulses.

TABLE-5.2 SIMULATED PULSE CHARACTERISTICS

Simulated PD Pulse No	Peak Amplitude (mV)	Duration (uS)
1	100	15
2	150	15
3	100	20
4	150	20
5	100	30
6	150	30
7	100	40
8	150	40
Noise	140 (mV) peak to peak	1 MHz frequency

Figure-5.12 (a, b, c) shows simulated input PD signal with two different amplitudes, Noise and PD signal with addition of Noise respectively. Figure-5.12 (d and e) shows obtained PD signals with universal threshold and Minimax threshold.

Extracted PD signal is much definable and the reflected pulse can be clearly seen in comparison to the simulated noisy PD signal. In this analysis, signal is de-noised using level- approximation and Daubechies db2 wavelet.

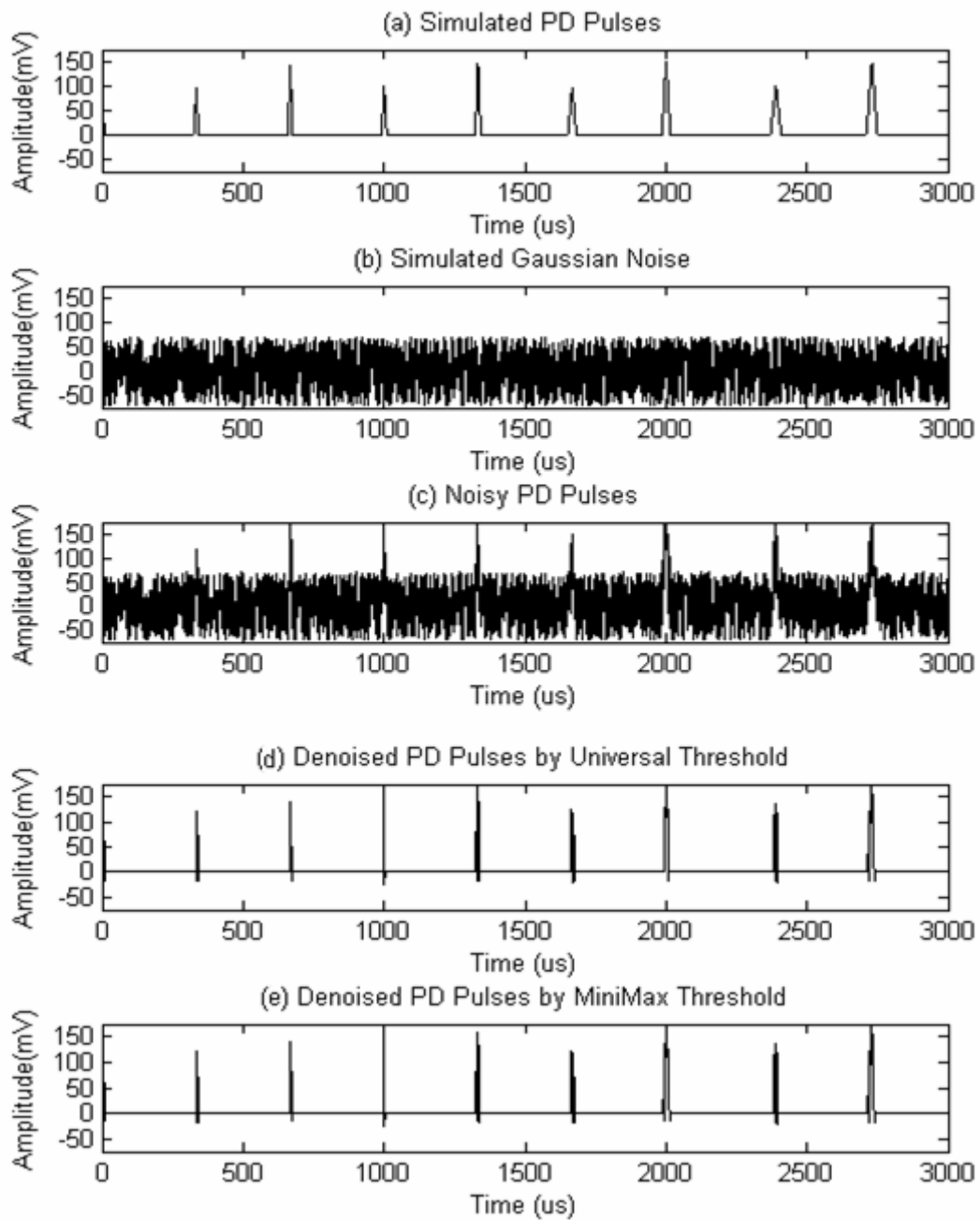


Figure-5.12 Simulated PD pulses, noise and pulled out PD Pulses

## **WT ANALYSIS ON DATA ACQUIRED**

PD measurements are recorded as per standard, which are with different time interval. During the measurement, waveforms are recorded for wavelet analysis. One of the recorded waveform is shown in figure-5.13. Stored waveform is referred to as data set in further theory. Summary of the WT analysis is shown in Table-5.3 and individual analysis on each data set (recorded at different time) are shown in Figure-5.14.

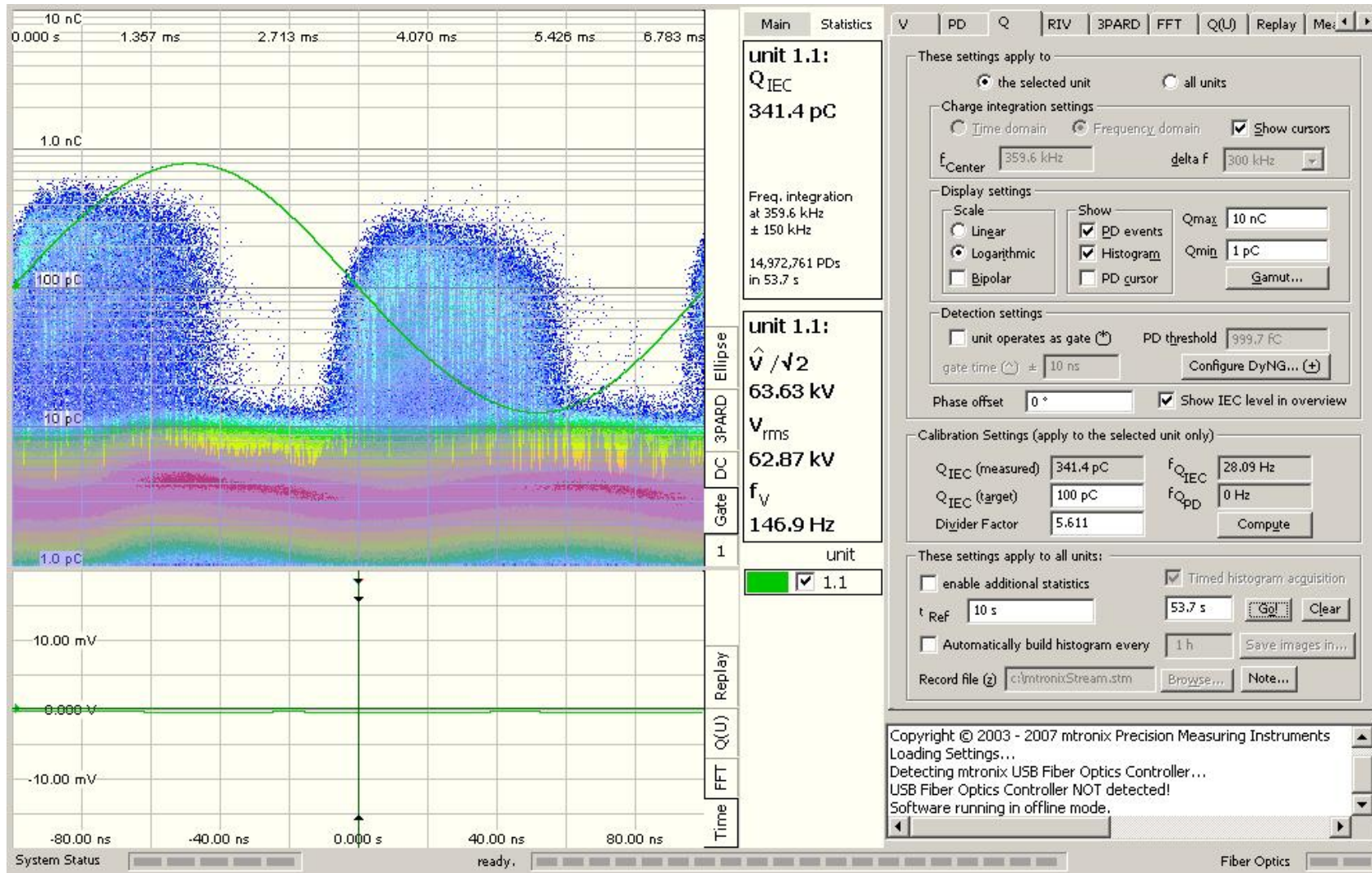


Figure-5.13 Recorded waveform using Mtronix software

TABLE-5.3 DATA ANALYSIS ON VARIOUS ACQUIRED DATA SETS

Data file No.	No of Samples	Universal Threshold (C)	Mean Value (C)	Positive Average (C)	Negative Average (C)	Average of Positive Samples Higher then Positive Avg * 2 (C)	Average of Negative Samples Less then Negative Average * 2 (C)	R <sub>pos</sub>	R <sub>neg</sub>	Absolute sum of Hard Threshold values (C)	Absolute sum of Soft Threshold values (C)	gain
1	5104	4.64E-11	3.99E-14	4.92E-12	-4.83E-12	1.16E-10	-2.32E-10	23.6132	48.0394	6.26E-09	5.09E-09	18.6467
2	8344	5.21E-11	-1.12E-13	6.11E-12	-6.35E-12	1.20E-10	-1.38E-10	19.556	21.6972	1.22E-08	8.89E-09	27.399
3	8725	1.05E-11	4.84E-14	3.26E-12	-3.23E-12	7.37E-12	-8.77E-12	2.2629	2.7198	1.38E-09	6.02E-10	56.2011
4	13197	1.57E-11	-6.52E-15	4.44E-12	-4.44E-12	1.15E-11	-1.25E-11	2.5814	2.8038	6.57E-09	1.88E-09	71.3512
5	12897	1.50E-11	5.05E-14	4.23E-12	-4.21E-12	1.18E-11	-1.34E-11	2.7855	3.1878	5.43E-09	1.89E-09	65.2451
6	8157	1.41E-11	3.83E-15	4.02E-12	-4.06E-12	1.04E-11	-1.12E-11	2.5727	2.7587	2.58E-09	8.35E-10	67.5753
7	10959	5.26E-12	3.17E-14	1.75E-12	-1.76E-12	2.81E-12	-2.88E-12	1.6092	1.6423	2.87E-10	4.20E-11	85.3829
8	9243	6.18E-12	-5.35E-14	2.04E-12	-2.09E-12	3.21E-12	-3.13E-12	1.5754	1.5002	2.55E-10	4.67E-11	81.6687
9	10627	8.83E-10	3.31E-13	6.35E-11	-6.55E-11	8.55E-10	-9.95E-10	13.4582	15.1922	3.78E-07	2.23E-07	40.8279
10	13272	6.08E-12	-1.26E-13	1.98E-12	-2.01E-12	3.10E-12	-3.33E-12	1.5673	1.6591	3.50E-10	7.65E-11	78.1158
11	12543	8.63E-12	5.14E-14	2.74E-12	-2.70E-12	4.16E-12	-4.69E-12	1.5169	1.7358	1.26E-09	2.55E-10	79.7783
12	7311	5.88E-12	-1.52E-13	1.95E-12	-2.01E-12	2.99E-12	-3.55E-12	1.5314	1.7654	2.57E-10	5.24E-11	79.5957
13	11123	8.64E-12	3.90E-14	2.75E-12	-2.72E-12	4.24E-12	-4.80E-12	1.5429	1.7617	1.20E-09	2.50E-10	79.172

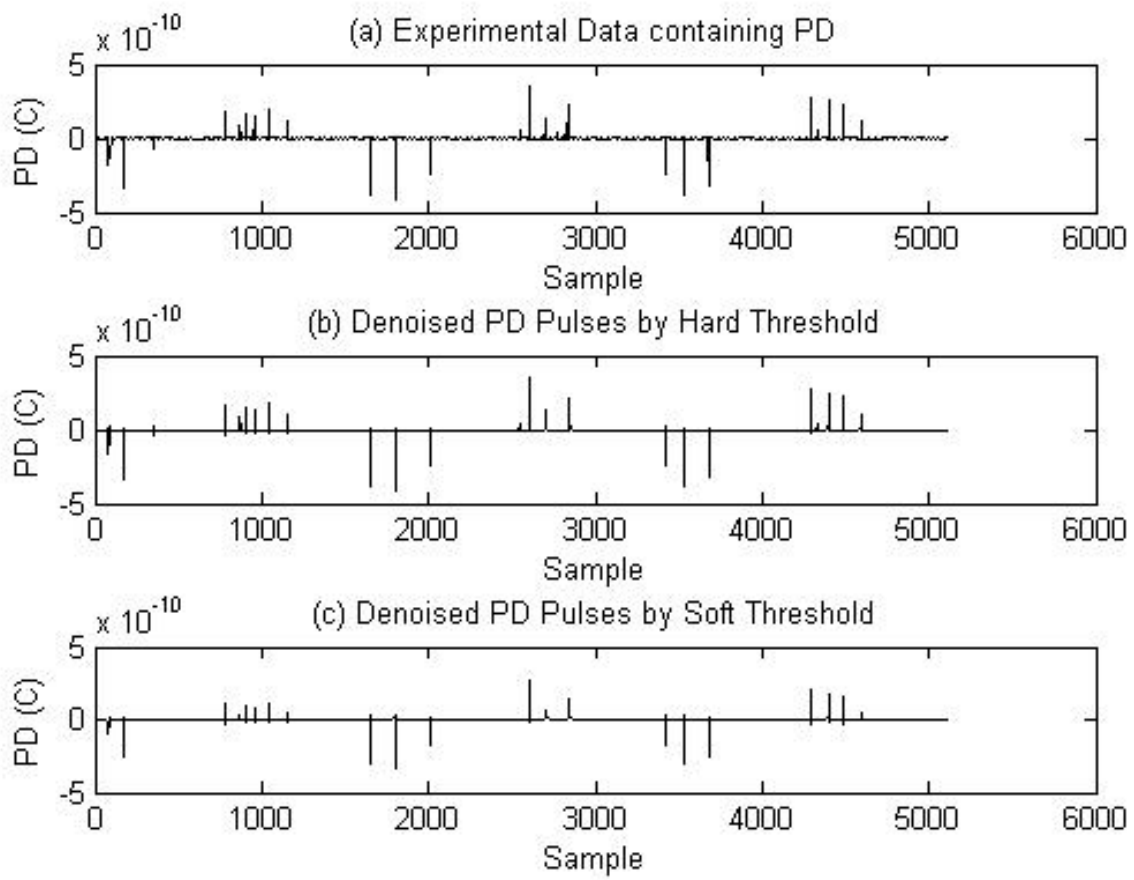


Figure-5.14 (a) Effect of hard and soft threshold selection on data set-1

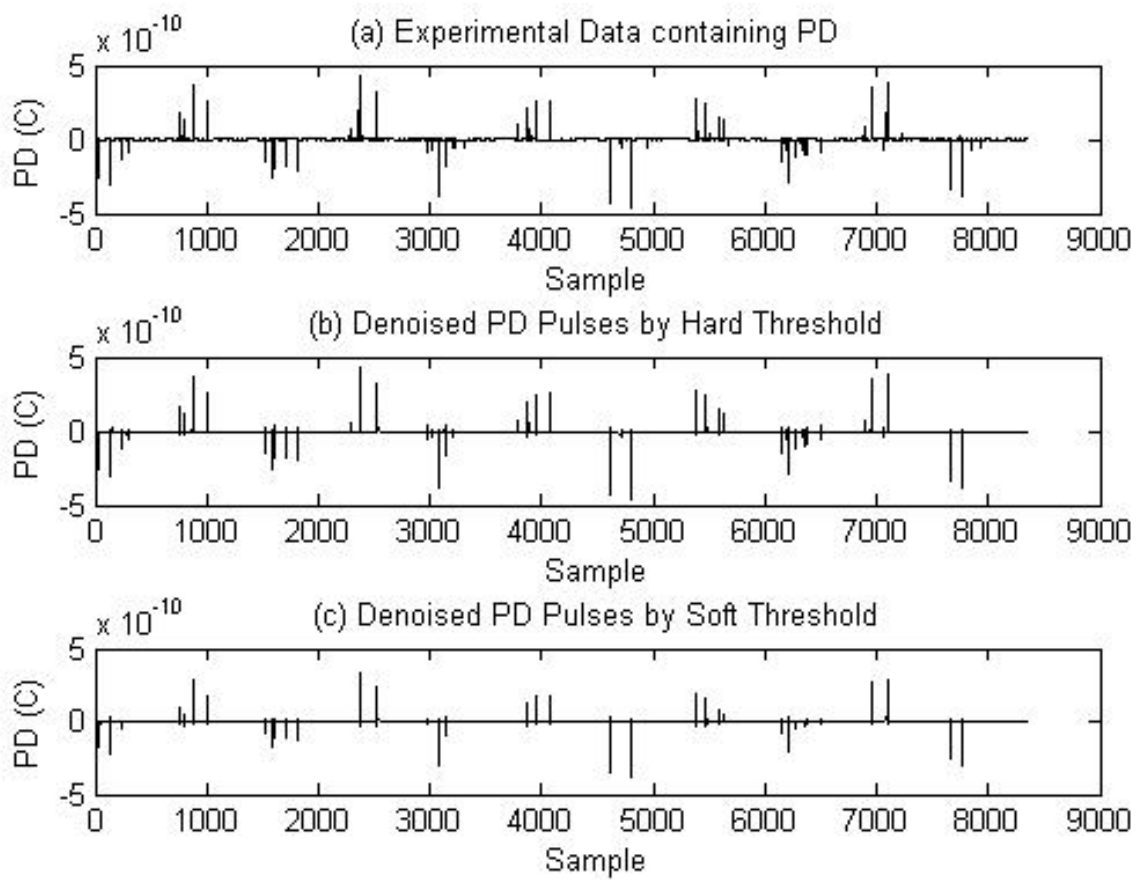


Figure-5.14 (b) Effect of hard and soft threshold selection on data set-2

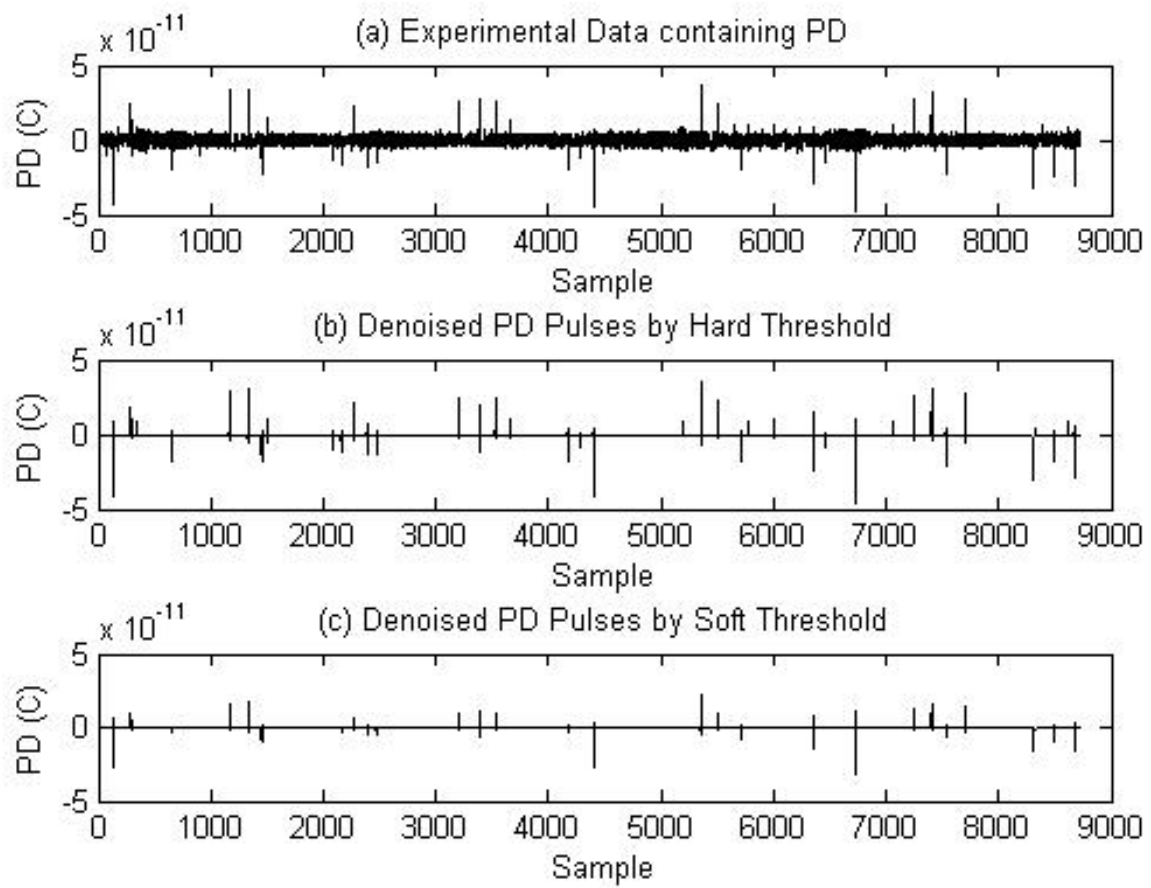


Figure-5.14 (c) Effect of hard and soft threshold selection on data set-3

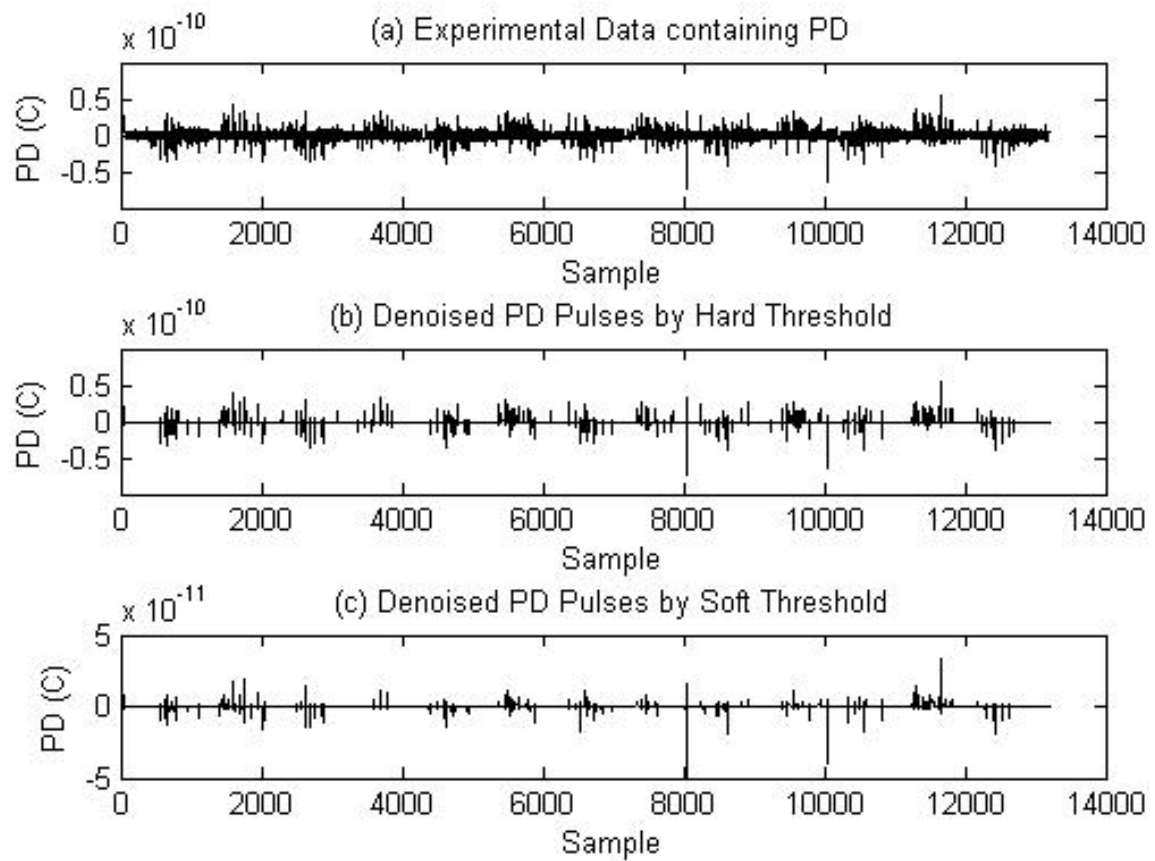


Figure-5.14 (d) Effect of hard and soft threshold selection on data set-4

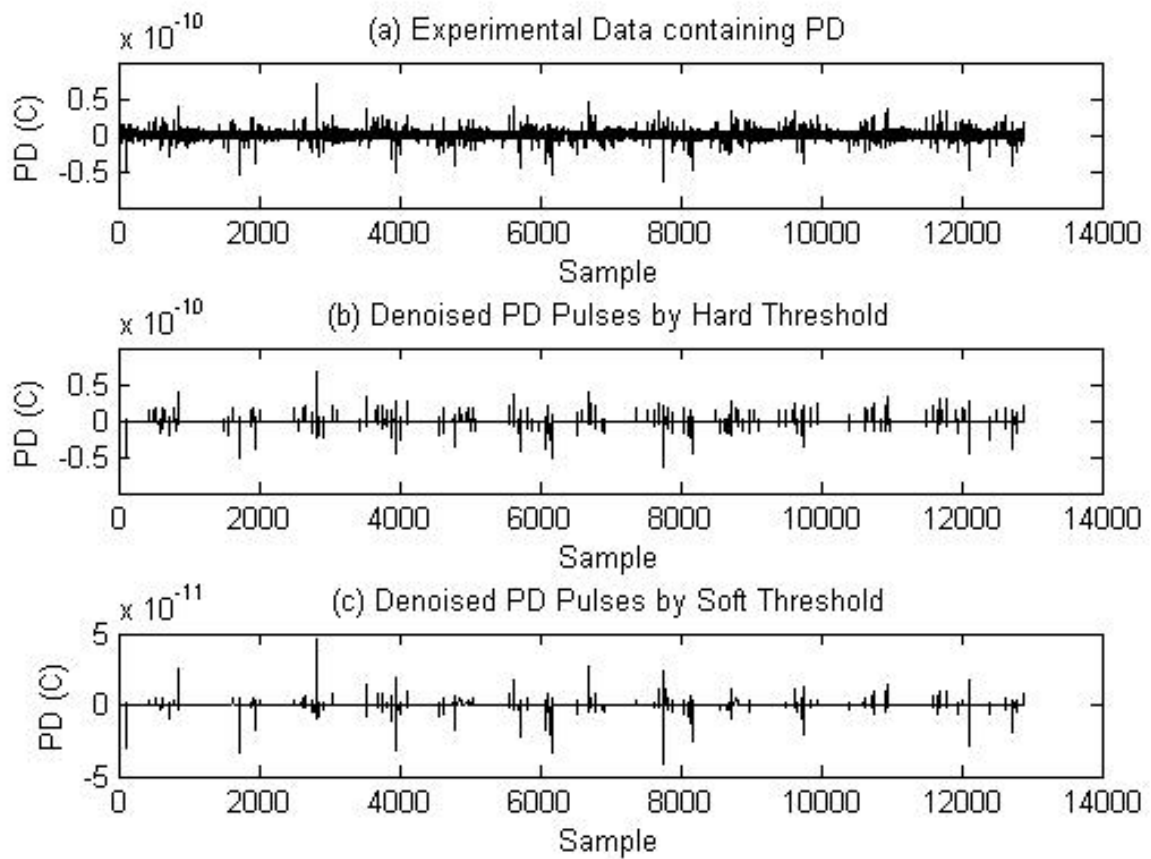


Figure-5.14 (e) Effect of hard and soft threshold selection on data set-5

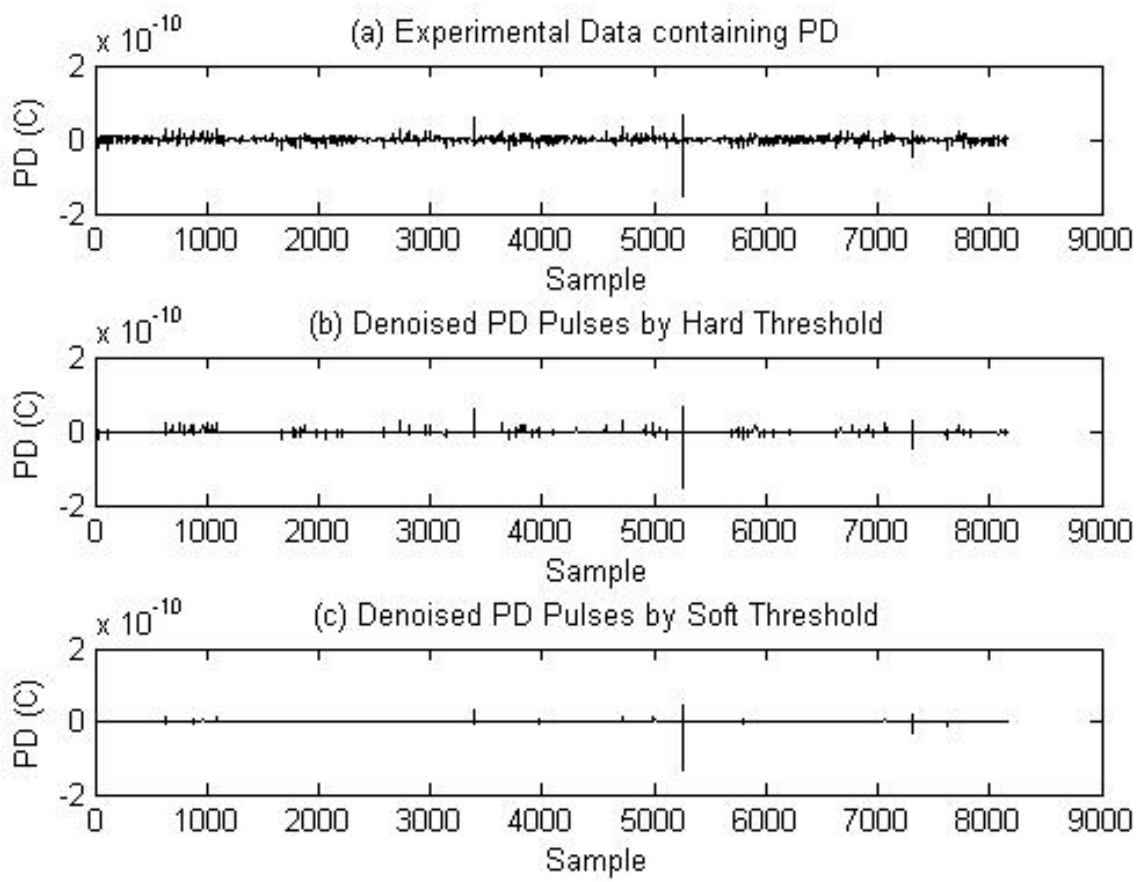


Figure-5.14 (f) Effect of hard and soft threshold selection on data set-6

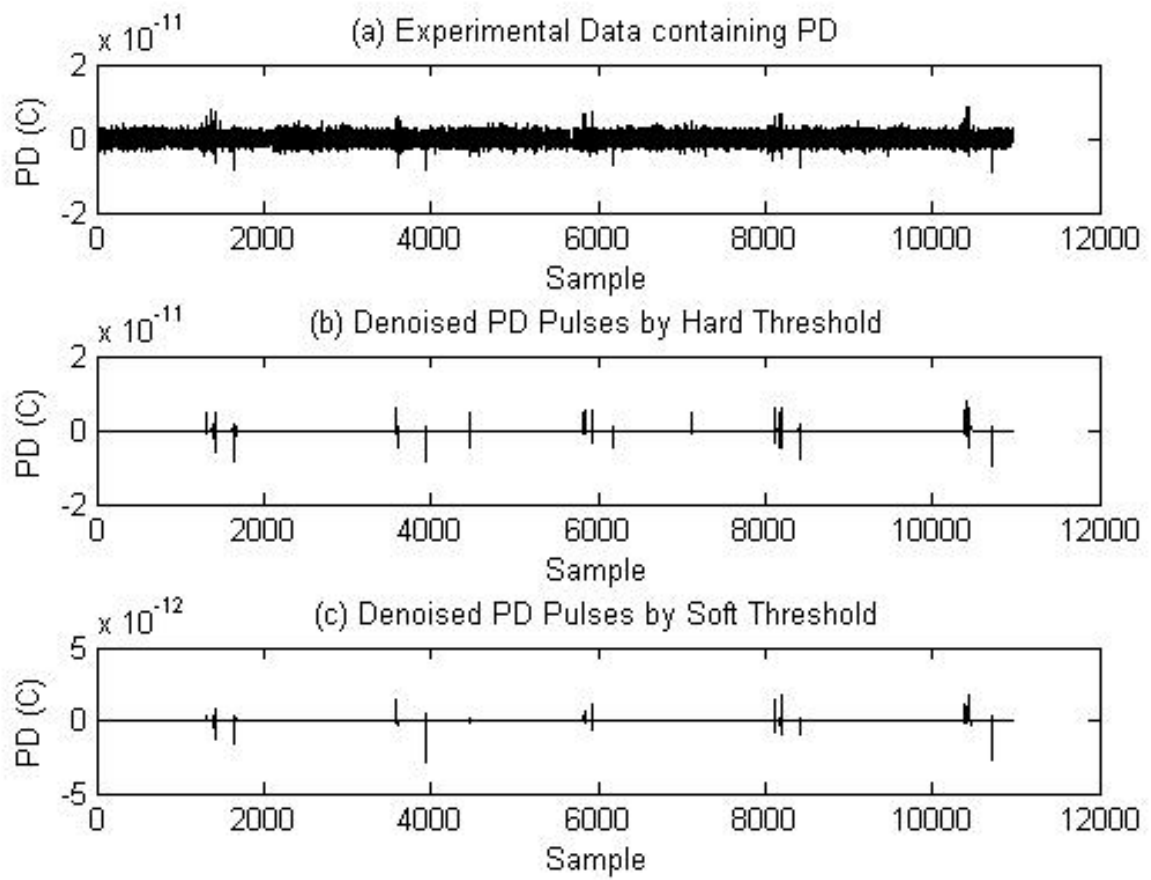


Figure-5.14 (g) Effect of hard and soft threshold selection on data set-7

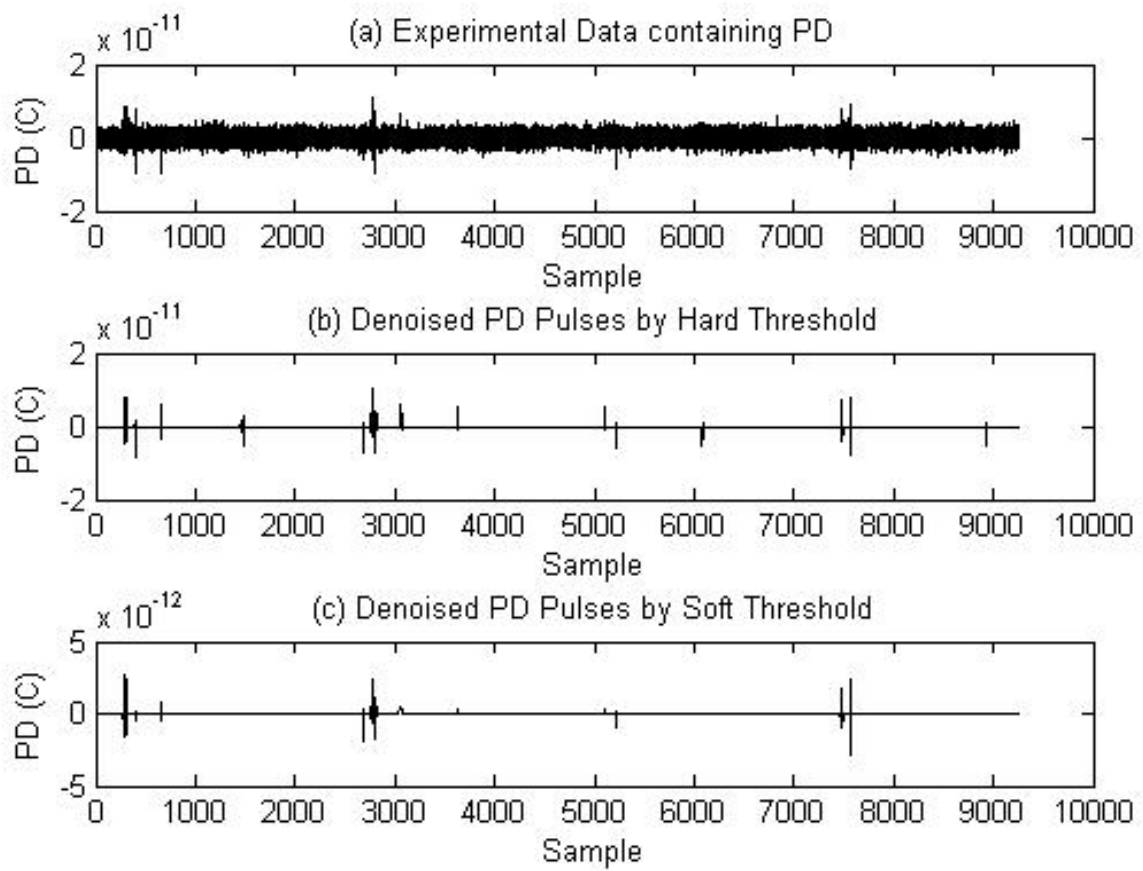


Figure-5.14 (h) Effect of hard and soft threshold selection on data set-8

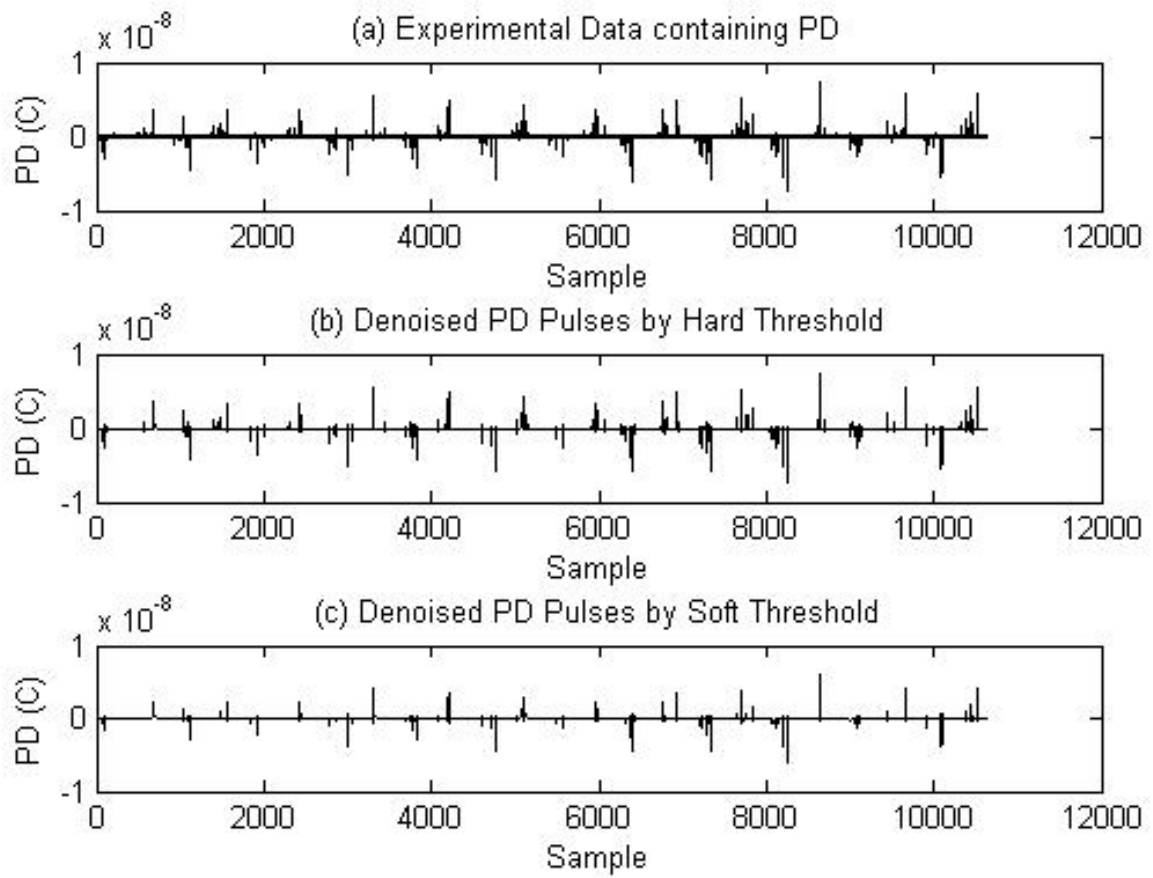


Figure-5.14 (i) Effect of hard and soft threshold selection on data set-9

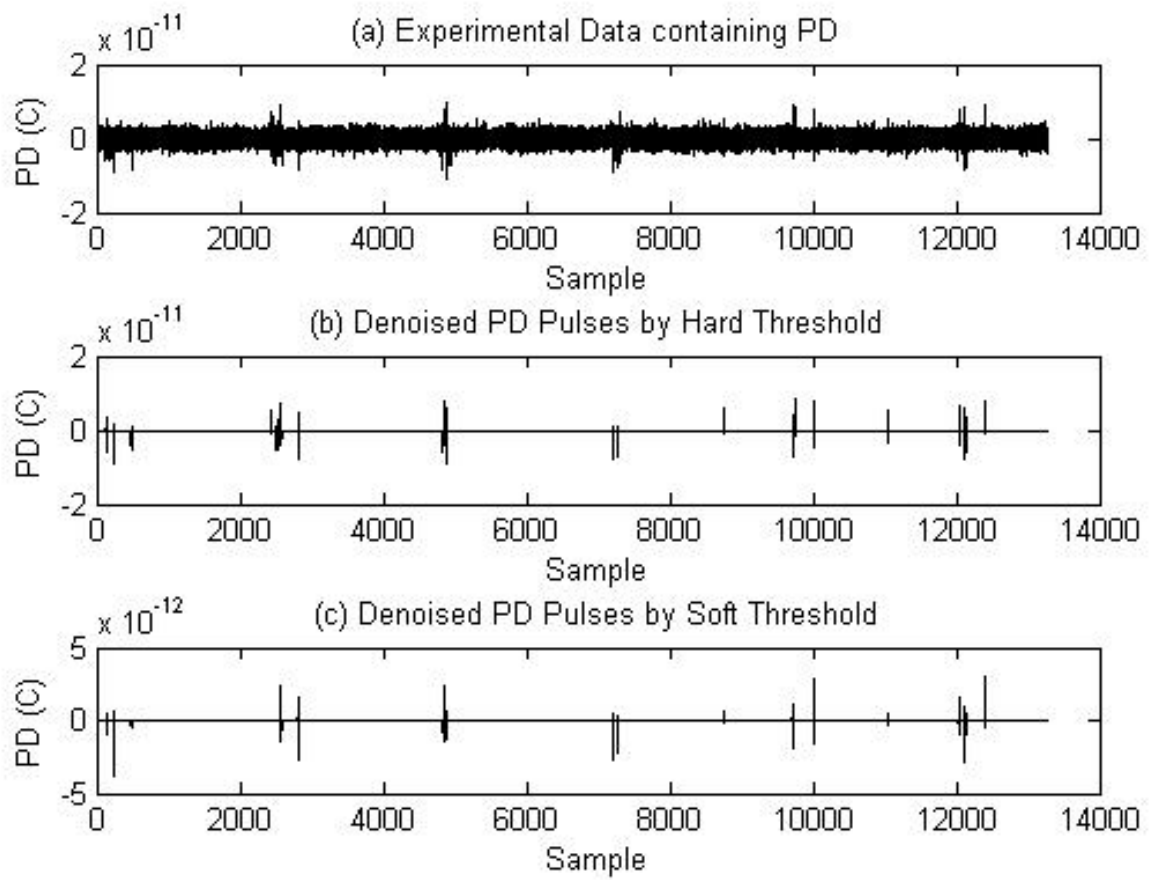


Figure-5.14 (j) Effect of hard and soft threshold selection on data set-10

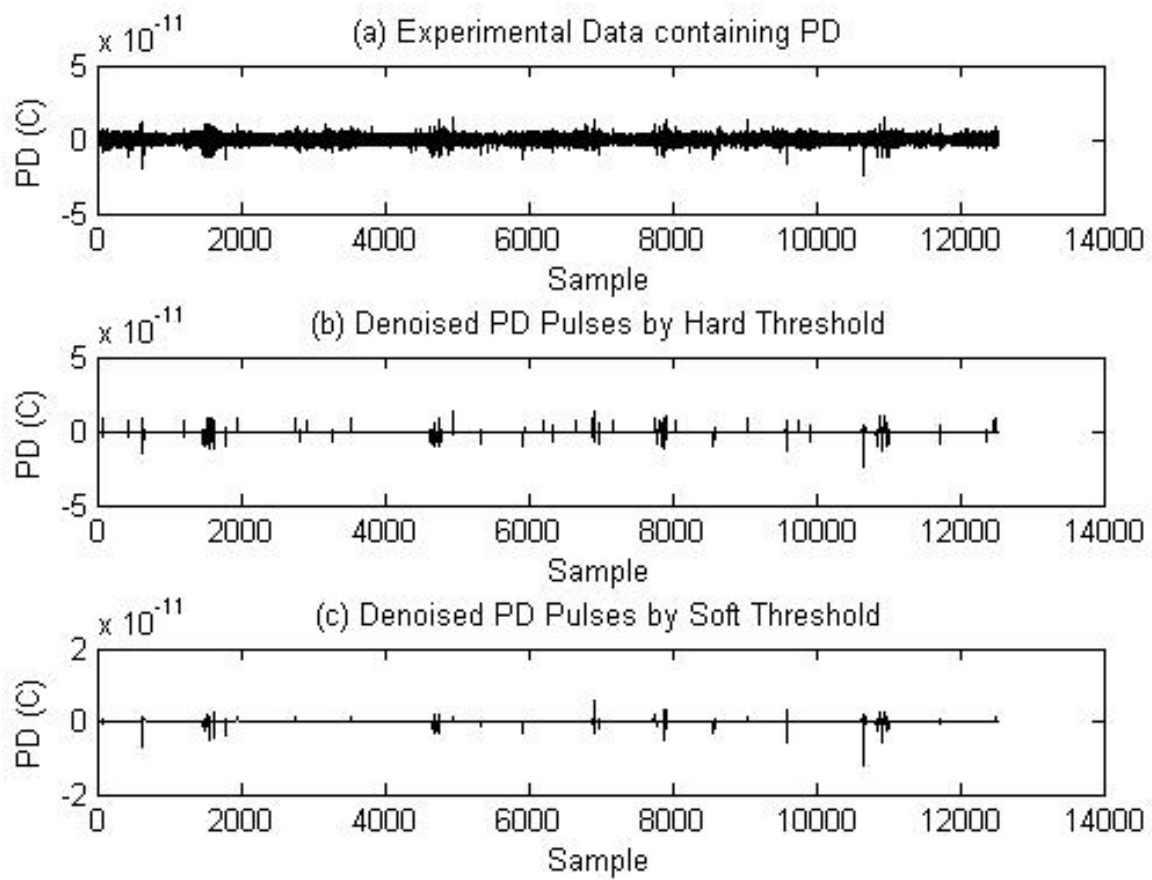


Figure-5.14 (k) Effect of hard and soft threshold selection on data set-11

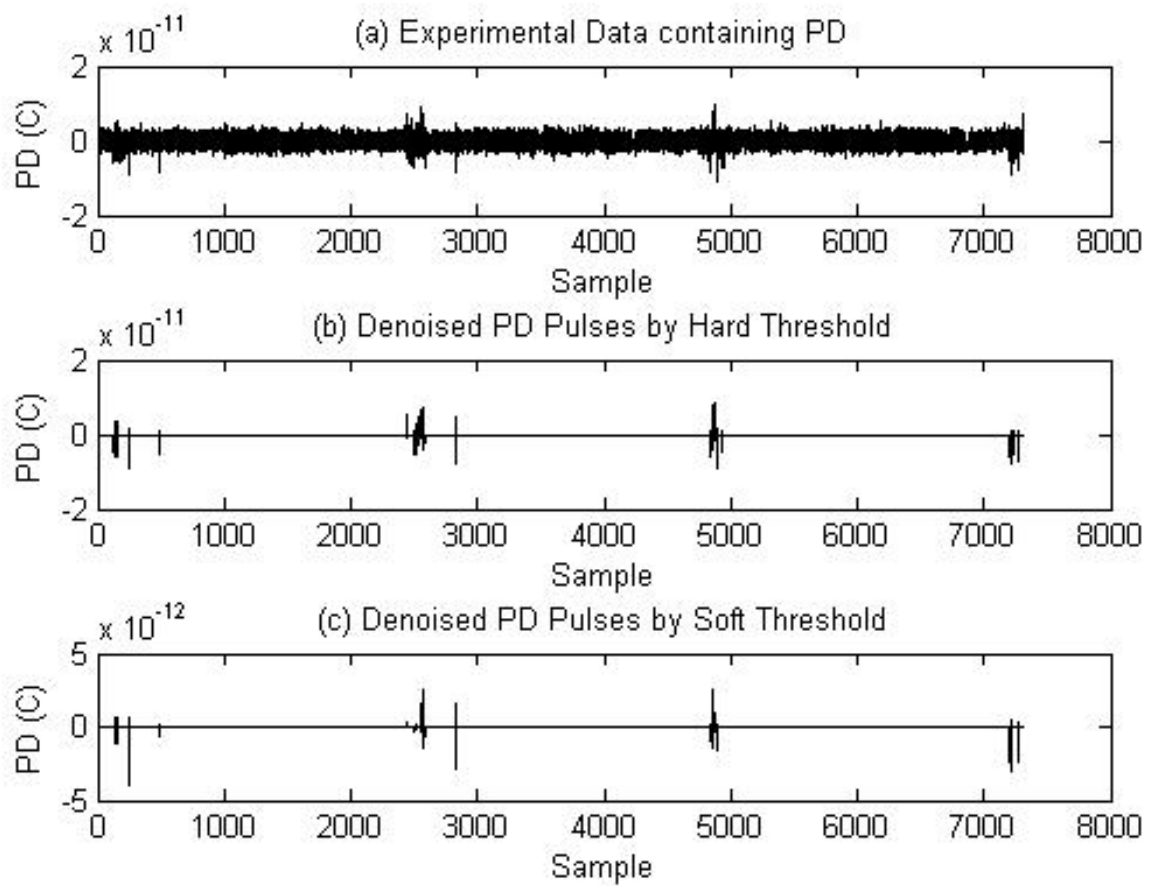


Figure-5.14 (l) Effect of hard and soft threshold selection on data set-12

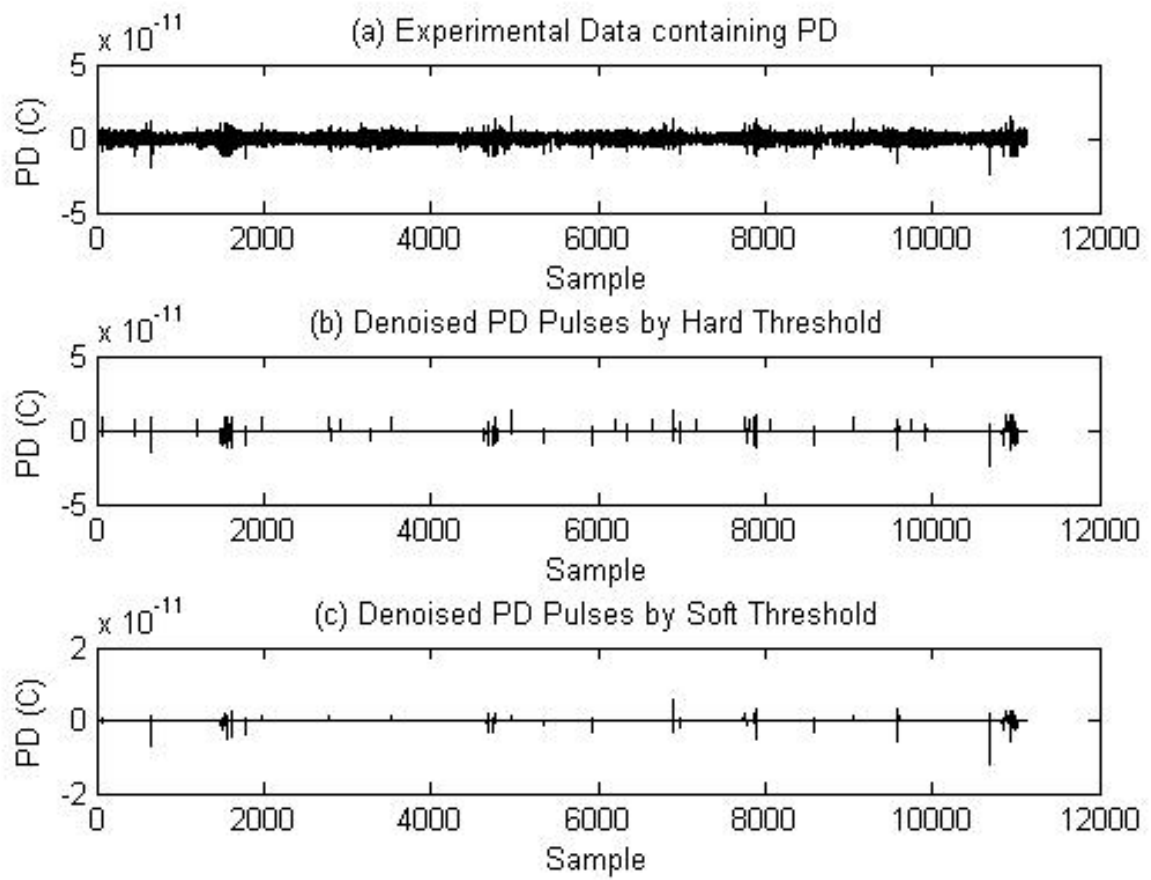


Figure-5.14 (m) Effect of hard and soft threshold selection on data set-13

During PD analysis of transformer, 13 different data sets are stored separately at different time interval. Signal analysis and wavelet analysis are carried out on each data set.

Figure-5.14(a) shows the data set, where PD values are much higher than noise. Here,  $R_{\text{pos}}$  and  $R_{\text{neg}}$  are much higher. In this case, the PD signal derived using hard and soft threshold are nearly same. Figure-5.14(g) also shows the data set where PD values are small. Here,  $R_{\text{pos}}$  and  $R_{\text{neg}}$  are much less and the threshold function selection plays important role. At this sample data, the hard threshold function can detect PD signals.

Subsequently, other data sets are analyzed their comparison is shown in figure-5.15. It is envisaged that, when  $R_{\text{pos}}$  and  $R_{\text{neg}}$  are higher, then implementation of hard threshold gain is of less advantage. In other words, when acquired signal is containing less PD pulse and more noise contribution; then only hard threshold gives good results whereas in other conditions, both threshold functions gives nearly same results.

This analysis is performed on the data obtained from transformer (referred as X'mer-1) at TRIL (Transformer and Rectifier Industries Ltd.), Ahmedabad. Also, another sets of data is obtained from transformer (referred as X'mer-2) at AREVA T&E, Vadodara and similar analyses are performed on the various data sets. The final results for X'mer-2 are shown in figure-5.14 which complement with the earlier one (figure-5.13).

### Gain (Hard threshold selection over Soft threshold selection) Vs. Actual signal parameters Rpos and Rneg (for p=2)

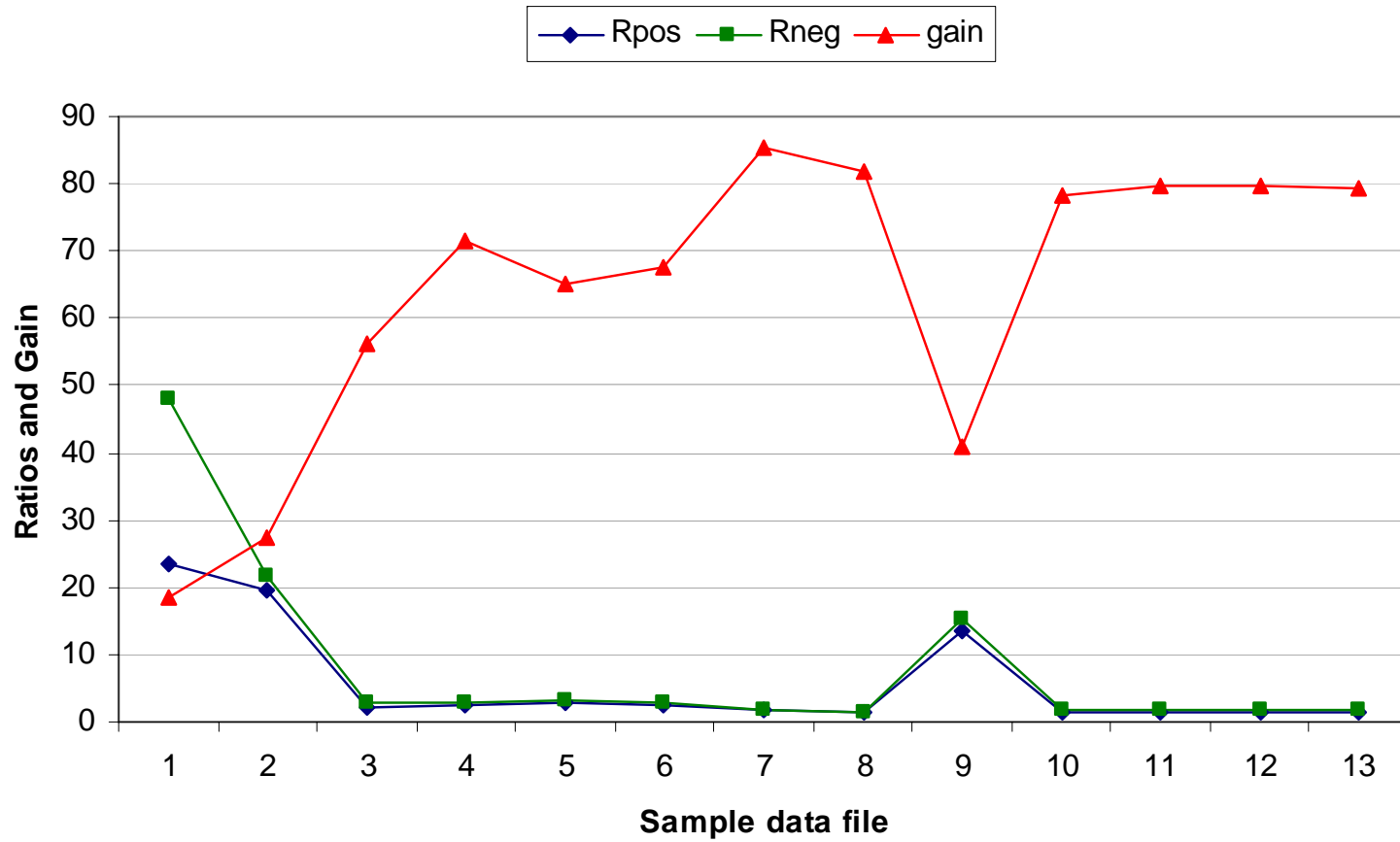


Figure-5.15 Comparison of Hard threshold Gain with Actual Signal (for p=2) Available from X'mer-1

### Gain (Hard threshold selection over Soft threshold selection) Vs. Actual signal parameters Rpos and Rneg (for p=2)

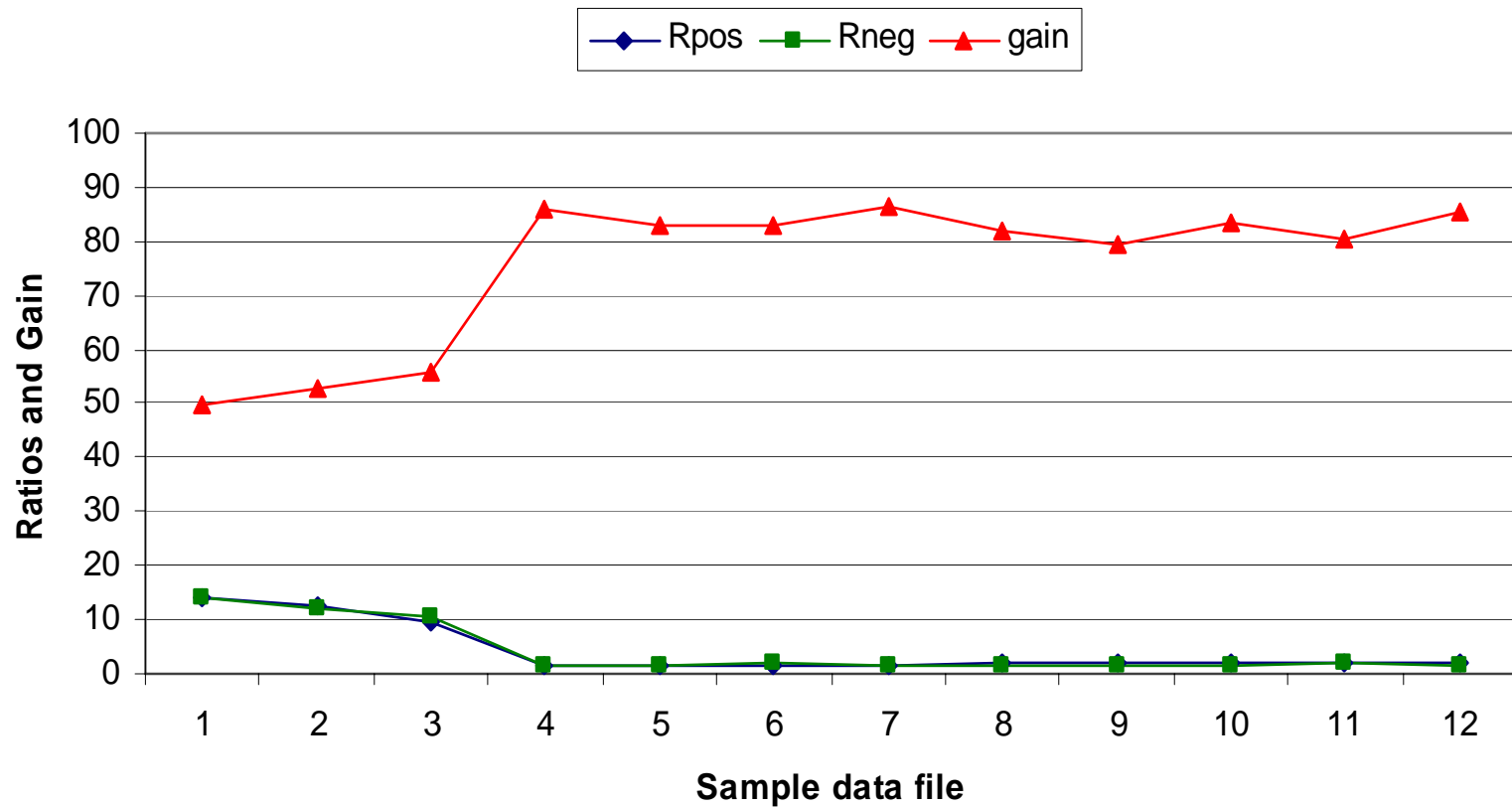


Figure-5.16 Comparison of Hard threshold Gain with Actual Signal (for p=2) Available from X'mer-2

## 5.6 CONCLUSION ON WT ANALYSIS

PD pulses de-noising is carried out using optimum WT, threshold function and threshold value selection. Wavelet transform can extract the PD signals effectively. Simulated PD signals are extracted by the Wavelet transform and the same method is applied to experimental data.

Simulated PD data has input of known PD pulses and noise whereas, test PD data has hidden PD pulses with noise. WT has successfully extracted PD samples, which match with simulated PD pulses.

The same WT method is applied on test data and extracted pulses. It is derived that extracted PD pulses (from testing data) are contains noise also and major noise is easily removed with this technique. It is concluded that WT technique can be utilized to de-noise the PD signals and thus enhance the detection sensitivity.

Later on, analysis is performed on acquired signal to determine in advance which threshold function is to be selected. Based on actual data and WT analysis, it is concluded that if the signal has low PD pulse intensity then hard threshold function selection has value, but when noise contribution is low compared to PD pulses then hard threshold function selection has marginal advantage over soft threshold function selection. So, based on amount of noise from surrounding environment at site, threshold function can be estimated in advance.

## **Chapter-6**

### **Conclusion and Future Scope**

In summary, this thesis focuses on the problems encountered by the conventional PD measurement during testing on solid insulating material, specifically focusing on problem of noise and temperature included during PD acquisition and off line PD measurement respectively. The work is carried on temperature and voltage stress parameters on insulation which are affecting its life operation. The present work introduces an experimental approach to obtain phenomenological and statistical life models based on the inverse power law, which has been defined and discussed in this work. The main goal is to describe the life of epoxy resin systems subjected to PD activity under thermal conditions, which are higher and lower than the ambient temperature as well as above the glass transition temperature ( $T_g$ ). After modeling the interaction between the temperature and PD activity, the main conclusions show that stress increases and life decreases with respect to ratio of  $T/T_g$  equal to 0.8 to 1.25. Also, average life increases when ratio of  $T/T_g$  is 0.25 to 0.6

During second phase, it is felt that noise has a prime concern in case of PD measurement and therefore a technique has been developed to reduce noise interference through WT de-noising method. WT is applied for suitability check for simulated data and real time data. Subsequently, WT is further considered for different threshold function and threshold value selection. It is concluded that WT can extract the PD signals effectively. During analysis, two factors are noticed; one is WT threshold function has great importance for small amplitude PD detection and another is by analyzing original signal, there is possibility of predicting which threshold function will give optimum WT result. Finally, by analyzing mathematically two conclusions are drawn: (1) if the acquired signal has low PD pulse intensity, there is great advantage of hard threshold function and (2) if noise contribution is low compared to PD pulses, then there is marginal advantage of hard threshold function over soft threshold function selection. In this work, a method is envisaged for optimum WT threshold function selection from real-time acquired data of Transformer. Finally, it is concluded that WT technique can be utilized to de-noise the PD signals and thus enhance the PD detection sensitivity.

Further research can be done on different parameters and a complete model can be developed which can estimates the life of any specimen.

Also, WT method can be used for anticipating appropriate WT threshold function selection for present data from previous one. Further research is possible on to define all WT parameters like, mother wavelet selection, different level selection etc. These WT parameters can be used for hardware realization for PD detection.

## **Publications**

## PUBLICATIONS

- [1] Vibhakar C. K., Kanitkar S. A., “A Novel approach for wavelet transform threshold function selection using acquired signal analysis for partial discharge extraction”, Indian Electrical & Electronic Manufactures Association (IEEMA) India, Journal, Vol. 3, No. 1, pp 138-142, Sept. 2011.
  
- [2] Vibhakar C. K., Kanitkar S. A., “Investigation on time domain signal to appropriate Wavelet Transform threshold function selection for Partial Discharge detection”, International Journal On Electrical Engineering and Informatics, Vol. 3, No. 1, pp 74-82, May 2011.
  
- [3] Vibhakar C. K., Kanitkar S. A., “Investigation and analysis of insulators aging tests under the effect of temperature on Partial Discharge”, International Conference IEEE AUPEC, Auckland, 5-8 Dec. 2010.
  
- [4] Vibhakar C. K., Kanitkar S. A., “Novel investigation on partial discharge signal in power transformer using wavelet transform”, 8th India Doble power forum program for PD Monitoring of High Voltage Assets at Modern Trends, Ahmedabad , (Doble Engg. USA) 2-4 Dec. 2010.
  
- [5] Vibhakar C. K., Kanitkar S. A., “Investigation on epoxies aging using Partial Discharge (PD) phenomena under different temperature and modeling of PD extraction using Wavelet analysis”, International Conference Organized by IEEE DEIS ICHVE, New Orleans, USA, 11-14 Oct. 2010.
  
- [6] Vibhakar C. K., Kanitkar S. A., “Extraction of PD Signals using Wavelet Transform with different thresholding methods”, International Journal of Electrical & Electronics Engineering, ISSN 0974-2042, Vol. 12, Issue 03, pp 12-19, Jun. 2010.

- [7] Vibhakar C. K., Kanitkar S. A., "Investigation and modeling of epoxies ageing test under the effect of variation of parameter on Partial Discharge (PD)", International Conference Organized by IEEE, IIT Kharagpur, 17-24, Dec 2009.
- [8] Vibhakar C. K., Kanitkar S. A., "Novel investigation for specimens ageing test under Partial Discharges and temperature." International Conference Organized by IEEE CEIDP, Virginia, USA, 18-21 Oct. 2009
- [9] Vibhakar C. K., Kanitkar S. A., "Modeling and Investigation of PD in Artificial Voids in Solid Insulating Material Used as a Capacitor", International Conference ICETA, Saurashtra University - Rajkot, 13-14 Jan. 2008.
- [10] Vibhakar C. K., Kanitkar S. A. "A new deterministic model for tree growth in insulating materials with barriers", National conference on emerging Technologies and applications, Saurashtra University - Rajkot, 1-2 Oct. 2006.
- [11] Vibhakar C. K., Kanitkar S. A., "Ageing in solid insulating material by studying the effect of variation of parameters", National Conference on Engineering Science, C. U. Shah, Wadhwan, 13-14 Oct. 2005.
- [12] Vibhakar C. K., Kanitkar S. A., "A study survey on solid insulating material by short term ageing test", National conference on emerging Technologies and applications, Amoghsiddhi education Society, Sangly, Oct. 2005.

## References

- [1] "High voltage engineering", M. S. Naidu & Kamaraju, Publishers: Tata McGraw-hill
- [2] "High voltage engineering", E. Kuffel & W. S Zoengle, Publishers: Newnes.
- [3] Mrs S.A.Kanitkar and Dr. M. R. Panchal "Study and measurement of partial discharges in solid insulations", M.E thesis, M.S. University of Baroda, 1981.
- [4] Schifani R. and Gagliardo V, "PD patterns and aging phenomena at different temperatures in filled and unfilled epoxy by a modified Cigre' setup, Method-I", Proc. ICSD'95 Leicester, UK, pp 329–333, 10–13 July 1995.
- [5] Montanari G C "Aging and life models for insulation systems based on PD detection", IEEE Trans. on Dielectrics and Electric Insulation, Vol-2, pp 667–675, 1995.
- [6] Simoni L, Mazzanti G, Montanari G C and Lefebvre L, "A general multi-stress life model for insulating materials with or without evidence of threshold", IEEE Trans. on Dielectrics and Electric Insulation, Vol-28, pp 349–364, 1993.
- [7] Di Lorenzo del Casale M, Romano P and Schifani R, "A life model for epoxy resins subjected to PD activity at different temperature", Proc. IEEE Conference on Electrical Insulation and Dielectric Phenomena, pp 564–567, 15–18 Oct. 2000.
- [8] Simoni L., "General equation of the decline in the electric strength for combined electrical and thermal stresses", IEEE Trans. on Electric Insulation, Vol-19, pp 45–52, 1984.
- [9] Ramu T S, "On the estimation of life of power apparatus insulation under combined electrical and thermal stress", IEEE Trans. Electric Insulation, Vol-20, pp 70–78, 1985.
- [10] Fallou B, Burguire C and Morel J. F., "First approach on multiple stress accelerated life testing on electrical insulation", CEIDP Annual Report, pp 621–628, 1979.

- [11] Crine J P, Parpal J L and Lessard G, “A model of aging of dielectric extruded cables” Proc. IEEE International Conference on Conduction and Breakdown in Solid Dielectrics, pp 347–351, Trondheim, Norway, July 1989.
- [12] Di Lorenzo del Casale M and Schifani R, “Investigation of temperature effect on an epoxy resin: aging due to PDs”, Proc. IEE 8th International Conference on Dielectric Materials, Measurements and Applications, pp 509–512, Edinburgh, 17–21 September 2000.
- [13] Schifani R, “Temperature dependence of epoxy resistance to PD”, IEEE Trans. on Dielectrics and Electric Insulation, Vol-2, pp 653–659, 1995.
- [14] Di Lorenzo del Casale M, Mirelli G and Schifani R, “On PD insulation ageing under electrical and thermal multistress in Cigr'e's method II: a methodologic approach”, Proc. NORD-IS99, pp 149–156, Copenhagen, 14–16 June 1999.
- [15] Schifani R “On a model for the comparative analysis of the ageing characteristics of epoxy resins subjected to internal discharges at various environmental temperatures”, Proc. 3rd Int. Conf. on Conduction and Breakdown in Solid Dielectrics, pp 456–460, Trondheim, Norway, 3–6 July 1989.
- [16] Gjaerde A C, “A phenomenological aging model for combined thermal and electrical stress”, IEEE Trans. on Dielectrics and Electric Insulation, Vol-2, pp 674–680, 1997.
- [17] Gulski E and Kreuger F H, “Computer-aided recognition of discharge sources”, IEEE Trans. on Electric Insulation, Vol-27, pp 82–92, 1992.
- [18] Schifani R and Mirelli G, “A computer-aided instrument for pattern recognition of PDs”, Proc. 9th Int. Symp. On Theoretical Electrical Engineering COMPEL 17, pp 765–772, Palermo, Italy, 9–11 June 1997.

- [19] Capponi G and Schifani R, "On PD measurements in solid dielectrics by an automated system", IEEE Trans. on Dielectrics and Electric Insulation, 27, pp 106–113, 1992.
- [20] Di Lorenzo Del Casale M, Holbøll J T and Schifani R, "PD activity tests at different temperatures measured by Cigr'e method II", IEEE Trans. on Dielectrics and Electric Insulation, 7, pp 133–140, 2000.
- [21] Di Lorenzo Del Casale M, "On multistress aging of epoxy resins, PD and temperature", IEEE Trans. on Dielectrics and Electric Insulation, 8, pp 299–303, 2001.
- [22] Di Lorenzo Del Casale M and Schifani R, "Investigation of temperature effect on an epoxy resin: aging due to PDs", Proc. IEE International Conference on Dielectric Materials Measurements and Applications (DMMA 2000), , pp 509–512, Edinburgh, 17–21 September 2000.
- [23] Gjaerde A C, "Multi factor aging of epoxy: the combined effect of temperature and Partial discharges", PhD Thesis Trondheim University, Norwegian Institute of Technology, 1994.
- [24] Stone G C, 1993, "The statistics of aging models and practical reality", IEEE Trans. on Dielectrics and Electric Insulation, 28, pp 716–728, 1993.
- [25] M Di Lorenzo del Casale and R Schifani, "Direct interaction between PD and temperature on epoxies: phenomenological life models", Journal of Physics: Applied Physics, Vol. 35, No. 1, pp 33-39, 2002.
- [26] Schifani R., Ramano P. and candela R., on "Partial discharges mechanisms at high temperature in voids included inside an epoxy resin", IEEE Trans. on Dielectrics and Electric Insulation IEEE, Vol. 8, pp 589-597 , 2001.

- [27] Dr. V. J. Pandiya, "Protection of series compensated transmission lines: Problem and solution", PhD thesis, M. S. University, 2009.
- [28] Iaideva C. Goswami and Andrew K. Chan "Fundamentals of wavelets: Theory, Algorithms, and Applications," Publishers: John Wiley & Sons inc, 1999.
- [29] L. Prasad and S.S. Iyengar "Wavelet analysis with applications to image processing", Publishers: CRC press, 1997.
- [30] Ingrid Daubechies. "'Ten Lectures on Wavelets," Society for Industrial and applied mathematics, 1992.
- [31] Olevier Rioul and Martin Vetterli, "Wavelets and signal processing," IEEE SP Magazine, Oct. 1991.
- [32] C. Sindney Burns, A. Gopinath, H.Guo, "Introduction to wavelets and Wavelet transform," Publishers: Prentice Hall, New Jersey, 1997.
- [33] Nikolaj Hess-Nielsen and Mladen Victor Wickerhauser "Wavelets and Time Frequency Analysis," Invited Paper, Proceedings of the EEE Vo1.84, No.4, pp 523-544, Apr. 1996.
- [34] Stephane G. Mdlat "A Theory for Multi-resolution Signal decomposition: The Wavelet Representation," IEEE Transactions on Pattern Analysis and Machine Intelligence, Vol. 11, No.7, pp 674-693, July 1989.
- [35] John R. Williams and Kevin Ammtunga, "Introduction to Wavelets in Engineering," International Journal for Numerical Methods in Engineering, Vo1.37, pp 2365-2388, 1994.
- [36] A.W. Galli, G.T. Hydet, P.F. Riberio, "Exploring the power of wavelet analysis," IEEE Cornputer Applications in Power, pp 37-41, Oct. 1996.

- [37] Andrew Bruce, David Donoho, Hong-Ye Gao, "Wavelet Analysis," IEEE Spectrum, pp 26-35, 1996.
- [38] Albert Cohen and Jelena K. b "Wavelets: The mathematical background," proceedings of the IEEE, Vo1. 84, No. 4, Apr. 1996.
- [39] Les E Atlas, Garry D Bernard, and Siva Bala Narayanan, "Applications of Time-Frequency Analysis to Signals from Manufacturing," Proceedings of the IEEE, Vo1. 84, Issue. 9, pp 1319-1329, Sep. 1996.
- [40] Wim Sweldens, "Wavelets: What Next," Proceedings of the IEEE, Vo1. 84, pp 680-685, 1994.
- [41] Perrier, Philipovitch, and Basdevant, "Wavelet spectra compared to Fourier spectra," Journal of Mathematical Physics, Vol. 36, No. 3, pp 1506-1519, March 1995.
- [42] Prof. Freeman George "Wavelets in Signal processing.", Course Notes, University of Waterloo, EME, Fall term, 1997.
- [43] Hsu H. P., "Applied Fourier Analysis," Publications: Harcourt College, 1984.
- [44] Brigham E. Oran, "The fast Fourier Transform and its applications", Publishers: Prentice Hall International, 1988.
- [45] Ribiero P. F., "Wavelet Transform: An advanced tool for analyzing non-stationary harmonic distortion in power system", Proceedings of IEEE ICHPS, VI, Bologna, 21-23 Sep. 1994.

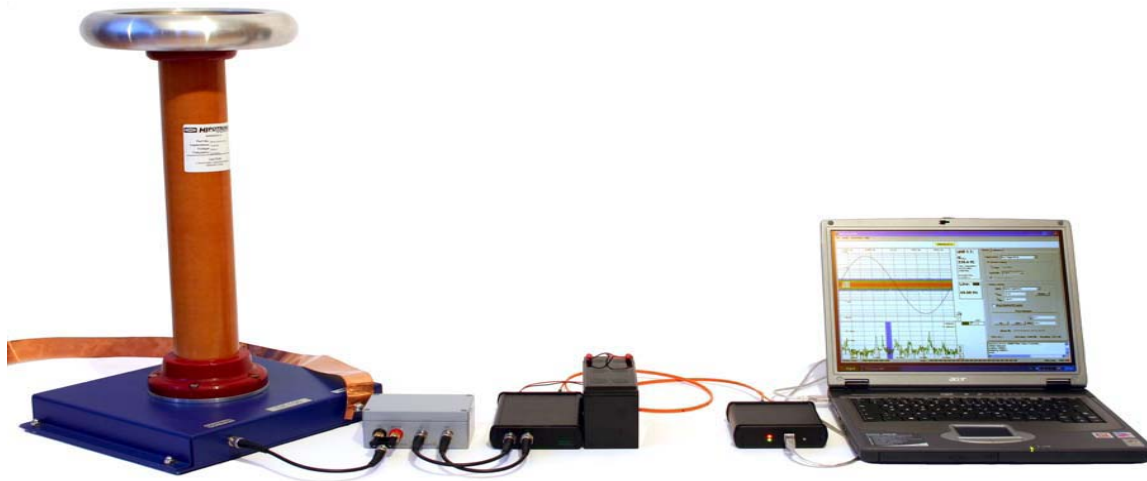
- [46] Robertson D., Camps O. and Mayer J. "Wavelets and Power system Transients", SPIE International Symposium on optical engineering in aerospace sensing, pp. 474-487, Apr.-1994.
- [47] Phung B. T., Liu Z., Blackburn T. R. and James R. E., "On-line partial discharge measurement on HV power cables", 11th International Symposium on HV Engineering (ISH), London, 23-27 Aug. 1999.
- [48] Odgen R. Todd, "Essential Wavelets for statistical Applications and Data Analysis", Publisher: Birkhäuser, ISBN 0-8176-3864-4.
- [49] Okubo H., Nayakawa H., "A novel technique for PD and breakdown investigation based on current pulse waveform analysis", IEEE Trans. on Dielectric and Electrical insulation, Vol. 12, pp 736-744, 2005.
- [50] James R. E. and Phung B. T., "Development of Computer-Based Measurement Systems for Recording and Analysis of PD Patterns", IEEE Trans. on Dielectric and Electrical insulation, Vol. 2, No. 5, pp. 838-856, 1995.
- [51] Evagorou D., Kyprianou A., Lewin P. L., Stavrou A., Efthymiou V., Georghiou G. E., "Evaluation of Partial Discharge Denoising using the Wavelet Packets Transform as a Preprocessing Step for Classification", IEEE Electrical Insulation and Dielectric Phenomena, CEIDP, Annual Report, pp 387-390, 26-29 Oct. 2008.
- [52] Yamada Ioya, Inui Akifumi, Kawaguchi Yoshihiro; "Distinction of Partial Discharge Signal from Noisy Signal by Daubechies Wavelet Transform"; Transactions of the Institute of Electrical Engineers of Japan, Vol. 123, No. 8, pp. 988-994, 2003.

- [53] Zhou X., Zhou C., Kemp I. J., “An Improved Methodology for Application of Wavelet Transform to Partial Discharge Measurement Denoising,” IEEE Transaction on Electrical Insulation and Dielectrics, Vol. 12, No. 3, pp. 586-594, June 2005.
- [54] Abramovich F., Bailey T. C., Sapatinas T., “Wavelet analysis and its statistical application,” The Statistician 49, pp 1-29, 2000.
- [55] Chang C. S., Jin J., Kumar S., “Denoising of Partial Discharge Signals in Wavelet Packets Domain,” IEE Proc. on Science Measurement and Technology, Vol. 152, Issue No. 3, pp. 129-140, May 2005.
- [56] Hettiwatte S. N., Crossley P. A., Wang Z. D., Darwin A., Edwards G., “Simulation of a Transformer Winding for Partial Discharge Propagation Studies”, IEEE Power Engineering Society Winter Meeting, Vol. 2, pp 1394-1399, 2002.
- [57] Mtronix Precision Measuring Instruments Germany (sources TRIL & AREVA), MPD 540 quick start manual, August 2006.
- [58] IEC 1985 the multi-factor functional testing of electrical insulation systems IEC Report Publication 792-1.

# Appendix

# APPENDIX

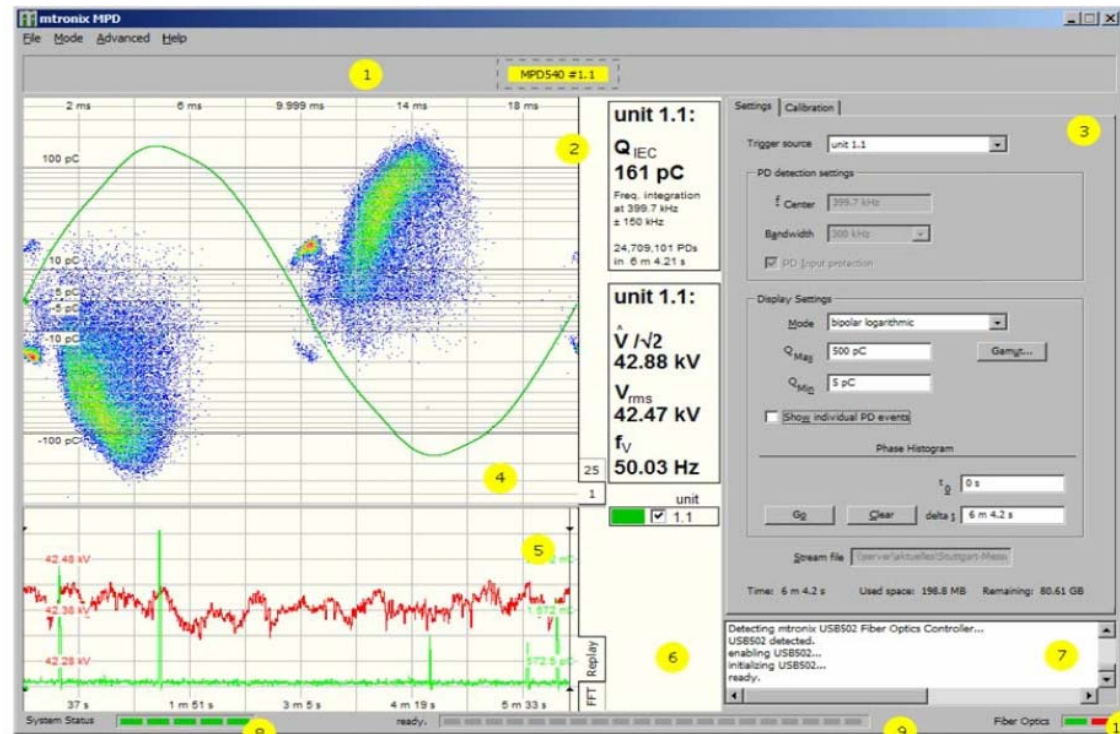
## Mtronix- Precision Measuring Instruments



MPD540 advanced partial discharge measuring system with coupling capacitor

### The MPD540 Software

The MPD540 software works in accordance of the hardware system (which is connected to specimen for interest). Here, the software is used to data record, export and analysis. Various MPD540 software features used in research are described here:



The different sections of the MPD540 window:

1. Acquisition unit display. The acquisition unit display shows which units have been detected by the software. Each detected unit is represented by a colored rectangle. A unit can be selected in the acquisition unit display by clicking on the corresponding colored rectangle; the selected unit then shows a dashed selection frame around its box. Selecting a unit prompts the software to show the rest of the workspace, which is not visible if no unit is selected. To hide the visualization and control panel views, click anywhere on the empty space next to the units. This will suspend any measurements currently in progress. To resume, re-select a unit. Hovering with the mouse over a selected unit rectangle will pop up a unit information window, which shows the unit's status, supply voltage, and any pending warning messages.
2. Visualization display. The visualization display is only visible if a unit is selected in the acquisition unit display. It takes up most of the left side of the workspace. The visualization display is further subdivided in the large scope view the small scope view and the measured quantities display.
3. Control panel. The control panel provides access to all measurement and display options.
4. Large scope view. The large scope view shows the high-voltage curve(s) of the connected acquisition units, as well as the phase-resolved histogram of the currently selected unit. Alternatively, the large scope view may be used to view an overview diagram showing the phase-resolved histograms of all connected acquisition units.
5. Small scope view. The small scope view can be configured to show many curves: the spectrum of the input signal at the PD input (DC through 20 MHz), the time signal at the PD input, trend curves for a variety of measurement quantities, and a replay log (in replay mode).

6. Measured quantities display. The measured quantities display shows the current values for the quantities being measured, such as IEC 60270-conformant charge estimation, voltage, high-voltage frequency, etc.
7. Log area. The log area displays status and warning messages in user-readable form.
8. System status bar. The status bar shows the initialization status of the software by means of 5 LEDs. During startup of the software, the LEDs in the system status bar will be illuminated in succession until all five LEDs are lit.
9. Progress bar. The progress bar visualizes the progress of the current operation. This is used, for example, to show the initialization progress of newly connected units. A message to the left of the progress bar shows what specific operation is being performed (or “ready.” if no operation is pending).
10. Fiber optical status. This display, consisting of two LEDs, shows the integrity of the fiber optical connections on the fiber optics controller. The left LED corresponds to the TX1 and RX1 connectors, the right LED corresponds to the TX2 and RX2 connectors. The LEDs turn green when the FO connection is set up correctly, and red if the connection is made incorrectly or if there is no connection. A yellow LED indicates that a temporary error was detected on the fiber optical network.

### **Microsoft Excel/Word 2007**

Microsoft Excel is used for various data sets processing and graph generation and Microsoft Word is used for the complete report generation.

### **MATLAB**

MATLAB is a high performance language for technical computing which integrates various functions for computation, visualization and programming with mathematical notations. Typical uses of the same are listed below:

- Math and computation algorithm development

- Data acquisition modeling, simulation and prototyping
- Data analysis, exploration and visualization
- Scientific and engineering graphics
- Application development including graphical user interface building

In the present work, it is used for life estimate modeling, Wavelet transform suitability check, WT data processing and result analysis.